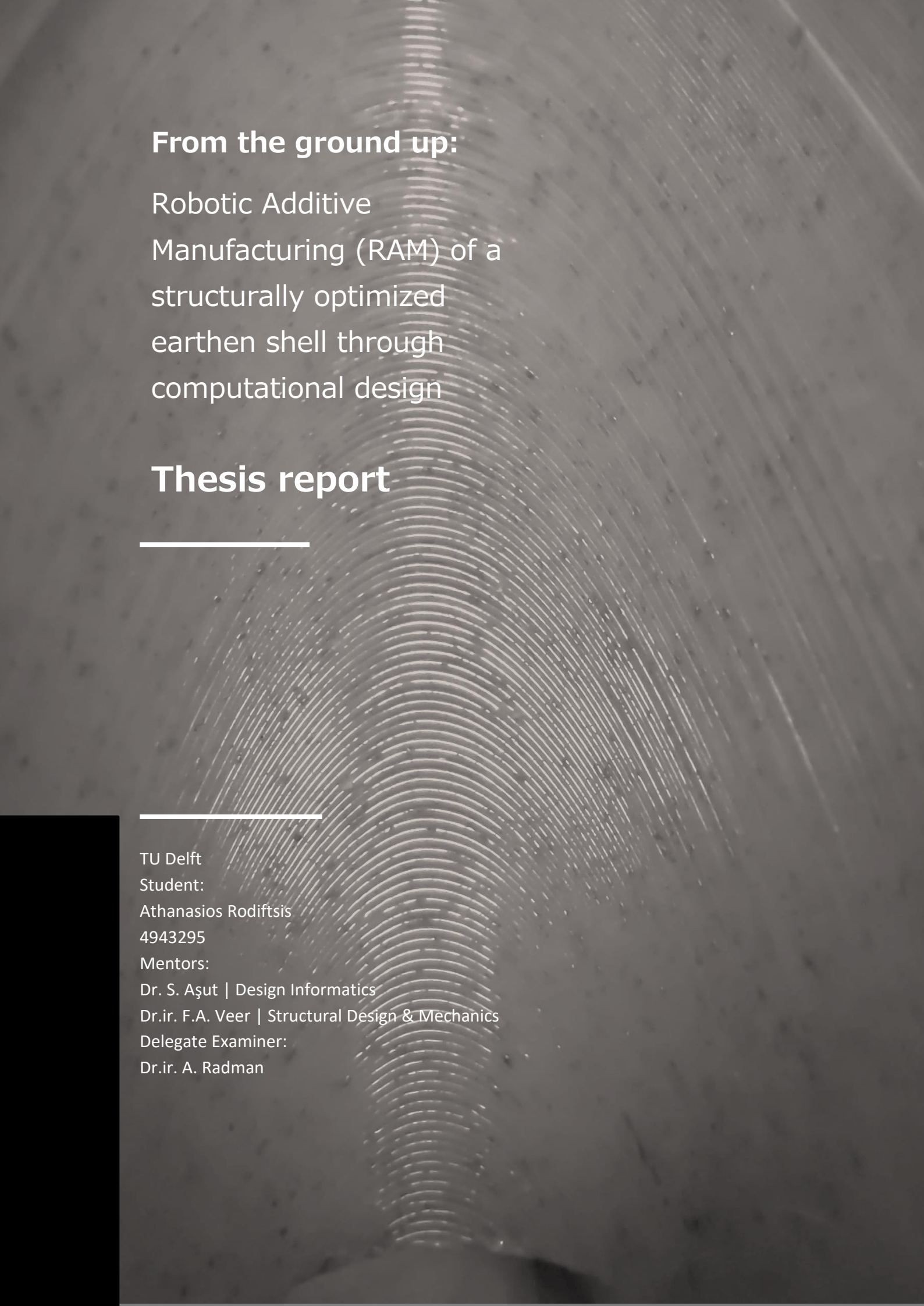

From the ground up:

Robotic Additive Manufacturing (RAM) of a structurally optimized earthen shell through computational design

Thesis report

TU Delft
Student:
Athanasios Rodiftsis
4943295
Mentors:
Dr. S. Aşut | Design Informatics
Dr.ir. F.A. Veer | Structural Design & Mechanics
Delegate Examiner:
Dr.ir. A. Radman

From the ground up:

Robotic Additive Manufacturing (RAM) of a structurally optimized earthen shell through computational design

Thesis report

In partial fulfillment of the requirements for the degree of

Master of Science

Personal Info.

Name: Athanasios Rodiftsis

Student number: 4943295

Studio

Name: Sustainable Design Graduation Studio

Tutors:

Dr. S. Aşut | Design Informatics

Dr.ir. F.A. Veer | Structural Design & Mechanics

Delegate Examiner:

Dr.ir. A. Radman

Themes:

- Robotic Additive Manufacturing (RAM)
- Structural Design optimization
- Sustainable materials innovation

Contents

Acknowledgements

During this thesis I have received a great deal of support and assistance by many.

First of all, none of this would have been possible without the scholarship granted to me by the Bodossaki Foundation. This honor gave me the opportunity to study abroad and chase my dreams in one of the best universities in my field. This experience matured me not only as a professional, but also as an individual by giving me a global perspective, a value that has become even more important due to the pandemic.

Secondly, I would like to thank my mentors, Serdar Aşut and Fred Veer for advising me in this endeavor. I am extremely grateful for their insight and giving me the opportunity to develop this project at the inspirational environment of the Architecture Faculty at the Delft University of Technology. In particular, I appreciate the freedom they gave me to pursue my ideas and make my own decisions on the direction of the project. Thirdly, I would like to thank Paul de Ruiter, not only for his feedback and direction on developing the extrusion system for the robotic arm, but also his hands-on involvement in the whole process.

This brings me to my friend and colleague Maximillian Mandat, with whom we collaboratively developed the extrusion system. We hope that it will become part of the department's toolkit and be developed further by students interested in this fascinating topic. I would like to acknowledge Maximillian's determination and enthusiasm in overcoming every obstacle encountered during the many iterations required when developing an actual product.

Next, I would like to thank my colleagues at team SUM. Being a part of a student team provided the necessary stimulus that is typically lacking in a solitary venture, such as the thesis. I wish them good luck in the competition of Solar Decathlon 2021 and promise to continue to support them with all the knowledge and skills I have acquired during my studies.

Finally, I wish to express my gratitude to my family for their patience during a challenging period that often tested my focus and resilience. Their support throughout my life allowed me to dream bigger and I dedicate this accomplishment to them.

Abstract

When designing for structural performance, the geometry of the load-bearing elements is crucial for achieving required stability. This is even more important in structural forms, such as shells and arches that are predominantly designed by their structural requirements. However, the typical design process starts with the design by the architect, and the subsequent analysis and development by the structural engineer, resulting in inefficiencies, not only in the process, but also in the sub-optimal result, as the more developed a project is, the least effective and more costly it is to optimize. Therefore, this report outlines the development of an automated pipeline that integrates the whole lifecycle of a structure, from conception to end-of-life.

The focus is on developing an integrated workflow for designing and fabricating a structurally optimized shell using computational methods for form-finding, structural and lifecycle analysis, as well as fabrication, with the end goal of facilitating an automated additive manufacturing production. The structure should be able to withstand applied wind and snow loads using construction materials that are strong in compression, such as earth as a load-bearing material. The design should also be adaptable, within the limits of the material strength or the spatial constraints of the system.

In the beginning, the topic is introduced and the research framework is defined. The relevant laboratory and numerical tests are mentioned. Next, literature research is conducted in the relevant fields. More specifically, the research are avenues are divided in form-finding shell structures utilizing computational tools, in earth as a construction material and in additive manufacturing in construction, as well as context. Then, a research by design method is adopted in two direction; a physical set-up and workflow for robotic additive manufacturing with earth is developed, as well as an optimal mixture that makes the most of the capabilities of the developed set-up. Next, a computational form-finding and digital fabrication process that are informed by the developed material and physical setup are defined. The generated form will be evaluated with finite element analysis (FEA) software. The algorithm integrates stress line additive manufacturing principles to direct load paths. The resulting forms are compared with corresponding non form-found and form-found shells in terms of material reduction, as well as with standard construction for environmental impact.

This project contributes towards the establishments of an optimized scientific workflow bridging the gaps between design and manufacturing, as well as the development of standards for assessing the safety and environmental advantage of 3D printed structures. In the end, the results will be discussed, some conclusions will be drawn, and further developments will be proposed.

Keywords - Robotic additive manufacturing (RAM), 3D printing construction, Parametric Design, Structural Optimization, 3D clay extrusion, Toolpath design

TiSD annotation

This thesis will also be part of the TiSD annotation. My interest in the concepts of sustainability and circularity led me to structure my electives with as many credits related to sustainable development as I could. The elective courses address issues related to sustainable development. Firstly, Zero Energy Design tackled an energy efficient renovation of multi-storey student halls as a case study. Renovation is an extremely relevant topic to address the environmental impact of construction. Secondly, in the Innovation and Sustainability course the assignments were a research paper and an educational animation on guidelines for Design for Disassembly [DfD]. DfD is a design strategy to facilitate circularity in construction, maximizing the construction materials' lifetimes, while reducing construction waste. Finally, in SWAT studio a strategy for a sustainable urban intervention and timeline in order to facilitate the transition to a Zero Energy Amersfoort was conceived and presented to local stakeholders and municipality.

Sustainability is central to the theme of the project, as the thesis aligns to sustainable development goals and attempts to address the issues through the development of a computational material use optimization workflow that integrates documentation of the lifecycle impact, as well as a robotic fabrication programming and simulation platform that takes fabrication constraints into account.

adapted from source: United Nations Sustainable Development, (2019)

Through efficient use of energy and resources, the impact of construction on the environment can be minimized. The project introduces a construction process with low environmental impact and reduced CO2 emissions. It achieves these through a reduction in transport operations and costs by the employment of natural material resources, providing an alternative to concrete. In addition, the presented method achieves a significant amount of material and cost reduction, while utilizing a globally available recyclable material delivering a cradle-to-cradle design. Moreover, this process of construction creates significantly less waste than typical construction where formwork as well as installation work, and end of life demolition cause an immense amount of waste. All these are factored in the lifecycle analysis that is integrated in the parametric tool, providing real-time information on the overall environmental impact. In this way, the assessment becomes a part of the decision-making process.

The adoption of the proposed technologies has the potential to create new jobs, while utilizing electric energy. The repeatability offered by the setup, due to its adaptive and parametric capabilities contributes to the promotion and expansion of a sustainable built environment that inhibits climate degradation. The multidisciplinary nature of the process enhances collaboration and partnerships between all related stakeholders, facilitating local economies due to the ubiquitousness of the main material.

1 Introduction

Circularity in construction and concepts like cradle-to-cradle design are gaining significant importance universally, as a new strategy to address the environmental impact of the construction sector. One of the pillars of circular strategies is the promotion of recyclable bio-based materials, as they do not contribute to the planet's resource depletion and have low embodied energy. Earth is a ubiquitous material that can be part of a more circular way of construction in a global context.

For thousands of years, earth has been used as a construction material. Time and practice led to the emergence of more climate-responsive, cost-effective and optimal construction techniques. Structures made with earth utilize locally sourced and environmentally friendly materials. That is why they are in harmony with the landscape, while contributing to local identity. Earth can be endlessly reprocessed or safely returned to the environment (Schroeder, 2015). Therefore, its relevance as a building material is becoming more and more noticeable, as sustainability becomes an important aspect of the construction sector and due to its compatibility with innovative construction methods, such as 3D printing.

At the same time, the energy consumption of construction industry amounts to 40% of the total energy used in most countries. In addition, carbon emissions of concrete amount to 8% of global emissions. Through the traditional way of construction, buildings end up as construction waste, as their lifecycle is not considered. Traditional on-site building involves the continuous pouring of concrete into formwork. The construction of a formwork is a highly-skilled and laborious process that utilizes a variety of materials, from plywood and lumber secured together to massive prefabricated assemblies. This causes a lot of waste and redundancy. The cost of formwork is estimated at around 60% of total construction (Shaeffer, 2009).

Despite their low weight, shells are very stable forms due to the high stiffness resulting from their geometry (Michiels, 2018). However, typical processes for arches and shells consider only the self-weight when defining the initial form. On the contrary, other types of loads, like seismic forces are omitted. This results in sub-optimal performance. By integrating a more complex load-case during the form-finding, there is a substantial potential in increasing seismic performance and efficiency of material use (Michiels, 2018). However, high-performance criteria are difficult to implement with standard manufacturing techniques. 3D printing in construction using earth could potentially address these issues through highly efficient performative design with an environmentally friendly, recyclable material. The lack of an established workflow and standards inhibits widespread adoption.

2 Research Framework

In this chapter, the research framework is presented. The structure starts with the background and the problem statement to indicate the research gap and the topic. This is addressed by the formulation of the main research question and related sub-questions. As graduation in Building Technology includes research and design, a case study is defined, where the research is

2.1 Background | Narrative

The building industry is increasingly adopting innovative manufacturing technologies, such as additive manufacturing in construction. This can lead to significant changes in the construction pipeline, as well as to a re-evaluation of construction materials. Building with earth, while having clay as the main binder has the potential to become an alternative to building with concrete, which is responsible for the big environmental impact of construction industry.

2.2 Problem Statement

The main problem this thesis attempts to address is the a one-size-fits all approach of the construction sector. This situation, not only results in inefficient constructions, but also has contributed to its high environmental impact through the excessive use of energy intensive materials.

2.2.1 Sub-Problems

The main problem can be decomposed to the following sub-problems:

- High environmental impact of process
- High cost and energy of transportation and operation (use of concrete)
- Unutilized local material resources
- Lack of affordability in construction
- Material waste due to formwork, installations & demolition at the end-of-life
- Outdated production techniques (compared to other industries)
- Sub-optimal design (due to construction limitations)

2.3 General objective

The general objective of the research is to utilize locally available materials and contemporary construction methods, in order to investigate the possibility and the extent of a more efficient solution for construction

2.3.1 Sub-objectives

The sub-objectives are directly related to the sub-problem:

- Minimal environmental impact of process
- Minimal cost and energy of transportation and operation (use of concrete)
- Utilized local material resources
- Affordability in construction
- Material conservation
- Contemporary production techniques
- Optimized design

2.3.2 Final product

The expected end product is a digital & physical design to fabrication method that integrates Life cycle assessment criteria. The process should be as automated as possible. Moreover, it should build upon the available tools of the Laboratory for Additive Manufacturing in BK faculty.

2.3.3 Boundary conditions

The boundary conditions of the project are:

- An extendable funicular vault will be the investigated geometry
- Structural stability and material use optimization will be the performance criteria evaluated. Therefore, comfort criteria such as thermal behavior, energy use or daylighting are out of the scope.
- Some assumptions will be made for the lifecycle analysis (LCA) The context of the LCA will be the Mediterranean hot and arid climate.
- The workflow will employ the means available at the Laboratory for Additive MAnufacturing (LAMA) of the architecture faculty, as well as the computational software available through the academic license, both for the prototype and the proposed solution.

2.4 Research Question

Based on the problems posed above, the research question is formulated as such:

> *"How to develop a design to fabrication workflow for a structurally optimized shell towards robotic additive manufacturing by earth?"*

2.4.1 Sub-Questions

To address the main question, the following sub-questions are specified

1. What are the advantages and limitations of using earth in RAM? What is the effect of material parameters (mixture design /kiln /drying time) in the mechanical properties of the component and what are the required material qualities for the proposed setup?
2. What are the design and performance criteria involved in designing a robotically 3D printed component out of earth? What is the effect of printing parameters (infill, layer height & direction, extrusion speed)?
3. What is the projected cost and environmental impact of the proposed construction?

2.5 Case Study

This thesis develops a computational structural optimization workflow, as well as a robotic fabrication programming and simulation platform that takes fabrication constraints into account, for the generation of shapes that ensure stability against the self-weight, wind load and snow load with optimal use of material.

A case study is an invaluable research method in a number of disciplines. It is particularly useful in construction, as it can capture the complexity of a real-life situation. In this situation, it will be a proof of concept of the proposed workflow:

> *"Structurally optimized earthen shell structure created through robotic additive manufacturing, using entirely reusable, recyclable materials sourced from the local terrain"*

2.6 Research Methodology

The research methodology demonstrates the systematic way the research is conducted. The method involves mostly research on quantitative data, both empirical and theorical, due to the experimental nature of the project. The structure of the research methodology is illustrated in the diagram 2.1:

2.6.1 Diagram

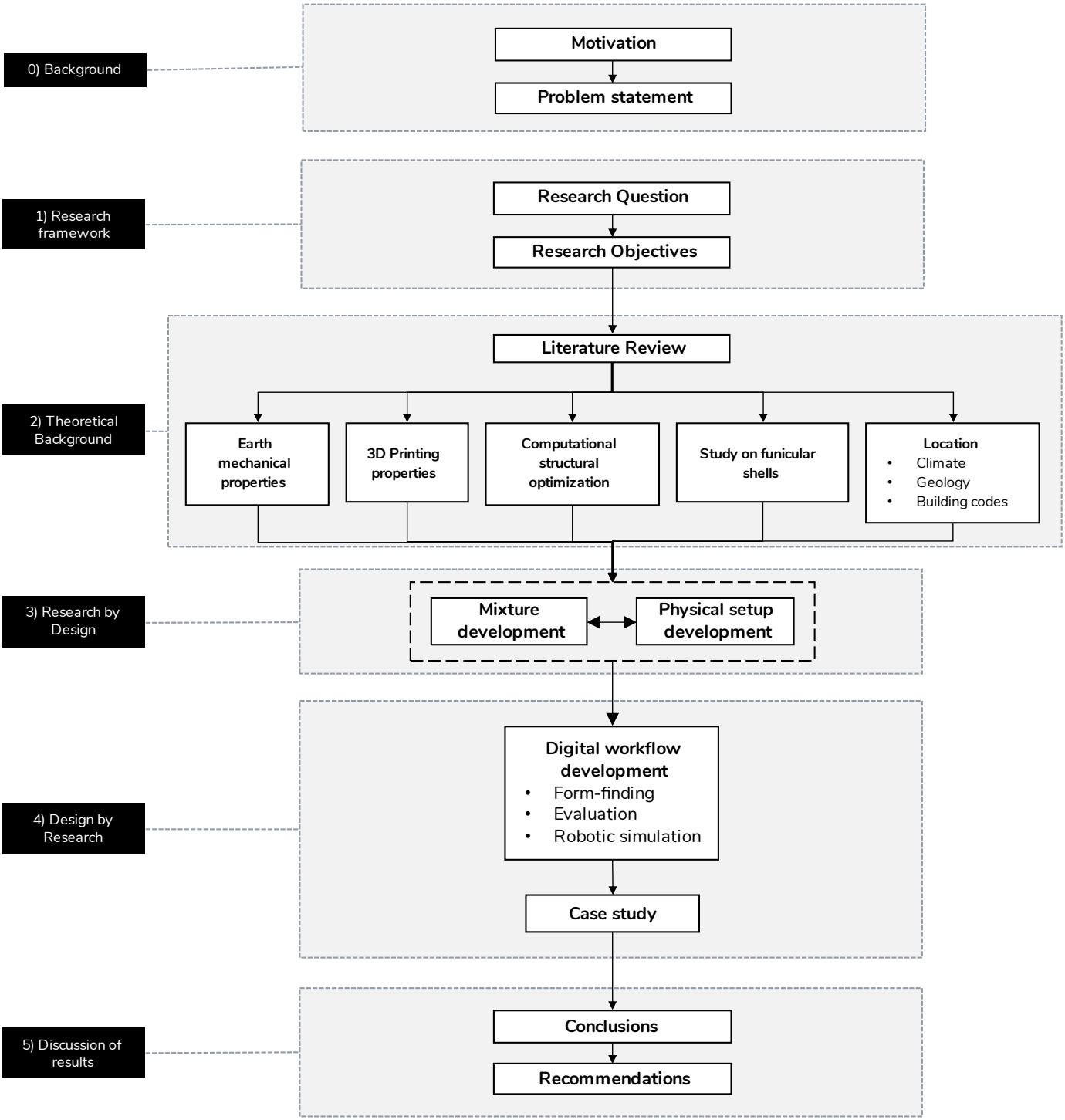

Figure 2.1 Research methodology diagram

2.6.2 Evaluation & Laboratory testing

This chapter describes the necessary laboratory tests for engineering uses. By performing these tests, essential parameters for the design are derived. The experiment design follows the process of similar researches on the mechanical properties of 3D printed materials, such as (Panda, 2017). These tests are

- Flowability test
- Extrudability test
- Open time test
- Buildability test
- Overhang test
- Green strength test
- Compressive strength test
- Shear strength test

The research incorporates physical tests, as well as simulations for evaluation of the results. Simulations are a vital part of design and construction. Finite Element Analysis (FEA) is a widely used simulation method in heat transfer, fluid dynamics, mechanical and structural problems. The principle of FEA is the reduction of a complex structure into small elements that represent local material properties. In this way, the overall structural response can be predicted. The degree of segmentation is determined by the computer processing power and memory.

The purpose of the FEA is to determine the maximum deformation and stress exhibited for the defined material and compare it with the maximum allowable displacement and stress. In the case of a compressive funicular vault the failure is predicted by the stress. A preliminary analysis is carried out in Karamba3D software, as it has a seamless integration with Rhino geometry and the grasshopper interface, making it an integral part of the digital workflow, increasing efficiency. In order to validate the Karamba3D results, ANSYS Workbench is used as a professional software as it supports additively manufactured materials, such as earth in our case.. For this reason, a Grasshopper script is defined to translate Karamba3D surface-based geometry, into a solid one, as ANSYS Workbench requires solid geometries.

2.7 Planning & organization

2.7.1 Research team

The research team consists of:

Execution: Athanasios Rodiftsis

Supervision: Serdar Aşut, Fred Veer

Advisor (informal): Paul de Ruiter

Collaborator(s): Maximilian Mandat (for the end effector development)

2.7.2 Timeline

Figure 2.2 illustrates the time-planning of the individual tasks allocated in the calendar weeks

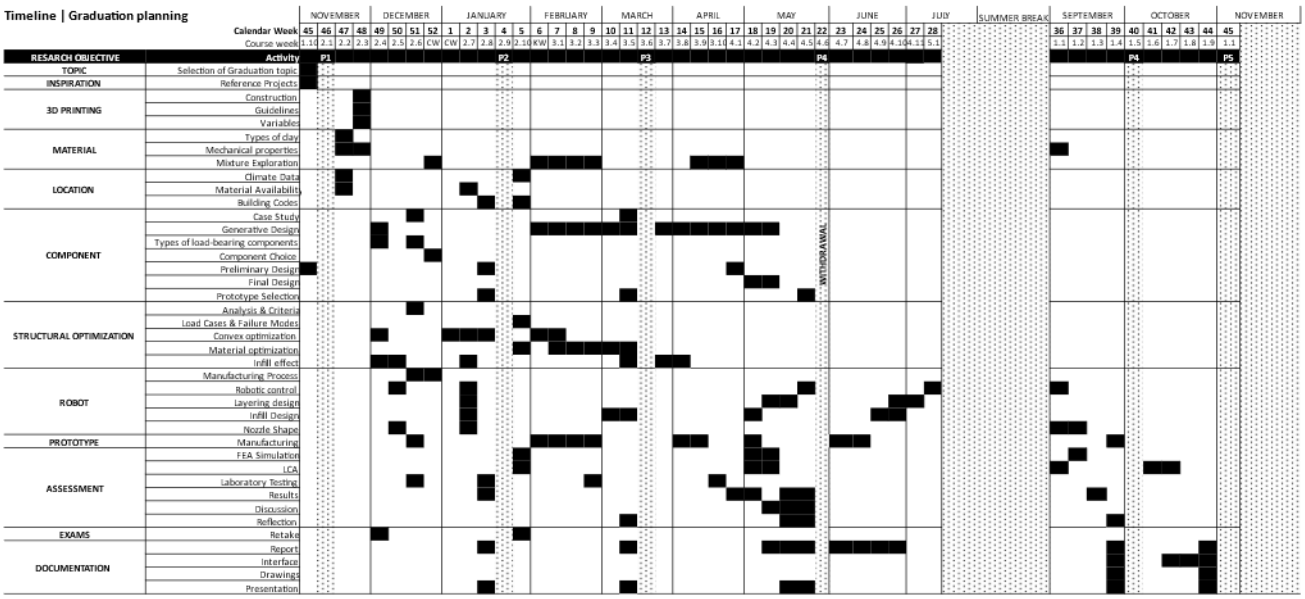

Fig. 2.2 Graduation planning

2.8 Topic Relevance

Soil constructed architecture can be found worldwide. As the most widely-used construction material, earth's relevance to contemporary architecture is undeniable.

Social relevance

The graduation work introduces a construction process with low environmental impact and reduced CO2 emissions. It achieves these through a reduction in transport operations and costs by the employment of natural material resources, providing an alternative to concrete. On a broader sense, the method promotes the capitalization of local workforce and resources for construction, since no advanced training is needed to utilize the tools and the materials are decided based on availability. The development of a physical setup with commercially available parts proves that this method can assist in the diffusion of production technologies, through an open-source construction paradigm and a reduction in the cost of construction. Proposed design guidelines contribute in the development of standards. Finally, as 3D printing in construction is an emerging concept, the project ultimately contributes to the expansion of human knowledge.

Professional / Scientific relevance

In the professional framework, the project achieves high construction performances, through the integration of computational optimization in the design and manufacturing process. This can contribute not only in mistake reduction but also in the integration of additional functions during printing, such as structural optimization, thermal insulation, natural ventilation and secondary working avoidance. In the scientific realm, the work adopts novel evaluation methods through the digitization of the construction process, such as BIM, file-to-factory. 3D printing offers the replicability of the architectural project, with high-quality standards, as well as realization of non-standard architectural geometries and material saving through algorithmic design.

3 Literature Review

This chapter outlines the main research avenues for the successful fulfilment of this project as defined in the research framework. The goal is to build a theoretical background in order to gain an understanding on the investigated structural system. First of all, a study on compressive forms with an emphasis on funicular shells is conducted. Secondly, research on state-of-the-art of 3D printing in construction is presented, as well as considerations in term of manufacturing and structural behavior. Thirdly, a brief introduction of earth construction and its considerations, as well as mechanical behavior is elaborated as a material that is suitable for additive manufacturing. Finally, a study on reference projects is conducted.

3.1 Shell Structures

Chris Williams, in the book "What is a shell?" describes shell structures, as curved surfaces with large dimensions in two directions and small in the third (Williams, 2014). Shells have been used in construction for their esthetic quality and structural efficiency, resulting from their continuous curvature, transferring forces in all directions along their surfaces in comparison to skeletal structures (Williams, 2014).

Shells are classified in in a number of ways. As geometries, they are described by their curvature, as a result of the surface's two main curvatures. This is defined as Gaussian curvature. When the curvatures have aligned directions, the Gaussian curvature is positive, resulting in a synclastic surface. In the opposite condition, the Gaussian curvature is negative and the surface is anticlastic. If one of the curvatures is missing the result is a zero Gaussian curvature shell and the surface is monoclastic. Naturally, flat surfaces have zero Gaussian curvature as well (Flügge, 1972). Gaussian curvature affects structural performance as a shell with increased curvature results in improved resistance against buckling. This is illustrated in *Figure* 3.1. As structural forms, shells are distinguished by their rigidity and are divided in three types: freeform or free-curved shells, mathematical or geometrical shells and funicular or form-found shells (Adriaenssens et al., 2014).

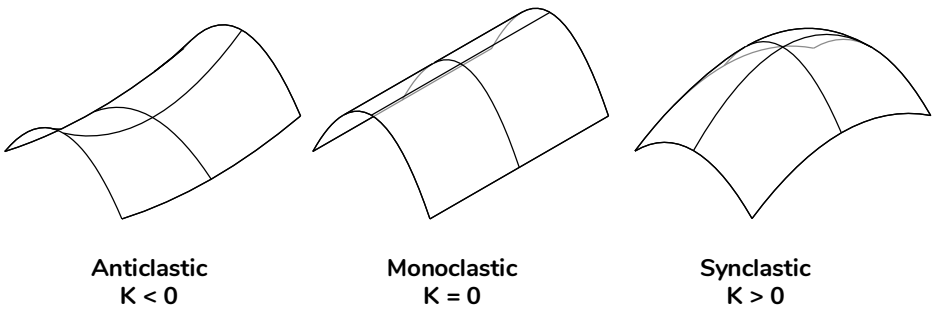

Fig. 3.1 Shell classification according to degree of curvature

3.1.1 Structural optimization

The adoption of technological advancements has the potential to reduce costs and energy, without compromising safety criteria. In the construction industry, this can be achieved through structural optimization. Its aim is to minimize the material needed for a structure by finding the optimal structural arrangement (Gordon,).

The methods employed are categorized in size, shape and topology optimization (Srivastana, Simant, & Shuckla, 2017) and illustrated in Figure 3.9:

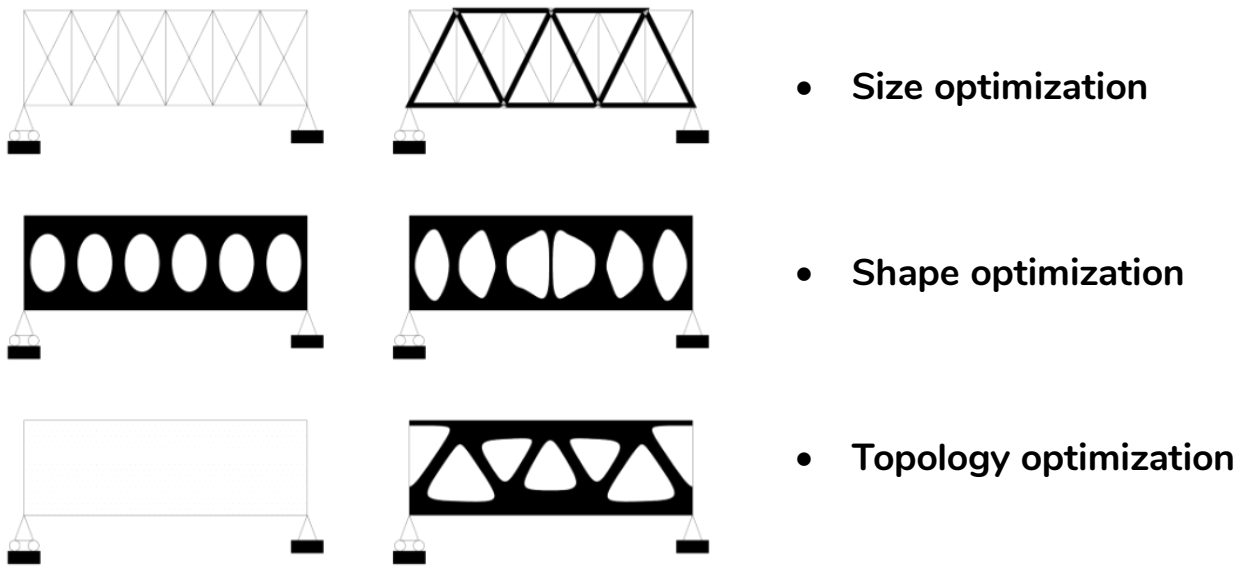

Fig. 3.2 Structural optimization methods, adapted from Srivastana, Simant, & Shuckla, 2017

- Size optimization refers to modifying the size and geometrical variables of the elements for a known structure, e.g. rod diameter
- Shape optimization involves the form finding process of the optimal shape, for certain structural conditions. The stages of shape optimization, as described by Yunliang Ding (1986) are "model description, selection of the objective function and shape variables, representation of boundary shape, finite element mesh generation & refinement, sensitivity analysis and solution methods".
- Topology optimization optimizes material distribution by assigning solid and void cells on a finite element mesh, according to boundary and loading conditions.

This thesis focuses on the shape optimization of a funicular vault.

3.1.2 Funicular Shells

Shells are very efficient structural forms, due to the way transverse loads are transferred, when compared to plane forms, as illustrated in Figure 3.3.

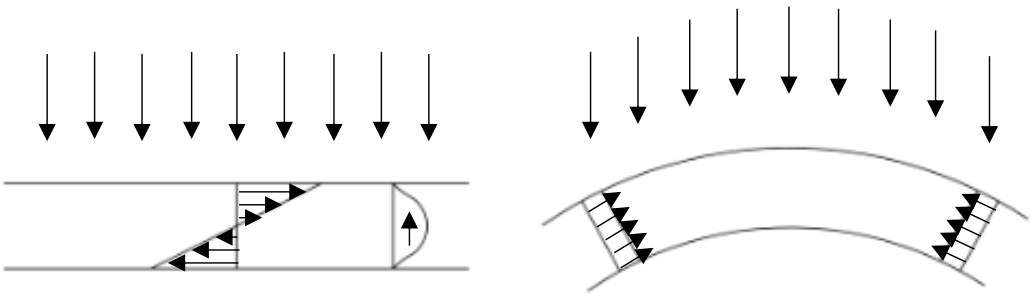

Fig. 3.3 Comparison of structural systems

A funicular shell is a compression only construction that transfers loads through axial forces and not by bending (Block, 2009) exhibiting membrane behavior (Michiels, 2018), resulting in a more efficient structure. Moreover, their small surface area for the same volume, compared to a rectangular form, results in a reduced shape factor. Form-finding is "the process in which a set of parameters is controlled to generate geometries for that design loading" (Adriaenssens et al., 2014). More than that, an understanding of form and forces is crucial for the design development (Michiels, 2018).

Before computational form-finding, hanging model methods were used to analyze and design funicular structures. Gaudi, Isler and Frei Otto are known for utilizing such methods (Addis, 2014). As a hanging chain is a form-active system, the resulting form adapts to different loading types to facilitate static equilibrium of the axial forces. The generated path is called thrust line. A hanging chain model is illustrated in *Figure 3.4*.

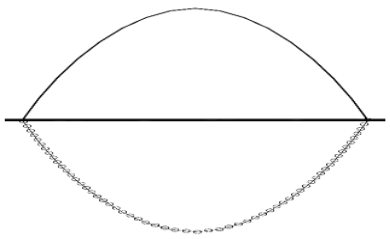

Fig. 3.4 Hanging chain model

As the stability is an issue of static equilibrium and not of stresses, these scale mock-ups offered reliable information about the performance of the actual structures. Normally, self-weight is considered in the form finding of arches (Michiels, 2018). These shapes are called catenary. When the same logic is applied to shells, the result is a structure that produces no bending moments. This structure is called funicular. However, when considering boundary effects or external loading, bending stresses develop. Computational tools have been used by researchers as more advanced form-finding methods to generate funicular shells that ensure force equilibrium and structural stability for complex loading cases (Block, 2009).

3.1.3 Structural Considerations

Open shells are not as rigid as closed shells and thus are prone to *inextensional deformation*. Essentially, they may experience bending without strain, while the surface length remains unchanged as they are more flexible. More specifically, as the force trajectories run through the arch, they push outward horizontally at the base. Therefore, an additional provision is required in the supports, for this so-called *kicking forces*. This phenomenon can be limited by increasing bending stiffness by ensuring sufficient boundary conditions. The phenomena are shown in *Figure* 3.5. Moreover, structures that rely on stiffness are sensitive to defects. As loads cause deflections, the structural efficiency of the ideal form is compromised, leading to buckling failure and collapse. This means that in this case the structural design is governed by the stresses and not the displacements. (Flügge, 1972).

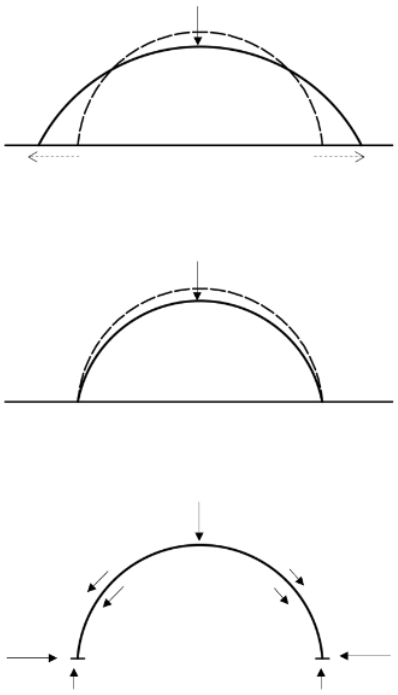

I. In-extentional deformation

- Open shells (rigidity)
- Boundary conditions

II. Buckling

- Sensitivity to defects (ideal shape)
- Stress-based analysis

III. Kicking forces

- Support conditions

Fig. 3.5 Structural considerations of shells

The failure modes are influenced both by geometry, as well as material properties. The latter, are more difficult to predict. In a global level of structural behavior, these are general instability, plastic collapsing or a solid to liquid phase change, and elastic buckling. These have already been mentioned by researchers, such as Carneau et al., (2020) and Wolfs et al., (2018). Regarding geometry, cantilever structures exhibit higher stresses than typical walls, with the addition of bending moments and tensile stresses. This increases the chance of failure.

To tackle this issue, there are two main strategies that have been devised: falsework printing, and maximum cantilever exploitation (Carneau et al., 2020). However, additive manufacturing in construction requires structural stability, not only of the final object, but also during the production. This condition entails risks in terms of potential failure modes. This thesis is directed in developing the latter, in the form of a printing strategy inspired by Nubian vault building technique.

3.1.4 Computational form-finding methods for shells

There is a number of different form-finding methods for shells. Generally, they are divided into two groups: geometric stiffness methods and dynamic equilibrium methods (Adriaenssens et al., 2014). The first group consists of methods, such as the Thrust Network Analysis (TNA) (Block, 2009), and the Force Density Method (FDM) (Linkwitz et al., 2014), not to be confused with Finite Deposition Modeling (FDM) which is an additive manufacturing method. These methods are widely used in practice, as they utilize force densities and trajectories to generate the form, and are therefore independent of the construction material. The second group comprises of Dynamic Relaxation (DR) (Barnes, 1988) and Particle Spring systems (PS) (Kilian et al., 2005). The principle behind them is the discovery of a static equilibrium solution for a dynamic equilibrium problem. By modifying mass or spring length and stiffness, the resulting geometry is affected. The advantage of this approach is that any type of loading case, including horizontal loads can be solved (Veenendaal, 2014). In order to develop a more universal workflow that allows external loading, such as earthquakes or wind load, the thesis will employ the dynamic relaxation method.

Dynamic Relaxation

In 1965, Day suggested Dynamic Relaxation for the analysis of indeterminate structures and it has been utilized since then for the nonlinear solving of a large number of analytical issues (Underwood, 1983). Examples of application consist of cable-membrane structures, tensegrity structures, tensile structures, grid-shells and continuous shells (Bagrianski et al., 2013). This method is based the second law of motion to convert a non-linear static problem to a pseudo-dynamic. An example of dynamic relaxation is shown in *Figure* 3.6. By following an iterative time-stepping process that revises deformations, a state of sufficient equilibrium is reached. However, for indeterminate structures, not only the shape contributes to the force distribution, but also the realized elements' stiffness. These are affected by the properties and dimensions of the materials, even though the processes are considered "material independent" (Veenendaal, 2014).

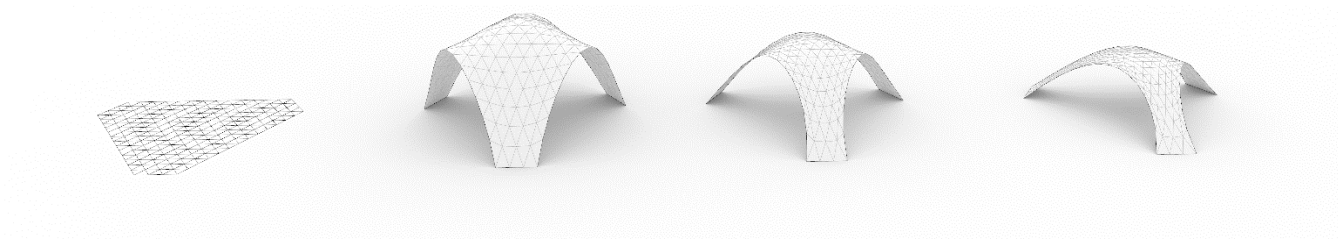

Fig. 3.6 Example of dynamic relaxation through the Kangaroo Physics (by Daniel Piker)

According to Bagrianski (2013), a form-finding procedure for compressive structures should possess three qualities:

1. Only axial loads should be transmitted by the elements
2. The process should include material properties and dimensions as parameters
3. The introduction of project-specific conditions should be done in a systematic way.

These are the ambitions for the parametric form-finding workflow.

Evolutionary Optimization

The design exploration will utilize an evolutionary form-finding process to achieve optimal solution. The theory behind this type of programming is based in principles of Darwinian evolution and was initiated in the 1950s (Bianchi et al., 2008). An evolutionary solver employs a metaheuristic research algorithm that investigates potential variations towards an optimization goal. It does so, by producing thousands of random alternatives, that are progressively evaluated with stochastic methods. In the end, the best solution, from the ones that are explored, is found. *Figure 3.7* illustrates a fitness landscape

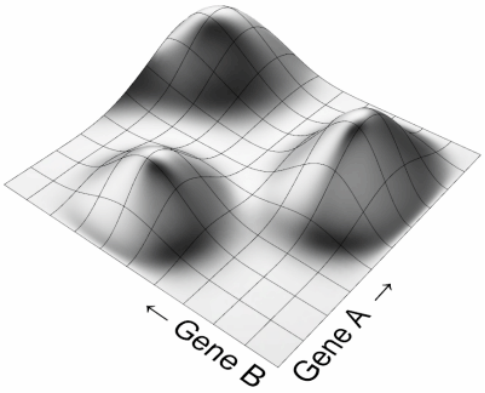

Fig. 3.7 Fitness landscape (Rutten, D. 2010)

Metaheuristics have a number of advantages. Firstly, they are applicable in variable ways as they are not problem-specific (Blum et al., 2003) and are able to operate under multiple constraints. This is why they are very valuable in design and engineering which tackle with multidimensional combinatorial problems. Moreover, the process can be stopped or influenced, when a desirable result is found. This allows high interaction with the user, since not all of the constraints need to be defined (Rutten, 2010). Lastly, evolutionary solvers do not require as high computational capacity as optimization algorithms (Blum et al., 2003). The tool Galapagos (Rutten, 2010) introduces evolutionary solvers in the Grasshopper3D environment, allowing seamless integration with computational design. Therefore, this method becomes more accessible to Building Scientists that aim to bridge design and engineering criteria and people that have no coding skills.

However, the main limitations of this method should be presented. First and foremost, compared to iterative methodologies and optimization algorithms, metaheuristic algorithms do not assure a globally optimum result. Instead, they explore in-between a finite number of options. In addition, they require a long time to produce results as each variation needs to be computed.

3.2 Additive Manufacturing in construction

Shell structures are non-standard geometries. Therefore, there is a big challenge in constructing them in an efficient and accurate manner. Traditionally, a large amount of material is wasted in temporary formwork and skilled labor is required. Digital fabrication methods, such as 3D printing, have the potential to address these challenges in a cost-effective way.

This chapter presents and overview of the state-of-the-art on 3D printing in the building industry, which is an emerging form of construction. Other industries, such as the automotive or aeronautics have already successfully adopted additive manufacturing of plastic and steel in their productions. The biggest advantage of this method is the capacity to manufacture building elements without the use of formwork, reducing cost and construction time. This method is still in research & development phase, with no standards set in place and significant deviations from standard constructions with cementitious materials, such as concrete. Therefore, to ensure structural integrity, creative engineering design and analysis is required.

3.2.1 Additive Manufacturing methods & State-of-the-art

Additive manufacturing comprises a series of methods, such as Fused Deposition Modelling (FDM), Binder Jetting and Paste Extrusion. FDM and Paste Extrusion are explored in this thesis.

In 1993 Binder Jetting, or powder-bed printing was developed at MIT. The process involves the spraying of a liquid binder on deposits of powder, resulting in a solid section of the printed object, as shown in *Figure* 3.8. The steps are repeated until the object is completed. Finally, the resulting print is excavated from the remaining powder. An advantage of this method is that complex forms which employ undercuts or overhangs are possible, as the unsprayed material functions as support structure. This powder can be reused, ensuing minimal waste (Rael and San Fratello, 2018). In terms of materials, this technology has been employed for glass, plastic, steel and concrete (Corneau, 2020). In the example of concrete, the method involves direct extrusion of paste in a gel-filled pool, in order to compensate for the weak strength of the fresh material. After the material sets, the gel is removed (Soliquid, 2019).

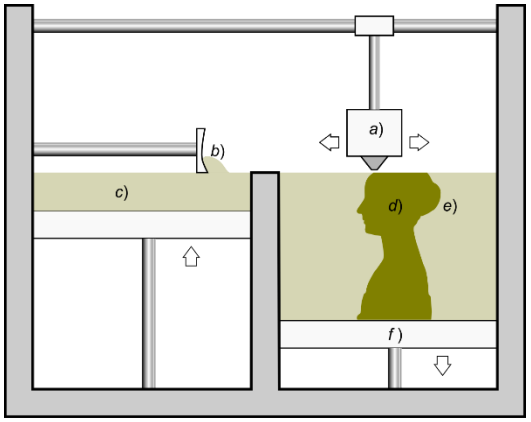

Fig. 3.8 Binder jetting (Cignoni, P. 2017)

Fused Deposition Modelling is the most popular method and was invented by S. Scott Crump and Lisa Crump in 1980s. It adopts additive manufacturing by depositing filament, usually plastic, on a programmed toolpath. A coil supplies the plastic thread to the heated metal nozzle. The melted plastic is extruded onto a build bed. The object is printed layer by layer, from bottom to top. The process is illustrated in *Figure* 3.9. Complex geometries that require overhangs are possible, up to a maximum angle. Cantilevers beyond this angle, as well as undercuts require printed falsework (Rael and San Fratello, 2018). The advantage of FDM printers is the low cost, both of the desktop printers and the filament. Even though plastic is the main material used, the However, the object size is limited by the printer frame dimensions, and the extrusion thickness by the nozzle. This is why this method is mainly used for prototyping.

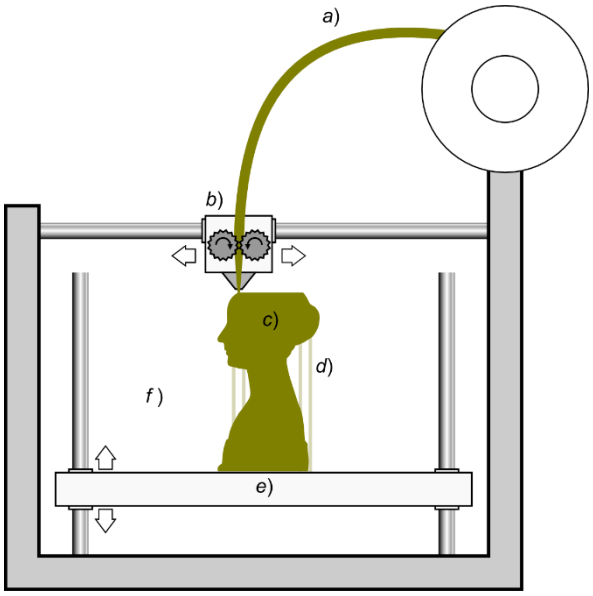

Fig. 3.9 Fused deposition modeling (Cignoni, P. 2017)

Paste Extrusion is similar to FDM, but allows the use of more diverse materials, such as resins, concrete and clay. The difference is that in this process, the material is not heated. This is due to the rheological behavior of the hydrated powders, a result of the colloidal flocculation of particles (Panda et al., 2019). Moreover, the material is kept in a tube and pressed through a nozzle, by means of ram press, compressed air or a screw. Like FDM, a line of paste is extruded on a surface or platform and the object is manufactured layer by layer. The diameter of the extrusion ranges from 0.0001 millimeters for the creation of cells through bio-nks, to 25 centimeters for building construction through concrete or mud (Rael and San Fratello, 2018). Compared to FDM with plastic, falsework printing, even with shape optimizations is avoided since tool path continuity is more practical when working with paste materials such as clay and concrete. The main reason behind this is that stopping and resuming the flow is difficult to control due to rheological parameters and gravity. (Carneau et al., 2020)

3.2.2 Paste Extrusion Setup and construction techniques

Additive manufacturing is at the forefronts of the fourth industrial revolution and can constitute a novel shaping method with new challenges and potentials that are currently under research.

Main potentials are:

- Reduction of cost / labor / time
- Environmental pollution mitigation
- High quality construction
- Integration of utilities
- Geometric freedom

Main limitations are:

- Dimensions limited by the printing frame
- Introduction of overhangs reduces efficiency
- Not cost-effective for typical structural elements
- Certification issues

3.2.3 Mechanical behavior of 3D printed structures

Shaping methods have a direct effect to the mechanical properties of the structure. Traditional shaping methods for earthen buildings consist of compression molding, hand-shaping, ramming, spraying and casting (Schroeder, 2012). In 3D printing, the material properties are affected by the relationship between time and material post extrusion in terms of yield stress development, as well as the possible types of failure during printing (Reiter, 2018). These assisted in determining the main criteria and requirements of the mixture paste. These parameters are extrudability, flowability, buildability and open time, as defined by researchers such as Lee, Maleb and Austin. The above parameters are defined as:

- *Extrudability* is the undisturbed pumping of a material from the extrusion pipe. It is a property of the additive manufacturing process that depends on the mixture and extruder compatibility. In general, high (static) yield stress impedes extrudability.
- *Flowability* refers to the easiness and continuity of material flow though the nozzle.
- *Buildability* is the resistance to collapse from the layer deposition. The material must be stiff enough to retain its shape, with minimized deformations, while being extrudable. In concrete 3D printing, chemical accelerators are used to facilitate this property.
- *Open time* is the period from when the material is pumped, until it is too stiff for extrusion or layer bonding. It is measured by testing shear resistance over time.

3.3 Earthen Architecture

Earthen architecture has existed for millennia. This chapter outlines the use of earth a global construction material. It highlights its structural material properties and its potential in sustainable architecture and defines a framework for its evaluation through a Life-Cycle Analysis.

3.3.1 Earth as a construction material

It is estimated that over one-third of global population resides in earthen buildings. Compared with typical buildings, earthen buildings utilize unfired earth as main construction material. In earthen architecture, load-bearing walls, infills, roof structures and finishes, as well as furniture are made of earth. The main constituents of a soil suitable for construction are clay, silt, aggregates and sand (Minke, 2012). Its scope is not limited by its poor strength, as entire settlements have been constructed by earth. A prominent example are the earth towers of Shibam and Tarim, commonly referred to as the "mud manhattans" of Yemen shown in *Figure 3.10*.

Fig. 3.10 The historic city of Shibam (Aiman titi. 2011)

Even though earthen buildings are more prevalent in hot-arid and temperate climates, a plethora of construction techniques and unique styles have empirically emerged due to the differences between cultures, climates and soils, as well as moisture contents, making earth one of the most versatile building materials (Reeves, 2006). Moreover, earthen architecture is not limited in vernacular construction. Its global application is highlighted by the range of typologies that share it as material, from humble shelters and dwellings, to palaces and mosques (Dethier, 1982). Many countries, such as Australia and France have successfully introduced earth in contemporary buildings (Reeves, 2006). This has managed to shift the common perspective of earth as an "old-fashioned" material (Dobson, 2000).

Drawbacks of earthen structures

There are a few disadvantages of earth, or loam in scientific terms, compared to industrial materials. First of all, its properties are highly dependent on the site. The different types of sand, silt, clay and aggregates, as well as processing techniques affect the end composition, leading to its lack of standardization. Its low compressive strength and very low tensile strength prohibit its use in contemporary building typologies that require multiple floors. Secondly, the loam mixture shrinks as it dries due to the water evaporating. This may result in cracks if the mixture design is not optimal. Thirdly, it is not completely water-resistant. Buildup moisture in earthen structures made of rammed earth walls, adobe, CEB can cause significant erosion. Therefore, provisions against rain must be taken (Minke, 2012). Finally, there is still prejudice against loam and other biobased natural materials.

Benefits of earthen structures

On the other side, earth has a series of advantages that industrial materials lack. One of the main benefits of earth buildings is the "feelgood" factor, claimed by the users. According to Gernot Minke (2000), this can be attributed to the stable relative humidity of 50% in the interior, as a result of the porous and breathable envelope, which is

the optimal value for the respiratory system. Its indoor climate balancing extends to its heat storing abilities, especially noticeable in climate zones with high temperature differences. Furthermore, its energetic impact is miniscule compared to reinforced concrete or baked bricks, providing a sustainable alternative. It can be endlessly recyclable, causing zero waste. Its ubiquitous nature minimizes, or in some cases eliminates, the transportation costs. Moreover, it is an extrudable material, making it compatible with additive manufacturing.

Earth mixture

Every earthen material consists of three types of components:

- Aggregates
- Additives &
- Water

In order to optimize certain properties of earth for construction, a plethora of additives and aggregates can be utilized during the mixing process.

Aggregates are responsible for altering the physical properties of the material. Some examples are better shrinkage behavior, tensile strength improvement, as well as erosion resistance. In order to improve the insulating properties of the material, aggregates that have low weight can be introduced. They can be of organic or mineral origin, as shown in *Table 3.1*.

Table 3.1 Earth Aggregates

Aggregates							
Mineral			Organic				
Natural		synthetic	Natural				synthetic
aggregates	Light aggregates	Glass fibers Rock wool Pumice slag Expanded glass Iron filings	Fibers	Short-fiber material		Wood-like materials	Synthetic fibers Polystyrene balls
Sand Gravel Crushed aggregate Rock dust Fireclay Asbestos fiber	Lava rock Pumice Sintered pumice Perlite Expanded clay Expanded slate Expanded mica		Straw Hay Herbaceous fibers Seaweed Hemp Jute Miscanthus	Plant-based Pine needles Flax shives Flax fibers Hemp wool Chopped straw Straw meal Chaff Rice husks Coconut fibers Sisal fibers Bamboo fibers	Animal-based Hair Bristles	Shavings Wood chips Small wood Slats Bamboo Paper Cellulose Reeds Cork	

Adapted from “Sustainable Building with Earth” by H. Schroeder, 2015

Additives are introduced to modify the chemical structure of clay in order to improve swelling and shrinking behavior, as well as increase compressive strength and weatherproofing. In earthen construction the most important mineral additives are the binders. They are separated into hydraulic and non-hydraulic. Typical hydraulic binders are hydraulic lime $CaCO_3$ and cement. These are referred as “chemical stabilizers”. This process is irreversible and therefore eliminates the replasticization of soil and return to the natural cycle (Schroeder, 2015). The main additives are shown in *Table 3.2*.

Table 3.2 Earth Additives

Additives				
Mineral		Organic		
Natural	Synthetic	Natural		synthetic
Clay	Gypsum	Plant-based	Animal-based	Petroleum products
Lime	Salt	Algae and seaweed	Fecal matter	Synthetic resins
Gypsum	Cement	Gluten	Urine	Was, stearin, paraffin
Salt	Sodium silicate	Starchy substances	Casein	Rubber
Grass	Soda	Molasses	Whey	Latex
Natural asphalt	Spent sulfite	Oils and substances	Blood	Soap
	Liquor	Resins	Animal-based glues	Flocking agents
	Ashes	Waxes	Glycogen	Quaternary
	Fired clay	Tannic acid	Termite structures	derivatives of amines
	Iron oxide	Saps		Acids
		Lignin		Alcohol
				“margines”
				synthetics

Adapted from “Sustainable Building with Earth” by H. Schroeder, 2015

3.3.2 Earth as a Sustainable Material

In 1987 the United Nations World Commission on Environment and Development proposed “sustainability” as a long-lasting progress for humanity. Sustainable Development is called the development that “meets the needs of the present without compromising the ability of future generations to meet their own needs” (United Nations Organization, 1987).

The ambition of sustainable architecture has renewed the interest in earth buildings, resulting in the adoption of traditional techniques in some countries and the maintenance in others. Provided that the on-site sub-soil is suitable, earth is a free building material, without the need for transportation. Moreover, when the structure is not required any more, the materials can be returned to the ground. As the construction process is fully reversible, there is no redundancy in the amount of material used (Reeves, 2006). *Figure 3.11* illustrates the lifecycle of earthen buildings.

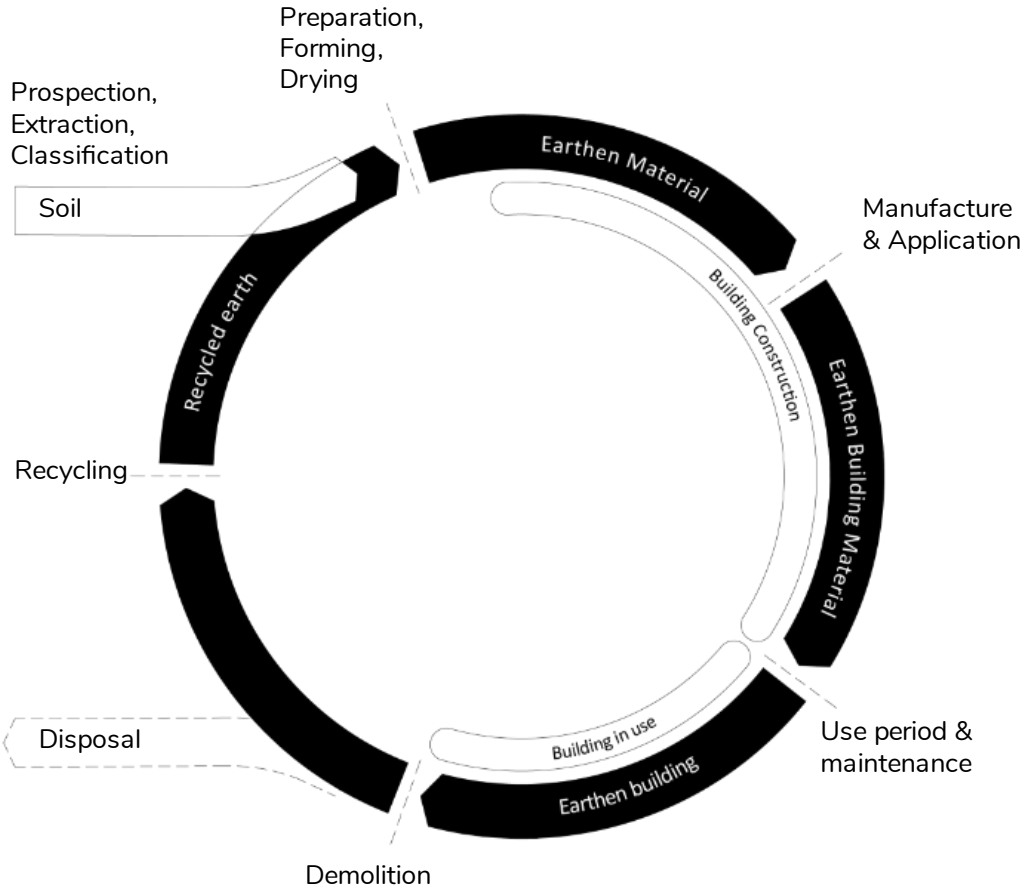

Figure 3.11 Life cycle of earth as a building material. Adapted from "Sustainable Building with Earth" by H. Schroeder, 2015

The aim of sustainable development in construction is to minimize the use of resources and the environmental impact in all phases of the building process. More specifically, structures must be designed, built, used and demolished with environmentally friendly and recyclable materials (European Parliament, 2011). General principles regarding sustainable buildings are categorized in materials, construction and surroundings.

Materials:

- Selection of renewable of long-term available materials, free from harmful substances
- Environmentally friendly and sustainable way of sourcing
- Minimization of transportation times in all stages
- Minimization of pollution

The evaluation of these strategies is conducted through Life Cycle Assessments (LCAs.

LCAs provide a reliable method of evaluating the environmental impact in all stages of the earth, from sourcing, to preparation and processing, the use and maintenance, all the way to the demolition and recycling.

"Primary Energy Intensity" indicates the energy for production and transportation of materials and is a popular gauge for comparing construction materials. *Table 3.3* contrasts the PEI of related materials. It can be observed that the preparation of the material requires little energy when compared to fired bricks

and concrete. The ideal situation of utilizing local earth results in zero PEI for transportation. Construction with earth as a load-bearing material has the ability to fulfil these conditions. Therefore, part of the research ambition is to inform the workflow with the parameters of Life Cycle Analysis.

Table 3.3 Construction material energy intensity

Construction material	PEI [kWh/m^3]
Earth	0-30
Straw panels	5
Timber (non-imported)	300
Timber derivatives	800-1500
Bricks (fired)	500-900
Cement	1700
Concrete	450-500
Glass sheet	15000
Steel	63000
Aluminum	195000
PE Polyethylene	4600-13100
PVC	13000

Adapted from Reeves, 2006. Schroeder, 2015

3.3.3 Soil as a structural material

This section focuses on the performance aspects of soil in construction, such as engineering behavior and mechanical properties. Loam is characterized by the grain size distribution of clay, silt, sand and gravel. Clay's purpose in earthen architecture is essential since it provides plasticity and cohesion during manufacture and strength during use, same as cement in concrete. Therefore, it was deemed necessary to elaborate on its characteristics as the main binder of the mixture.

Clay

Clays are an essential part of soils through their different applications and forms. In fact, soils are characterized by their clay content into from lean to rich in clay. Soil mechanical strength is dependent on the binding properties of clay, the frictional forces of the aggregate particles and the voids and bridges caused by free water molecules. (Houben & Guillaud, 1989). There is no universal consensus on considering and quantifying the contributions of each, so it is done on a case by case basis. However, in general, earth is a material with low compressive and shear strength, and very low tensile strength (Miccoli et al., 2014). *Figure 3.12* shows a simple soil model.

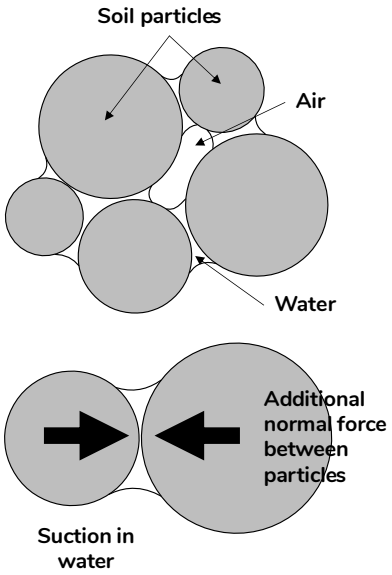

Fig. 3.12 Unsaturated soil model, Adapted from (Jaquin et al. 2012)

As a definition, the term clay "may mean a material made of clay-sized grains (smaller than 2 ~tm or 0.002 mm) or of grains consisting of clay minerals. Grains smaller than 2 μm may be clay minerals, or other materials, such as finely ground quartz or rock flour. Clay mineral grains may be larger than 2 μm and they are often bound into silt-sized (0.002-0.06 mm) aggregates" (Reeves, 2006). The mineralogy of clay has been investigated by Shaw & Weaver (1965), as a heterogenous mineral mixture of: 60% clay minerals, 30% quartz and chert, 5% feldspar, 4% carbonates, 1% organic matter and 1% iron oxides. Clay minerals are part of aluminum silicates (Schroeder, 2015). Soil types are categorized by their clay content according to *Figure 3.13*.

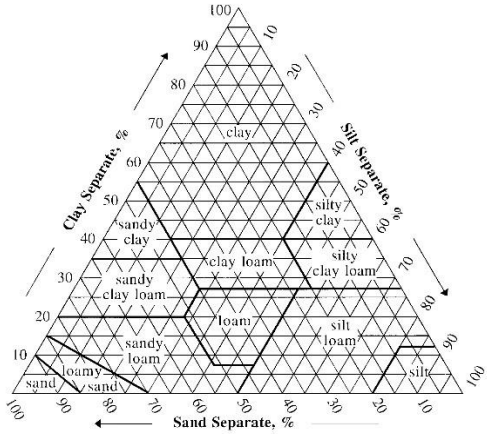

Fig. 3.13 Soil types by clay, silt and sand composition (Reeves, 2006)

The clay cycle is illustrated in *Figure 3.14*. It starts with the emergence and gathering of clay minerals in soils due to the erosion of rock forming minerals and glassy volcanic ash. Next, by being transferred, weathered and sorted due to physical processes, they become the main element of muddy sediments. Then, the diagenesis process occurs, causing the development of mudstones and shales from mud, which can change to slates If tectonic forces are present. In the end, the buried mudrocks rise to the surface due to tectonic uplift and the cycle starts again (Reeves, 2006).

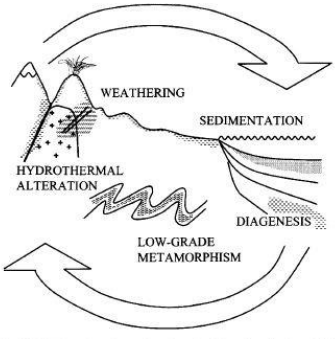

Fig. 3.14 Clay cycle (Reeves, 2006)

The role of clay in the economy is major due to its diverse applications, from cosmetics and medicine, to paper and cups, as its material species can be found everywhere and have an array of characteristics and properties. In construction, clay is typically used in brick-making or in water-retention barriers. Table 3.4 outlines the main applications of clay and relevant properties.

Table 3.4 Uses of clay and related properties

Use	Properties
All	Plasticity, density, porosity, particle distribution
Ceramics	Rheology, plasticity, vitrification, modulus of rupture, shrinkage, thermal properties, color
Fills, earthworks	Compaction, consolidation, in situ and remolded strength, plasticity, moisture condition value, permeability, suction
Earth moving	Shear strength, durability, bulking
Barriers	Permeability, compaction, viscosity, thermal properties
Agronomics	Density, pore size
Absorbents	colloidal properties, cation exchange

Adapted from "Clay Materials Used in Construction, Engineering, Geology," by G. M. Reeves and I. Sims and J. C. Cripps, 2006, Geological Society of London, p. 73.

Clays are classified as aluminum silicates from a chemical point of view. They consist of the elements Al, Si, hydrogen and oxygen, as well as Fe, Mg, K and Ca. Characteristic properties of clay, such as plasticity and shrinkage/swelling cycles are direct results of its mineral structure, cation-exchange capacity, surface tensions and bound water, as well as color (Schroeder, 2015).

Regarding their *mineral structure*, clay minerals form crystal lamellae with diverse contact types, as illustrated in Figure 3.15. These types greatly affect the emergence of the different properties. For example, *band structure*, which refers to planar contact increases structural stability and handling resistance. On the other hand, a *house-of-cards structure*, which refers to a dot-related contact assists water molecule evaporation and drying, while reducing the effect of shrinkage and swelling (Schroeder, 2015).

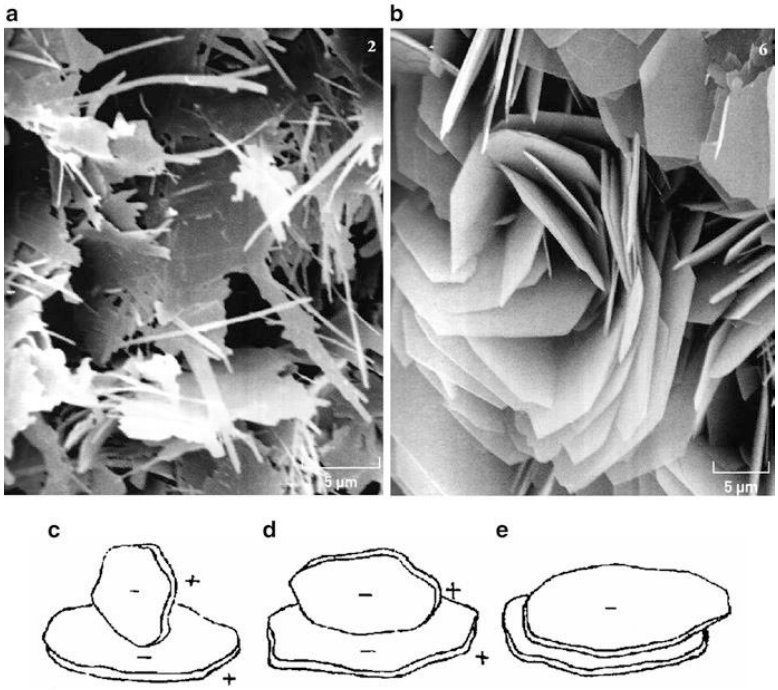

Fig. 3.15 adapted from Schroeder (2015) Structure and types of contact between clay minerals. (a) Needles/acicular or cemented, illite; structure, "house of cards," (b) Platy, chlorite; structure, "house of cards," Types of contact between clay mineral lamellae [20]. (c) Dot-like. (d) Linear. (e) Planar

Cation-exchange capacity has a significant influence on the hydration and plasticity of the material. This is the result of excess electric charges binding more water. Moreover, as the particle size is reduced, so is the porosity, resulting in an increase in cohesion (Kezdi, 1969).

Clay is an air-setting non-hydraulic binder as it hardens through drying. At the same time, its plastic characteristics are not lost as it can be "replasticized" with the addition of water (Schroeder, 2015). The importance of this property is crucial in ecological and sustainable construction as it allows endless recycling of the material.

Sand

Sand is an abundant aggregate of the earth mixture. Through the erosion of rock particles, natural sands are produced. According to the specific needs, the properties of the material can be influenced by the amount of sand. Aggregates improve tensile strength, erosion resistance and insulating properties, while reducing shrinkage throughout drying. Sand, gravel and straw are common examples of aggregates found in local soil (Schroeder, 2015).

Processing Parameters

Plasticity refers to the condition where the shape of a material deformed under pressure is retained when the force is removed (Reeves, 2006). This characteristic property of clay stems from its contact with water and is present over a specific range of water contents. Free and absorbed water molecules, as well as clay particles develop friction when mixed together, resulting in a viscous mix. If the water content is reduced, the clay paste exhibits ductile deformation and rupture. An additional reduction of moisture results in brittle behavior, prone to fracture. A clay material may fail either by plastic yielding or brittle fracture. These conditions are defined by the elastic and plastic limits of clay, as shown in Table 3.5. The plastic limit (PL) is the moisture content at the bounds between plastic and semi-solid conditions (Reeves, 2006).

Table 3.5 Clay phases

Phase	SOLID	SEMI-SOLID	PLASTIC	LIQUID-PLASTIC	LIQUID	SUSPENSION
Water	← Water content decreasing →					
Atterberg Limits	Ws	Wp	STL	Wl	WSL	WSL
Condition	Stiff –v. stiff	Stiff – workable		Sticky	Slurry	Suspension
Strength(kPa)	← Shear strength increasing →					
Shrinkage*	Residual	Normal	Structural			

Adapted from (Reeves, 2006)

There is a direct correlation between moisture content and strength. Stress-strain curves illustrate how clay behaves under constant applied stress. *Figure 3.16* displays the plastic deformation of clay for different moisture contents until the yield strength is reached. It can be observed that in principle, the lower the water content, the higher the final strength of the material.

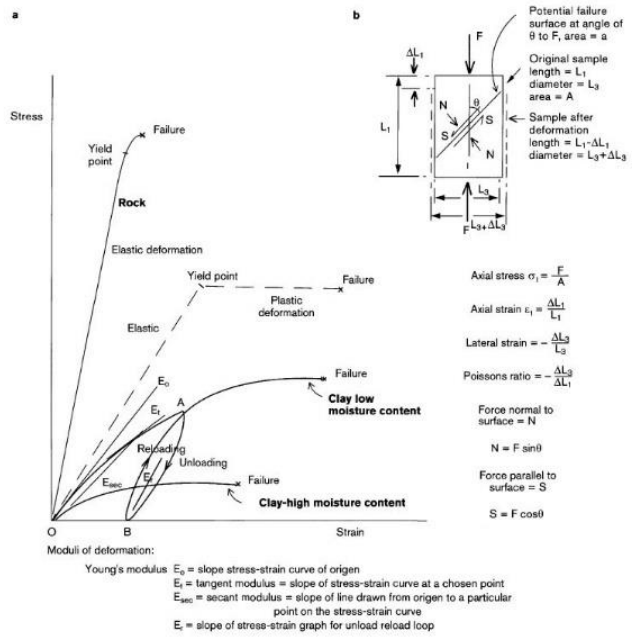

Fig. 3.16 Ideal and typical forms of stress-strain relationships in elastic and plastic solids. Adapted from "Clay Materials Used in Construction", by G.M Reeves, 2006

Drying Process

Change in moisture content results in swelling and shrinkage in clays. As the bounded water evaporates naturally, "shrinkage during drying" occurs. The degree of shrinkage is affected by the amount of water and clay in the mixture, the aggregates and the environmental conditions. High moisture and clay content results in higher shrinkage, as well as faster drying (Schroeder, 2015).

"Firing shrinkage" refers to the permanent shrinkage of the sintering process due to the use of a kiln. During sintering, a vitreous bond is formed between minerals and other materials, significantly increasing the compressive strength (Reeves, 2006), as shown in *Table 3.6*. In robotic additive manufacturing, the curing process occurs in the air, as no moulds are used. Therefore, post-deposition deformations should be minimized as the green strength is a fraction of the dry.

Table 3.6 Compressive strength of materials

Process Comparison	Compressive Strength [MPa]
Drying (e.g. unfired bricks)	2-5
Firing (e.g. Bricks)	20
Standard concrete	25

Adapted from (Reeves, 2006)

Structural Parameters

To guarantee the structural integrity of a structure under load, it is important to know the structural parameters of the material. In literature, they are distinguished between strength and deformation parameters. Strength parameters express the stress limits of the material before failure. On the contrary, deformation parameters define the way to failure and are generally expressed by the volume change exhibited. In actual conditions, different types of stresses occur in a load bearing structure. *Table 3.7* illustrates the main structural parameters that are investigated during the dissertation.

Table 3. 7 Main Structural Parameters

				Effects
Structural Parameters	Strength Parameters	Compressive Strength	Force vertical to cross section (important)	Dimensioning
		Tensile Strength βT	Cohesive strength	Wet (preparation)
				Dry
			Splitting tensile strength	Shock resistance (quality control)
			Tensile adhesion strength βTA	Mortar adhesion
			Flexural strength	Load perpendicular to plane (bending)
		Buckling strength	Plastic buckling	Overhangs
		Shear strength βS	Internal stresses from horizontal loads	Load parallel to joint
		Torsional strength	Twisting load	Extruder motor
	Deformation Parameters	Load-Independent	Thermal strains	Expansion (+)
			Moisture strains (reversible)	Shrinking (-)
				Swelling (+)
			Chemically induced strains (permanent)	Chemical Shrinkage (-) (e.g. lime)
				Chemical Swelling (+) (e.g. gypsum)
		Load Dependent	Modulus of elasticity	• Dead loads • Other permanent loads • Live loads
			Poisson's ratio	

Sources (H. Schroeder. 2015, G. M. Reeves. 2006)

It should be noted that these are affected by the type and quantity of clay minerals, particle size and plasticity (Reeves, 2006). Moreover, in earth building materials, the final dry state as well as the wet one during construction should be considered. When the material is still wet, it is important to minimize load transfers (Schroeder, 2015).

The most important dry material criteria are the compressive strength, the flexural strength and the tensile bond strength, which can be derived from laboratory testing.

- *Compressive strength* is the most important structural parameter in earth buildings. In this respect, clay rich mixtures have higher strength than lean ones. However, they exhibit higher shrinkage due to drying. The use of additives and special treatments can influence the compressive strength. In principle, earth structures must be in compression.
- *Flexural strength* refers to the maximum bending stress that can be applied before failure. The significance of this property lies in the structural form studied and the orthotropic behavior of printed materials. This is caused by the differences in porosity dur to layering (Rahul, 2019).
- Tensile bond strength. Since the tensile strength of the dry material is very low (about 10% of the compressive strength), it is generally not considered in the calculations.
- *Shear Adhesive Strength* is Therefore, the ultimate permissible strength is based on the value of this.

3.3.4 Mixture development parameters

The relevant parameters for a successful mixture development are showcased in *Figure 3.17*.

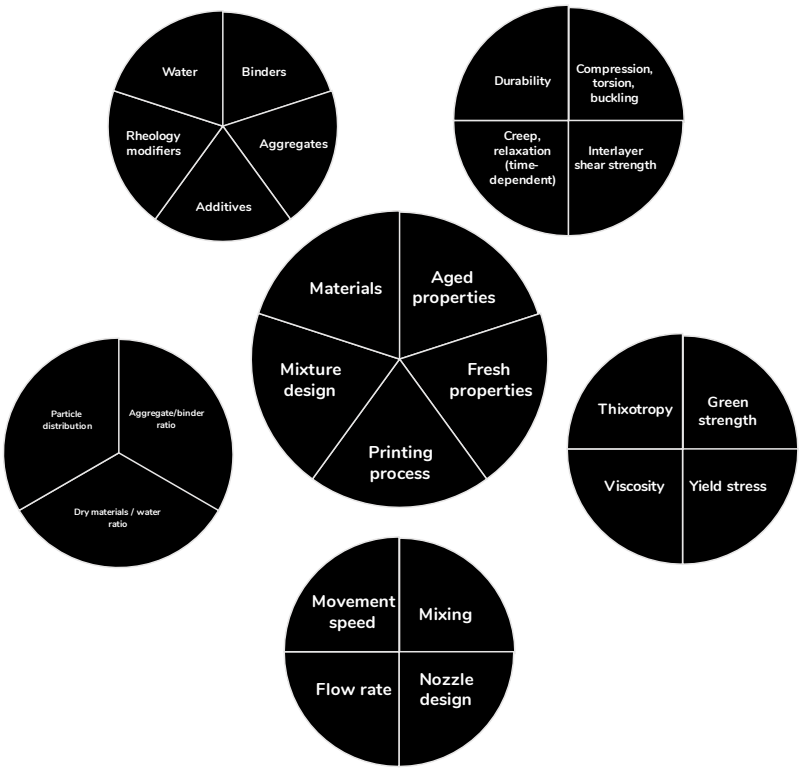

Fig. 3.17 Mixture design parameters

3.4 Precedents

The three research avenues explored in the previous chapters are the main variables that need to be incorporated for a well-informed proposal. These reference studies demonstrate successful integration of the aforementioned variables. The reference studies are divided in two types of construction systems: masonry construction and earth 3d printing presidents

3.4.1 Masonry Construction as a precedent to 3D-printing

Masonry and 3D printing are both additive manufacturing methods. Therefore, even if 3D printing is the latest and least developed construction method, there is a lot of knowledge that can be transferred from masonry systems. In principle, they are both additive and layered structures. Moreover, the layers are horizontal typically and have a specific height. The most important similarity is in the material behavior. Both systems perform well in compression, but not in tension. This limits the possible structural elements to columns, straight walls and form-found shells. This thesis investigates the latter.

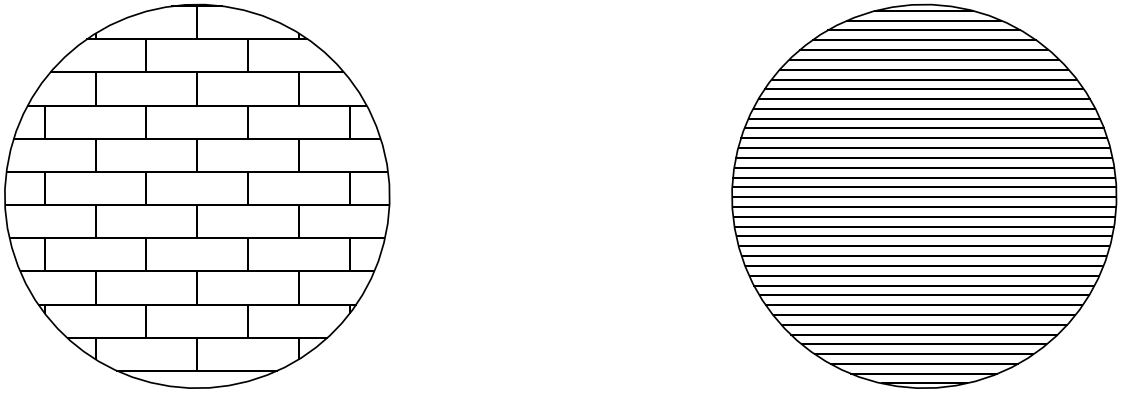

Fig. 3.18. Masonry wall vs. 3D printed wall

Cantilever strategies in Masonry Construction

Normally, shells require a customized and complex scaffold that significantly increases the cost and the material waste of the construction. This has led to the development of techniques that take advantage of the evolving mechanical behavior during construction, instead of thinking only about the final structure (Carneau, 2020). This is extremely relevant to 3D printing where even the mechanical properties of the material change during construction.

Carneau (2020) classifies cantilever structures in a number of ways. According to the element stress state during construction, he notices the following situations, as illustrated in Figure 3.19.

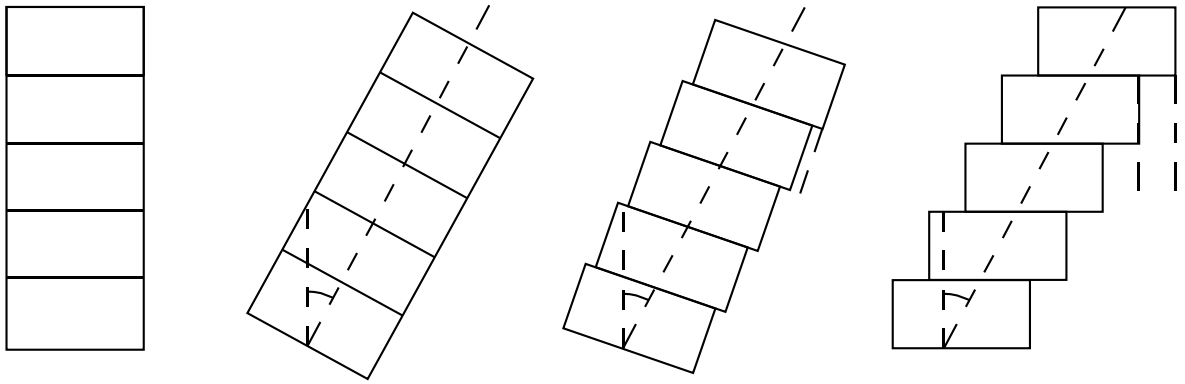

Fig. 3.19. a) Vertical wall, b) shear stress due to inclination, c) bending and shear, d) bending

By analyzing and comparing the different cases he noticed that inclined layers perform better than local cantilevering, as they exhibit bending moments in addition to shear. This means that a cartesian 3d printing process is not sufficient, and a 6-axis robotic 3D printing process is required. Moreover, in curved geometries in order to minimize sliding on the interface, trapezoid cross sections are needed. In this way, the contact area between the bricks is maximized, as well as the material utilization.

A third categorization involves the degree of element continuity, which refers to the different brickwork patterns and is more relevant in masonry than 3D printing.

Nubian Vault

Nubian vaults are barrel vaults constructed by the Nubians in Egypt in the last 3300 years ago. The main principle is the assembly of inclined arches that are layered in front of each other until a vault is formed. The process starts with a gable wall. Then, an inclined bed joint is formed as a base for the bricks. When an arch is completed, the thrust line is formed locking the bricks in compression and becoming the base for future arches. As more and more inclined arches are constructed, the principal stresses are not affected by their weight and the structure behaves as a shell, as shown in *Figure 3.20*. It should be noted that with this construction method, a curved geometry can be formed by bricks with rectangular cross sections. With normal arches, the bricks should have trapezoid cross sections, so that they are normal to the thrust line.

Fig. 3.20. Nubian vault construction (Aga Khan Award for Architecture, 2009)

3.4.2 Reference projects

Delta" system (WASP)

The most relevant precedents in additive manufacturing technologies is the works of WASP company. WASP is a company based in Italy that researches and develops sustainable 3D printed structures by means of natural materials, such as soil and straw. Recently, a collaboration was initiated with Mario Cucinella Architects to develop the TECLA project, to erect a 3D printed global habitat for sustainable living. The design is illustrated in *Figure 3.21*.

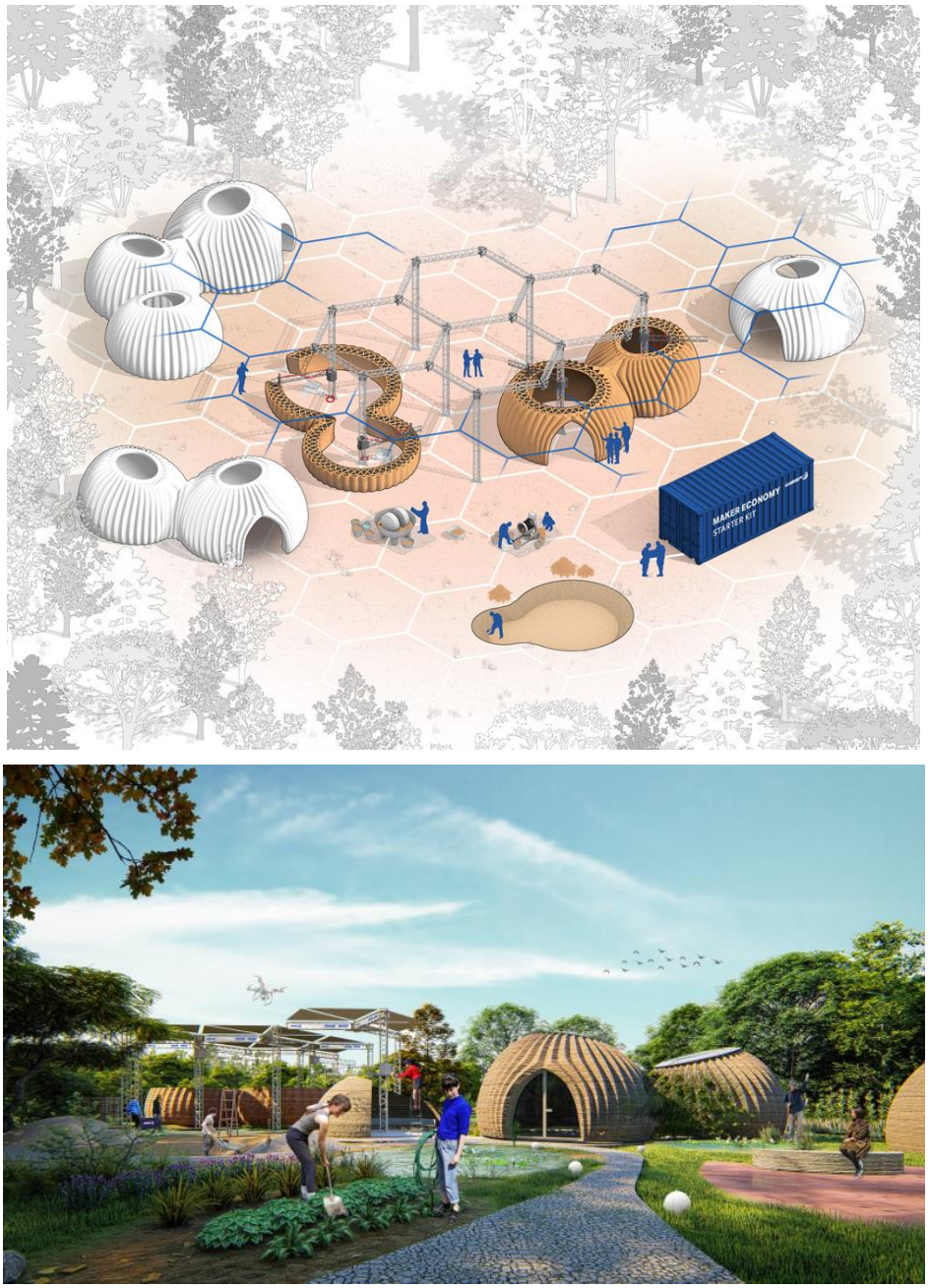

Fig. 3.21 Sustainable Habitats: TECLA by Mario Cucinella + WASP (Mario Cucinella Architects, 2019-to be finished)

4 Research by Design

The research by design task can be summarized in *Table 4.1*:

Table 4.1 Research by design task

Design tasks		Sub-tasks
Physical setup	Extrusion	Controller
		Extruder Design
		Nozzle Design
		Feeding tube
		Extruded material properties

4.1 Physical setup Development

This chapter briefly documents the main decisions and steps taken for the design and assembly of the earth printing setup. A more elaborate description is provided in the thesis of Mandat M. (2020).

4.1.1 Setup Design Considerations

Part of the research consists of the development of the required tools. The printing setup follows the process of similar types used in research and industry and is based on the connection of the following systems:

- a robotic arm [COMAU Nj2.2]
- a material storage vessel and pump
- extruder and print nozzle [custom extruder development, ch.3.2.2]
- mixer and hose pipe
- software control system [FURobot]

4.1.2 Printing Apparatus

The earth printing system was designed and assembled at the Delft University of Technology. The system consists of the following parts, as illustrated in Figure 4.1. The robotic arm, operates in a radius of and height frame. The machine utilizes step-motors in order to achieve high precision of millimeters. The extrusion system is based on a barrel and die principle to ensure a laminar flow, incorporating commercial and 3D printed parts. It is comprised of three main parts. Firstly, it utilizes a PFT hose with a length of 1,5 meters and an inner diameter of 25 millimeters connects the main extruder with the refillable cartridge. The extruder is connected with a series of 3D printed nozzles for different applications. The moving speed can be tuned between 0 mm/s and 120 mm/s, in accordance with the extruder motor speed.

4.1.3 Robot type

For paste extrusion, there are two types of robots that are predominantly utilized; a 3-axis Cartesian robot and a 6-axis robotic arm. The 3-axis Cartesian robots utilize the same principle as desktop 3d printers, such as X, Y and Z-directional translations. A horizontal plane is generally used as printing bed. On the other hand, 6-axis robotic arms are designed with 6 rotating joints, allowing 6 degrees of freedom in terms of rotation, as well as translation. Therefore, inside the boundaries of the robotic arm reach, extrusion is possible at any point and from every direction. This freedom allows more complex and optimized toolpath generation. In this thesis, the latter type is utilized in the form of a COMAU NJ 2.2, that is available at the LAMA lab of the BK-city.

4.1.4 Extruder & Nozzles

For the purposes of this study, a new extruder & nozzles were decided to be manufactured in collaboration with Maximillian Mandat and the assistance of Serdar Aşut, Marcel Bilow and Paul de Ruiter, as the current clay extruder is limited to a 5 mm diameter nozzle. On the contrary, the maximum nozzle diameter allowed by the extruder setup is around 1.8 cm. The extruder diagram and final product are shown in *Figures 4.1 & 4.2* respectively. Each element is briefly described below.

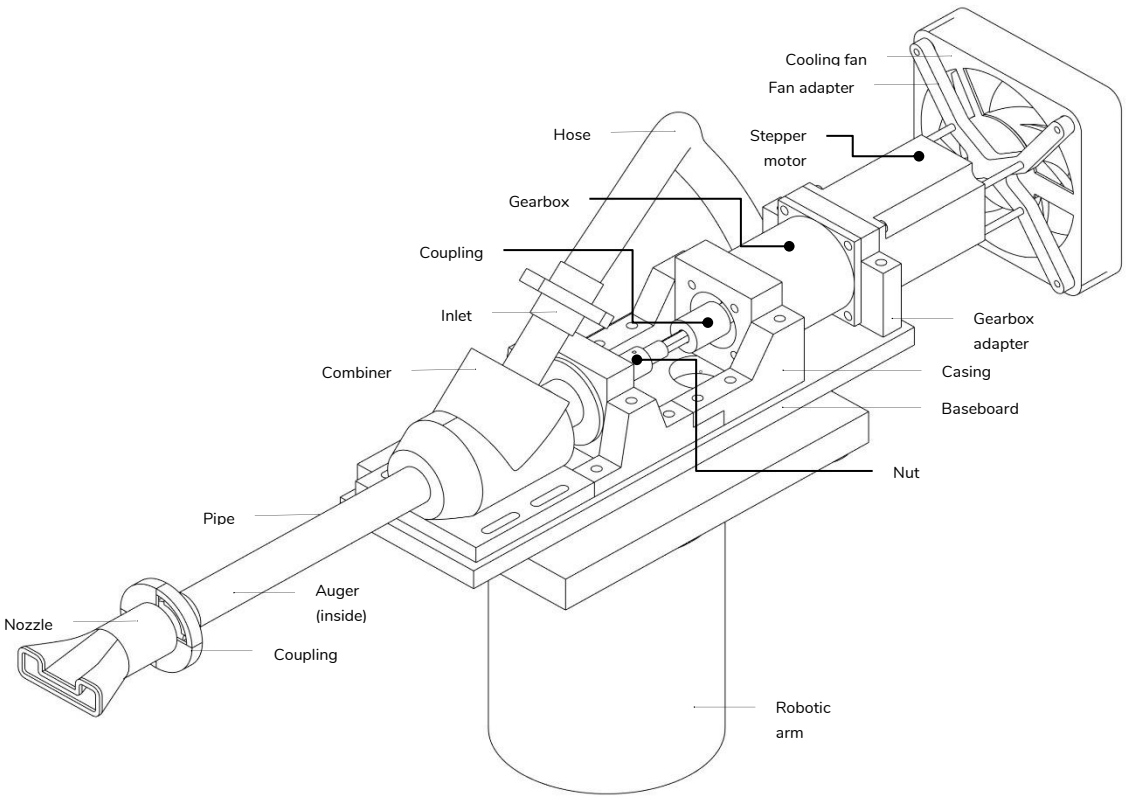

Fig. 4.1 Extruder design

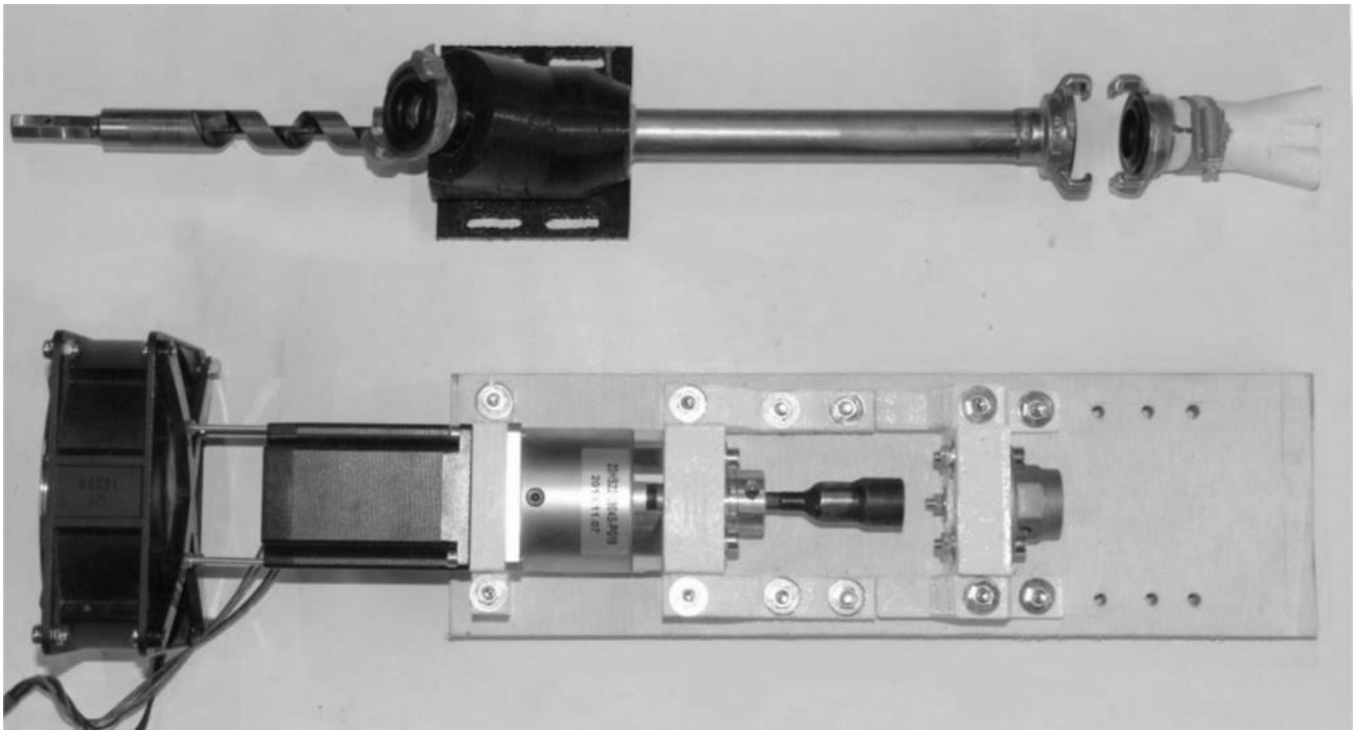

Fig. 4.2 Extruder assembly (photo by Mandat, M. 2020)

Cooling fan & fan adaptor

The addition of a cooling fan was deemed necessary due to the overheating of the motor, ensuring lower temperatures for extended periods of time. A 3D printed adaptor was designed and manufactured with PLA in order to mount the cooling fan to the motor using 4 long bolts. The wires are connected to the 24V power supply.

Stepper motor

A stepper motor was incorporated in the extruder to ensure a more controlled and accurate flow by driving the snail. The motor is driven through an Arduino setup, which is described in chapter 4.1.5. The stepper motor is a NEMA 23 Bipolar with the following specifications:

- Step Angle: 1,8 [deg]
- Holding Torque: 3,0 [Nm]
- Rater Current/phase: 4,2 [A]
- Voltage: 3,78 [V]
- Phase Resistance: 0.9 [ohms]
- Inductance: 3.8 [mH] ± 20%(1KHz)
- Frame Size: 57 x 57 [mm]
- Body Length: 113 [mm]
- Weight: 1.8 [kg]

Even though the stepper motor is relatively strong, the torque was not sufficient, leading to motors stalling and unsuccessful extrusion. Sand particles trapped between the steel pipe interior and the snail flank clogged the system. As the development of a proper snail was beyond the available means, a gearbox was needed to increase the torque strength.

Spacer & Connector

The stepper motor and the gearbox were not directly compatible, as the motor axis was longer than the gearbox socket. To overcome this, a spacer was designed and 3D printed with PLA to facilitate their connection. It is mounted on the stepper motor entries with four screws.

Gearbox

The gearbox decreases the load-to-motor inertia ratio, increasing motor torque and performance. At the same time, while torque is multiplied, speed is reduced by an equal factor. In order to achieve a combination of successful extrusion and printing speed, a gearbox of 1:15 ratio was successfully tested.

Upper/lower casing

The casing functions as the main connector where the motor, snail and hose meet to form the extruder. It is designed to allow visibility between the parts, indicating possible issues, as well as taking demountability into account, as the lower parts should be able to be removed for cleaning and repositioned without disassembling the whole system. As with previous custom-made parts, it is 3D printed with PLA.

Baseboard

The baseboard is the board where casing and the motor are mounted to the robotic arm. It is made from a 19mm plywood sheet in order to dampen vibrations and carry the weight of the extrusion system.

Coupling

The coupling connects the gearbox nail with a diameter of 12mm to the transformation nut with a diameter of 8mm. In our case, a flexible aluminum coupling was chosen to reduce vibrations and misalignment of the auger due to the inaccuracies in the welding of the transformation nut. The two parts are fixed to the coupling by two grub screws.

Transformation nut

A custom-made transformation nut was required in order to connect the snail, having a 14mm diameter hexagonal shank, with the coupling, having an 8mm round diameter. Due to the strength requirements of this part, a 3D printed option was rejected. Instead, a bit socket and a hex bit were welded on a steel ring. In order to fix the snail to the transformation nut, a hole was drilled that runs through both and a holding pin is bolted.

Inlet connector (GEKA coupling)

A GEKA coupling was utilized as the inlet connector that attaches the hose to the combiner part due to their easy of locking and unlocking. Therefore, the paste is successfully pushed through the hose at 4 bar by the compressor into the combiner with no leakage, as the couplings can withstand up to 40 bars pressure.

Combiner

The earth mixture is fed to the snail through the combiner. The combiner is a solid 3D printed part where the steel pipe and the paste inlet are joined by a foaming polyurethane glue ensuring a stiff connection between steel and plastic. Up to that point, the material is transferred by the atmospheric pressure. Once it is fed to the die, the paste is moved by the rotation according to the Archimedes screw principle.

Steel barrel

The extrusion barrel is made from a steel pipe, having an inner diameter of 18mm, same as the die diameter, and a wall thickness of 2mm. A rectangular opening was sawed in the upper side, allowing entry of the earth paste to the barrel.

Auger

The design of the snail extruder is based on the extrusion die geometry. In our case, a commercial steel drill for wood was utilized. By reversing the direction of rotation, the wood drill functions as an Archimedes screw.

Coupling

Another GEKA coupling was used to mount the different nozzles to the steel barrel. One part of the lock is glued to the steel pipe, while the other is fastened to the nozzle. In this way, different nozzles can be easily changed.

Nozzles

Nozzle design should facilitate extrusion through minimization of obstacles and mixture fluidity. In order to increase strength and reduce shrinkage cracking, the nozzle size should allow coarse aggregate integration (Ø > 2-4mm) to the mixture. The nozzle is used to modify the cross section of the earth filament according to the user specifications. A number of different nozzles was 3D printed with PLA. In terms of structural properties, a higher thickness results in fewer layers and weak interfaces, resulting in higher shear strength. Additionally, a larger width increases the buckling resistance. A smaller layer height will improve layer adhesion. Using the maximum size will affect surface resolution and aesthetics. Therefore, the optimal balance of both is required. As buckling failure is more likely during printing and lateral strength is required, a large width is required, which is one of the main reasons for the development of the extruder. Moreover, a saw-like cross section may increase the surface bonding and shear strength. The nozzle evolution is illustrated in *Figure 4.3*.

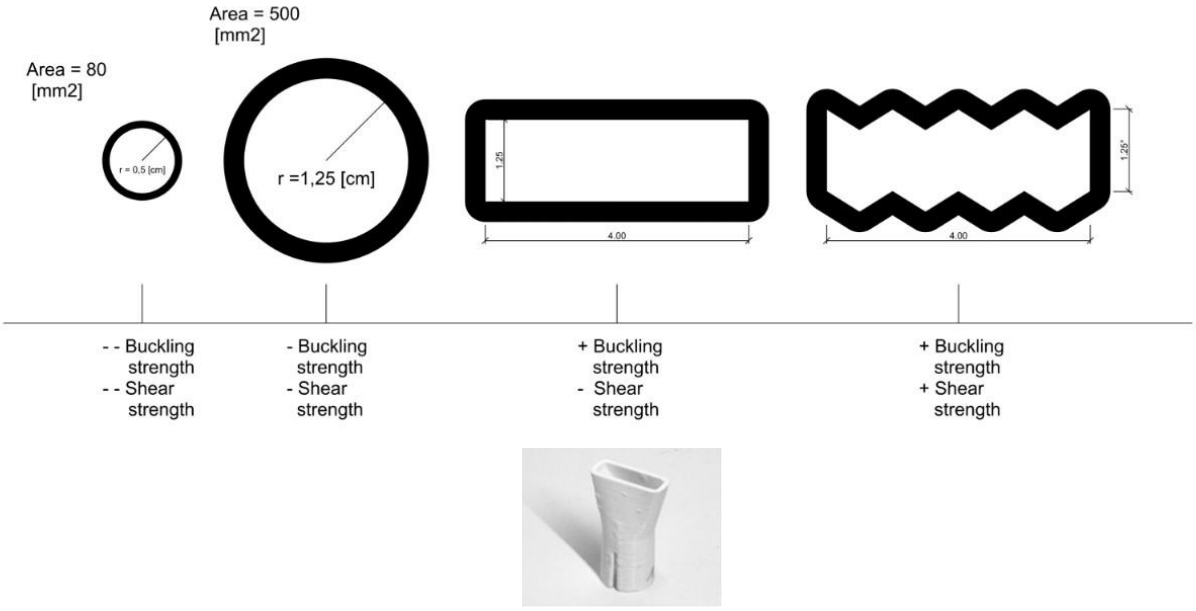

Fig. 4.3 Nozzle design evolution

4.1.5 Motor Control

As previously mentioned, the barrel & die principle of the extruder is made possible through an Arduino controlled stepper motor. In this chapter, the Arduino setup and sketch are developed as they were part of the focus of the author's research.

Arduino & Stepper motor wiring

The wiring of the Arduino to the microstep driver module is illustrated in Figure 4.4. It should be noted that the negative inputs of the modules are driven, and not the positive ones. The positive inputs are all wired to the 5-volt output of Arduino. A potentiometer and a push button switch are also added. The potentiometer controls the stepper motor speed while the push button halts the printing. A 24-volt power supply is utilized. This is important not only for the micro-step driver function, but also for the cooling fan integration.

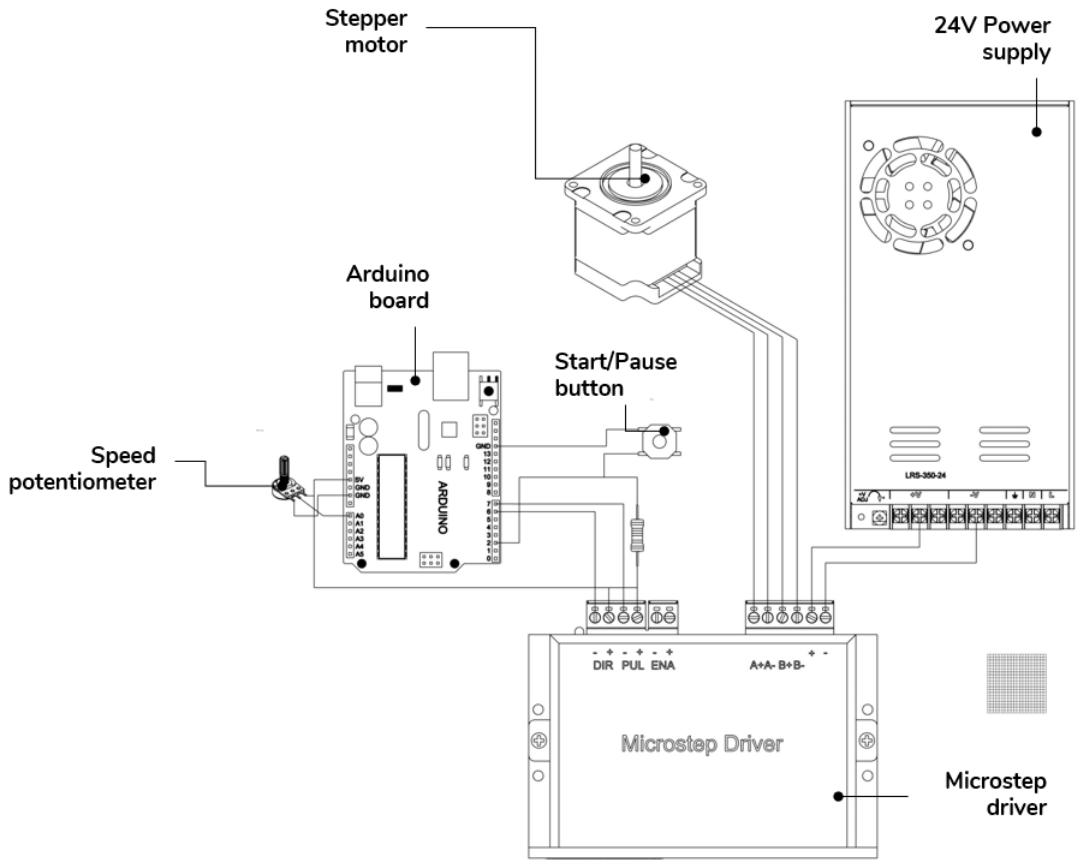

Fig. 4.4 Arduino wiring diagram

Arduino sketch

The Arduino sketch to the microstep driver module is illustrated in *Figure* 4.5. The sketch introduces the stepper library to define and control the wired stepper motor. The Arduino code allows adjusting the rotation speed through the potentiometer, while visualizing the resulting speed on the screen. Moreover, the button is controlled by a toggle script to pause and start the extrusion by halting or continuing the rotation.

```
1. #include <Stepper.h>
2.
3. const int stepsPerRevolution = 19800;  // change this to fit the number of
   steps per revolution for your motor
4.
5. // initialize the stepper library on pins 6 through 7:
6. Stepper myStepper(stepsPerRevolution, 6, 7);
7. int driverDIR = 6;  //DIR- pin
8.
9. int reverseSwitch = 2;  //limit switch as toggle
10.  boolean setdir = LOW;  //toggle start/stop
11.
12.  int stepCount = 0;  // number of steps the motor has taken
13.
14.  //Interrupt Handler
15.
16.  void revmotor (){
17.    setdir = !setdir;
18.  }
19.
20.  void setup() {
21.     attachInterrupt(digitalPinToInterrupt(reverseSwitch), revmotor,
   FALLING);
22.     Serial.begin(9600);
23.     delay(25);  //millisecond delay between pulses
24.  }
25.
26.  void loop() {
27.    // read the sensor value:
28.    int sensorReading = analogRead(A0);
29.
30.    Serial.println(sensorReading);
31.    digitalWrite(driverDIR,setdir);
32.    // map it to a range from 0 to 100:
33.    int motorSpeed = map(sensorReading, 0, 1023, 0, 100);
34.    // set the motor speed:
35.    if (motorSpeed > 0) {
36.      myStepper.setSpeed(motorSpeed);
37.      // step 1/100 of a revolution:
38.      if (setdir==LOW){
39.      myStepper.step(stepsPerRevolution / 100);}
40.      else
41.      {myStepper.step(stepsPerRevolution / 100000);}
42.  }
```

Fig. 4.5 Arduino sketch

4.1.6 Physical setup assembly

The finished setup is shown in *Figure 4.6*.

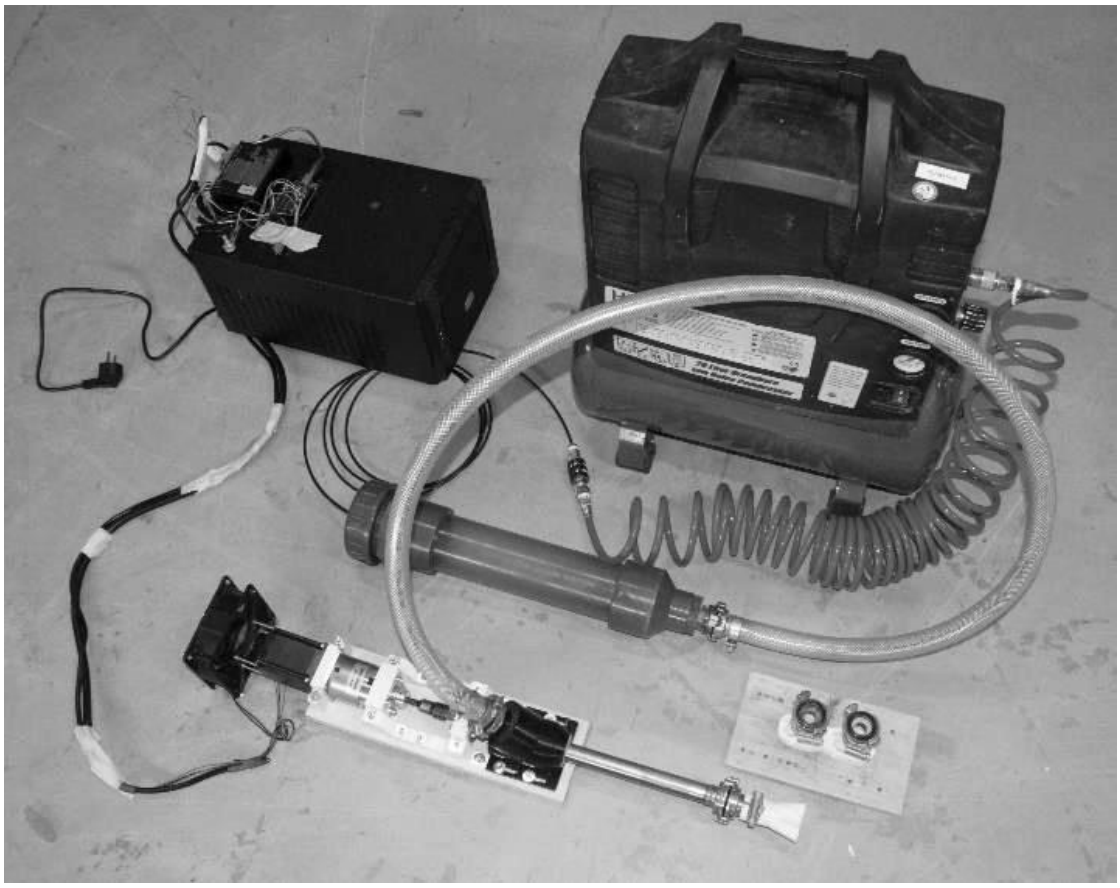

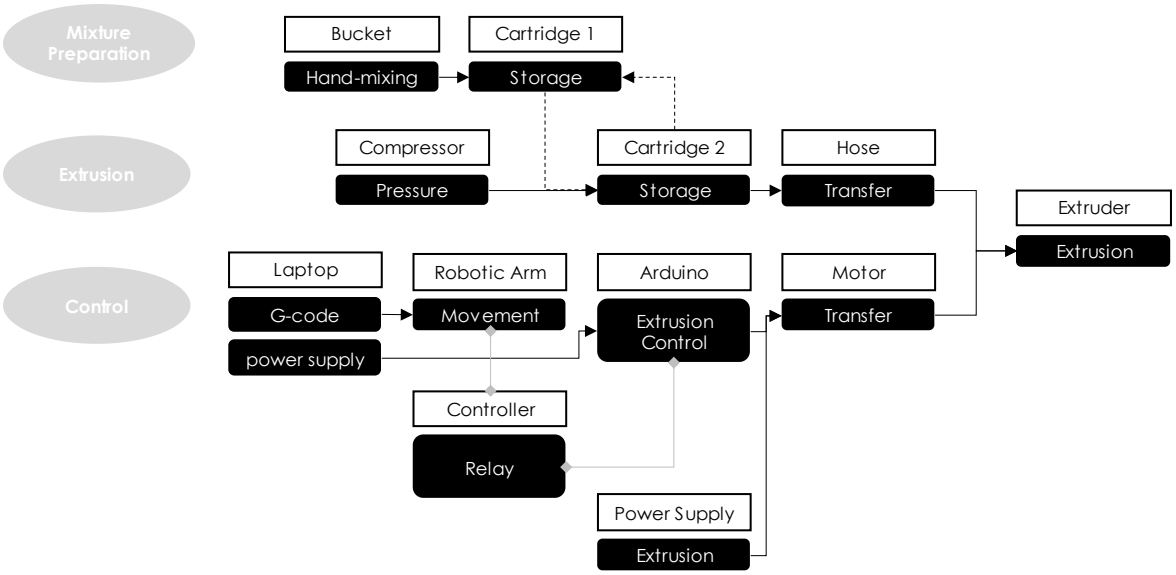

Fig. 4.6 Physical setup assembly (photo by Mandat, M. 2020) & physical setup diagram

4.2 Material Exploration

This chapter covers the development of the earth building material according to the criteria established in the literature review. The following experiments were conducted in collaboration with Maximilian Mandat, as his graduation project falls within the same field. His focus is on optimizing the production technique via tooling and extrusion strategies.

4.2.1 Initial Experiments

Active experimentation is important to determine the limits of the setup and material. This is why a first quick round of experiments was conducted to investigate a broad range of mixtures in a qualitative manner. At the end of this round, mixtures with desirable qualities are investigated further in a round of refined experiments that quantify the specified properties.

Tools

For the initial experiments a mortar extruder was used to simulate the process of the robotic 3d printing for different nozzle dimensions. It should be noted that the mortar extruder utilizes pressure extrusion, while in the final setup, a barrel & die extruder is developed. This will inevitably cause deviations. The mortar extruder is shown in *Figure 4.7*.

Fig. 4.7 Mortar extruder

Method

In principle, locally available materials with low impact that do not hinder the recyclability and circularity of the soil are preferred to ensure a low-cost solution. The ratios and mixtures were decided according to literature and modified to achieve optimal extrudability in terms of aggregate size and water content.

As in typical earthen construction, the dry materials are sifted and mixed prior to the addition of water. However, there are differences between typical earth mixture and a printable paste. In this phase, a compromise between maximum compressive strength -as defined by the plastic limit- and extrudability is made to facilitate optimal deposition. For the stage of experiments, the materials chosen are displayed in Table 4.#. The relevant rheological and compositional parameters are facilitation of extrusion through the nozzle, post-deposition shape retainment, layer adhesion, layer superposition without collapsing, as described by Panda (2018).

The mixtures tested were evaluated in 4 criteria through visual inspection:

- *Extrudability* of the mixture from the extrusion pipe. This is evaluated by the ease of extrusion
- *Particle Distribution* of the material. This is evaluated through microscopic tests
- *Layer adhesion* is evaluated through the microscopic tests, as well as visual inspection by making transverse cuts on multi-layered samples.
- *Buildability* is evaluated by the shape retention of the sample while multiple layers are superimposed.

Figure 4.8 shows some of the samples.

Fig. 4.8 Preliminary test samples

The mix compositions are displayed in *Table 4.2*.

It should be noted that *the quantities are all in volume parts and not percentages*. The highlighted mixtures are the ones chosen to move on to the second phase of experiments.

Table 4.2 Preliminary mixtures

	Mixture	1	2	3	4	5	6	7	8	9	10	11	12	13
Aggregates	Sand	70	50	70	70	70	60	30	70	70	70	70	70	70
	Straw	10	-	-	10	-	-	-	30	30	-	40	30	-
	H_20+ Cellulose	-	-	-	-	-	-	-	-	30	-	-	-	-
Additives	Clay	30	50	30	30	30	40	70	30	-	30	30	30	30
	Rice husk ash	-	-	-	-	-	-	-	-	-	-	-	-	-
	Milled grain	-	-	-	-	-	-	-	-	-	20	-	-	20
	Lime	-	-	-	-	-	-	-	-	-	-	-	-	-
Water		30	25	35	30	25	25	25	30	-	45	35	35	60

Note: all values are in volume parts

4.2.2 Results

In this section the evaluation of the mixtures is presented, while some notable mixtures are briefly discussed.

Mixture #3

Figure 4.9 shows a microscopic view of the sample. In this mixture we can observe a high degree of homogeneity in the particle distribution. The clay particles have sufficiently coated the sand particles signifying a good ratio, even though the mixture is lean. There are minimal cracks, resulting in a good surface finish. However, the water content has caused a wide spread and deformation. Therefore, a high porosity is expected due to water evaporating.

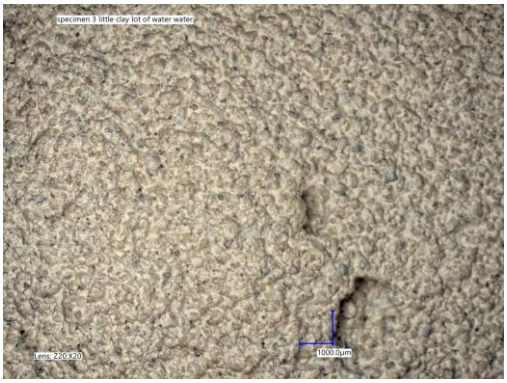

Fig. 4.9 Mixture #3 microscopic view

Mixture #7

Figure 4.10 shows a microscopic view of the sample. This mixture is very rich, as can be noticed by the sparce sand particles inside the clay. Combined with the low water content, the mixture exhibited high consistency and no visible deformation during deposition and layering, as well as low porosity. The seam between the layers is visible which might indicate poor layer adhesion. Higher shrinkage is expected due to the amount of clay which may cause cracks if the drying process is fast.

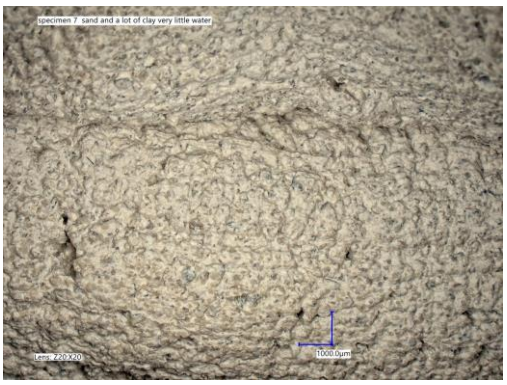

Fig. 4.10 Mixture #7 microscopic view

Mixture #9

Figure 4.11 shows a microscopic view of the sample. This mixture is interesting due to the addition of fibers in the form of cellulose. A microscopic view is illustrated in Image 4.5. The sample exhibited significant cracking during extrusion. This may be due to the fibers not being integrated sufficiently in the mixture. Significant effort was required for extrusion as the fibers built up near the nozzle, which may pose risks when trying this mixture with the motorized extruder.

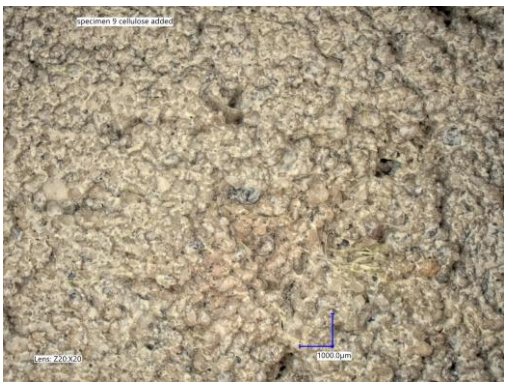

Fig. 4.11 Mixture #9 microscopic view

Discussion

Table 4.3 contains the evaluation of the mixtures. Naturally, all four criteria are essential. In general, increasing the clay content, while reducing the sand improves extrudability and surface finish, as well as shape retention. Aggregate addition eliminated shrinkage and cracking. However, it may compromise extrudability when a barrel & die extruder is used. Moreover, due to the clogging in the nozzle, the fiber content needs to be minimized further or eliminated. Slight changes in moisture content have a significant impact in mixture plasticity. This effect is increased when the sand ratio is higher. On the contrary, richer mixtures are more forgiving.

Mixture		1	2	3	4	5	6	7	8	9	10	11	12	13
Aggregates	Sand	70	50	70	70	70	60	30	70	70	70	70	70	70
	Straw	10	-	-	10	-	-	-	30	30	-	40	30	-
	H_20+ Cellulose	-	-	-	-	-	-	-	-	30	-	-	-	-
Additives	Clay	30	50	30	30	30	40	70	30	-	30	30	30	30
	Rice husk ash	-	-	-	-	-	-	-	-	-	-	-	-	-
	Milled grain	-	-	-	-	-	-	-	-	-	20	-	-	20
	Lime	-	-	-	-	-	-	-	-	-	-	-	-	-
Water		30	25	35	30	25	25	25	30	-	45	35	35	60

Note: all values are in volume parts

Evaluation Criteria						
	Extrudability E	1	E: ••	PD: •••	LA: •••	B: ••••
		2	E: ••••	PD: •••••	LA: •••••	B: •••••
		3	E: ••••	PD: •••	LA: •••	B: •••
	Particle Distribution PD	4	E: ••	PD: •••	LA: •••	B: •••••
		5	E: ••••	PD: •••	LA: •••	B: •••••
		6	E: ••••	PD: ••••	LA: ••••	B: •••••
	Layer Adhesion LA	7	E: ••••	PD: •••••	LA: •••	B: •••••
		8	E: •	PD: •••	LA: •••	B: ••••
		9	E: •	PD: ••	LA: ••	B: •••
	Buildability B	10	E: •••••	PD: •••	LA: •••	B: ••
		11	E: -	PD: •	LA: •••	B: •••••
		12	E: ••	PD: ••	LA: •••	B: •••
		13	E: •••••	PD: •••	LA: •••	B: •

Table 4.3 Mixture evaluation

4.2.3 Refined Experiments

In additive manufacturing using earth, contradicting rheological properties are required. More specifically, for extrusion and pumping the mixture should be highly fluid, whereas it should be stable and viscous during rest in order to ensure buildable layers. These material behaviors arise due to the interaction between the networks of particles. The tests described in this section aim to investigate these properties and their relation with time for three mixture candidates. The mixtures investigated in this phase are named by their contents with the order Sand-Clay-Water.

Tools & method

The ambition for these experiments was to conduct them with the physical setup. However, due to the pandemic and faculty closing, another way needed to be found. Thus, it was decided to modify the manual mortar extruder, in order to be able to receive different nozzles, as shown in *Figure 4.12*. The mixtures are:

a) 50-50-30

b) 50-50-40

c) 65-35-30

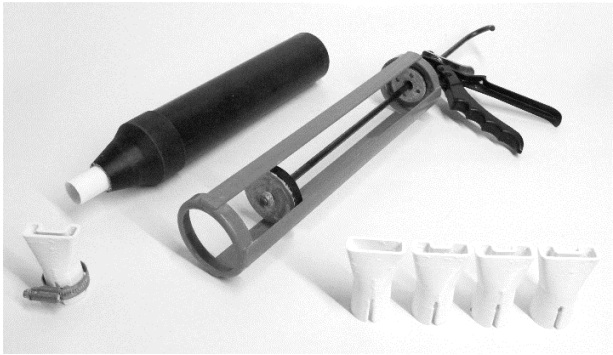

Fig. 4.12 photo & nozzles by Maximillian Mandat

Table 4.4 Time specification of fresh property tests.

Type	Material age	Test duration (per time)
Flowability test	10 min to 120 min (20 min of the time interval)	2–3 min
Extrudability test	30 min	10 min
Open time test	30 min to the terminated time (10 min of the time interval)	0.5–1 min
Buildability test	30 min	5 min
Green strength test	30, 45, 60, 90, 150, 240 min	2 min

Flowability test

Flowability is directly related to what is referred in practice as workability. Yield stress is the main parameter that evaluates this property. First parameter of investigation is the amount of water and time, until the mixture loses thixotropic behavior. This occurs during rest time and causes an increase in the yield stress, which can be reversed by remixing (Roussel, 2011). Second parameter is the clay to sand ratio. As sand is more abundant than clay, this test will determine the influence of the binder ratio in flowability.

The tests will be conducted according to ASTM C1437-15 (Standard Test Method of Hydraulic Cement Mortar, 2015). A cone mold required for the test will be 3D printed. Its dimensions are illustrated in *Figure* 5.5. Normally, mold oil should be used to lubricate the interior surface of the cone before testing. For simplicity water will be used. Firstly, fresh mixture will be poured in half of the mold and disturbed with a wooden stick for 15-20 times. This procedure is repeated for the rest of the mixture, until the mold is full. Secondly, the mold is released and the spread diameter of the specimens are documented. This test will be performed for material ages from 10 to 180 minutes, with 10-minute intervals. Each test will be performed three times. A photo of the samples is shown in *Figure* 4.13.

Fig, 4.13 Flowability test cone samples

Extrudability test

The extrudability test explores the extent of a consistent and continuous extrusion from the prototype setup. The nozzle moving speed should be constant as it affects the consistency of the printed filament (Nerella et al., 2019). Therefore, the speed of extrusion should be synchronized with the speed of the robotic movement to ensure continuous flow for a more accurate test. Aim of this test is to assess the link between extrusion pressure through the compressor and the flow rate of the mixture. By adjusting the air pressure, as well as the snail rotation speed through the controller, different flow rates (Q) are investigated. As the test will be performed with the manual extruder, one flow rate will be investigated and deviations will occur. For this test, the material age at the time of the test is 15 minutes, while the extrusion speed is equal to the material flow rate (Q) achieved by the extruder. This is calculated by the equation:

$$Vlin = \frac{\mathrm{Q}}{\mathrm{A}} \qquad (4.1)$$

where:

Q: material flow rate [L/sec]
A: interior nozzle area [mm^2]

Open time test

Open time is the timeframe while printing remains continuous. This property conveys important information about the print quality, as well as insight about the effect of age in interlayer bonding. The testing follows the process described by earlier studies (Ma et al., 2017). For a specified quantity of mixture, a single strand of paste, with a length of 800 mm and a width of 20-25 mm is printed at a series of material ages with time intervals of 20 minutes. All tests started with a rest time of 20 minutes. A ruler is utilized to assess the shape retention ratio (S_1) of the filament. Examples of samples are shown in *Figure 4.14*. Panda et al. (2019) and Bong et al. (2019) defined this property as:

$$S1 = \frac{\mathrm{Wf}}{\mathrm{Wn}} \qquad (4.2)$$

where:

W_f: extruded filament width [mm]
W_n: interior nozzle width [mm]

Fig. 4.14 Open time specimens

Buildability test

Buildability is the ability of a fresh extrusion to retain its form under its self-weight and the loading of the subsequent layers (Cheng et al., 2020). The evaluation follows the settlement tests of Kazemian (2017). According to it, after the mixture has rested for 20 minutes, five straight layers with a cross section of 40 x 10 and a 200 mm length are superimposed before the open time limit. A Vernier caliper is used to measure the shape ratio (S_2) that is defined as:

$$S2 = \frac{H}{h} \tag{4.3}$$

where:

H: measured height of deposited layers [mm]
h: designed height of layers [mm]

Green strength test

A green strength test should be conducted to investigate the material strength as it evolves in the first 4 hours of the mixture. Since the strength test was not possible due to the university closing, the test procedure is described for the time that they are possible. A pocket penetrometer may also be used for convenience and on-site evaluation. The samples should be manufactured from printed objects that are sawn to 50x50x50 mm cubes. The specimens are sealed in plastic bags to retain moisture until testing. The testing equipment is an Instron universal testing machine (8872), with a load cell of 10 kN. A plastic film covers both surfaces to minimize friction between them and the base plates. A rate of 0.2 mm/s displacement is applied until maximum displacement of 20 mm is achieved. The free software ImageJ can be used to analyze the lateral and vertical deformations. The material ages of the mixture are shown in *Table 3*. 3 Samples are prepared for every age and nozzle type, as displayed in *Figure 4.15*.

Fig. 4.15 Compressive strength specimens

Compressive strength lab test

Due to absence of building standards for earth additive manufacturing, the experimental procedure was determined based on related literature. In order to assess the mechanical characteristics, a series of monotonic compressive strength tests will be performed in accordance with NEN-EN 196-1 (2016) with a loading rate of 2.4 kN/s. A uniaxial testing machine will be utilized for the tests. For the mixture preparation, the same samples as in green strength are printed, but measured 7 days after being left to dry in a controlled environment (20±2 °C and plastic covering). This decision was made to prevent cracking failure due to shock drying. As illustrated in Figure 4, 5 specimens are tested for each of the X, Y and Z directions due to the orthotropic behavior of the material (Panda, 2017). The compressive strength was calculated by determining the average value for each direction. Additionally, a loading-unloading test should be conducted to research the post-yield and elastic mechanical behavior of 3D printed earth. For this test, the same samples will be loaded at a constant rate, while unloading cycles are applied when the load equals 10, 50, 100, 150 and 200 kN successively.

4.2.4 Results

In this section, the results of the aforementioned tests are presented.

Flowability test

The results of the flowability tests for different material ages are recorded in *Figure* 5.5. The mixtures that contain higher amounts of water achieve a spread diameter of 97 mm up to 40 minutes. Compared to the ones with higher clay content, mix 65-35-30 demonstrates a delay of 50 minutes. It can be observed that after the first 40 minutes of rest, there is an increase of the flowability rate of decrease. In general, flowability is reduced with time for all samples. This is caused by the gradual moisture decrease due to drying, resulting in development of stiffness. Mixture 4 displayed considerable shape retention. Mixture 65-35-30 exhibited higher spread diameter than mixtures 50-50-30 and 50-50-40. As yield stress is determined by the structure and distribution of clay, mixtures with less amount of clay exhibit higher flowability. This is likely due to the clay forming a network around the sand particles, which is responsible for the thixotropic behavior of the paste (Roussel, 2011).

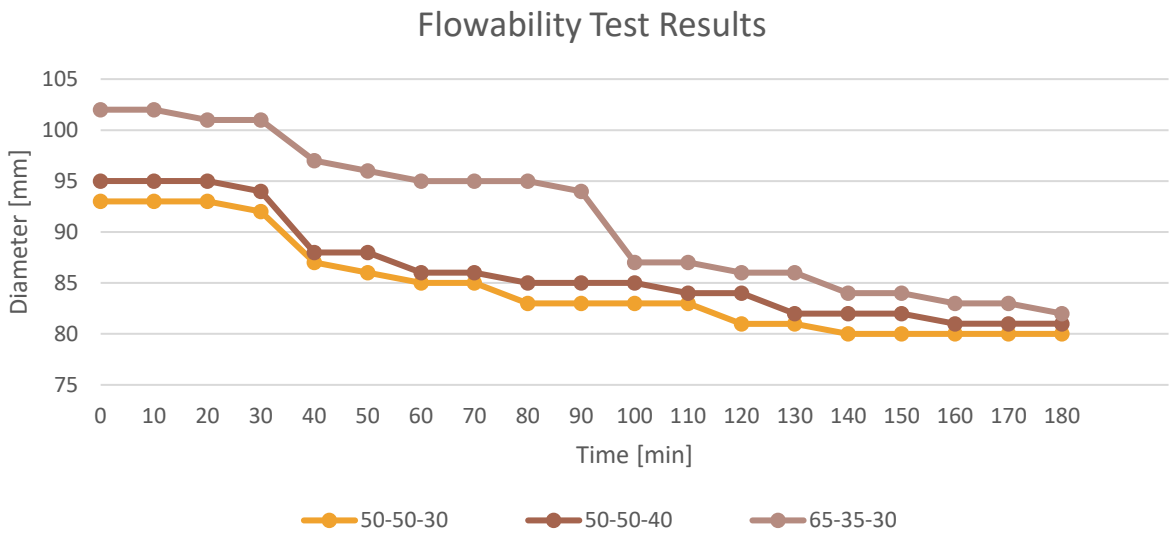

Fig. 4.16 Flowability test results

Extrudability test

During extrusion, the material is subjected to shear stress, leading to the emergence of the characteristic thixotropy of soil suspensions (Mitchel, 1961). All geological sediments, apart from coarse sand and gravel demonstrate partial thixotropic behavior (Boswell, 1949). The effect is dependent on mineralogical composition, grading and size, as well as the presence of electrolytes. Earth exhibits thixotropic weakening when agitated and strengthening during rest under constant water content. Moreover, the higher the moisture ratio, the more apparent the thixotropic behavior becomes (Zhang, 2017). This property suits additive manufacturing, as the paste can be extruded easily, but retain its shape and the weight of subsequent layers (Alghamdi et al., 2019). Higher extrusion pressure leads to an increase in material flow rate and shear rate for all mixtures. The higher the shear rate, the less viscous the mixture becomes. Mixtures with more water and less sand experience greater shear thinning and require lower pressure to achieve the same material flow. To ensure consistent extrusion, a constant flow-rate is required. The extrusion speed determined is 2 cm/sec

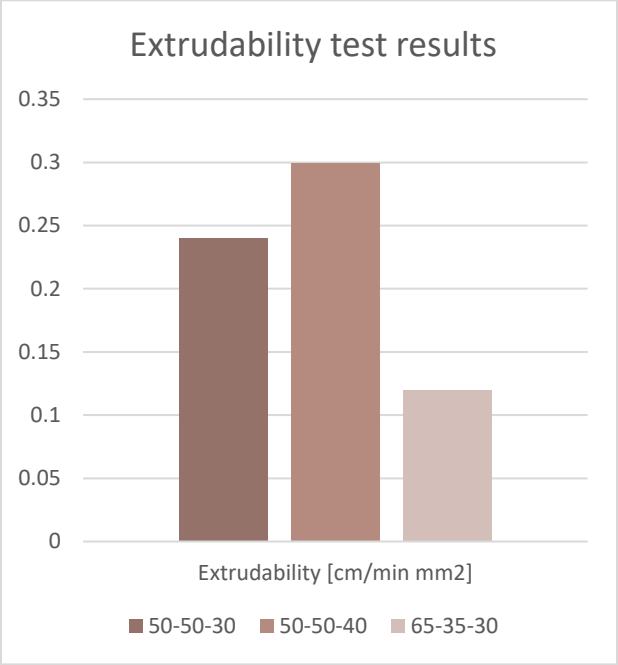

Fig. 4.17 Extrudability test results

Open time test

Open time test results are shown in Figure 4.18. The material flow selected for the test was 3,14 cm^3/sec, while the extrusion movement speed was 1 cm/sec. The degree of precision was evaluated through shape retention. As can be observed in *Figure* 4.18, Mix 50-50-30 displayed an open time of 40 minutes, while Mix 50-50-40 and 65-35-30 exhibited open times of 30 and 20 min respectively. Similar to Chen's (2020) results, it can be observed that shape retention ratios decreased during printing. Initially, S1 figures higher than 1 were detected, as the filament width was larger than the nozzle's inner width. Then, values equal to 1 were measured. In the later stage of extrusion, values lower to 1 were documented. This was the result of changes in rheology and particle flocculation around the inner surface of the nozzle over time. The flow rate decreased even further, resulting in eventual rupture.

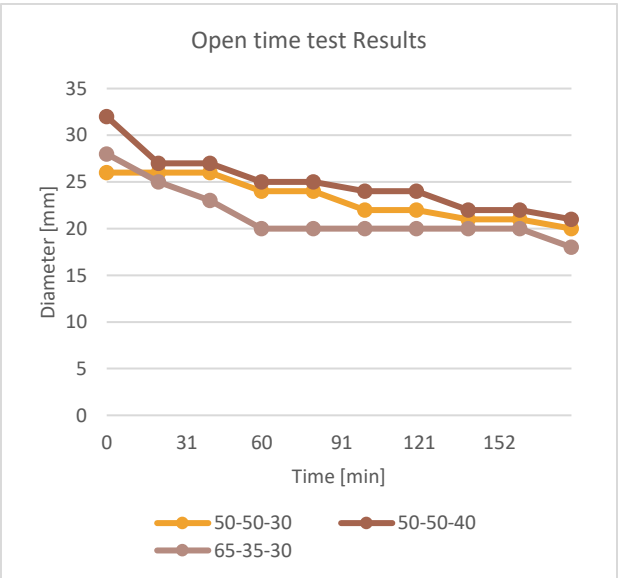

Fig. 4.18 Open time test results

\Buildability

the buildability results of Mixtures 50-50-30, 50-50-40 & 65-35-30 are exhibited in *Figure* 4.19. They were compared by building identical five-layer straight extrusions. The time gap between layers was 20 minutes and the test was initiated after a rest time of 20 minutes. As the results suggest, the buildability is influenced significantly by the moisture content. Mixture 50-50-30 performed the best, with an S2 factor of 0.88. However, all tests achieved a buildability index of at least 0.7.

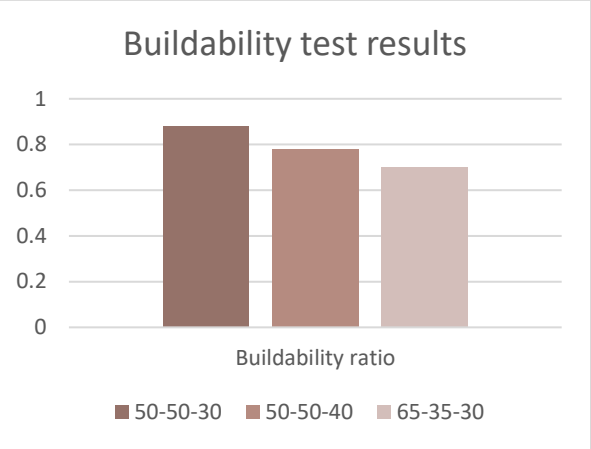

Fig. 4.19 Buildability test results

4.2.5 Mix design discussion

Effect of binder to aggregate ratio and moisture content

The binder to aggregate ratio has a major effect in the processing and mechanical behavior of the material. Compressive tests to investigate the effect of binder to aggregate ratio in the mechanical strength of the material were not possible before the completion of this thesis. However, some observations can be made as the strengths of the individual mixture components has been well documented in the past. The most important condition is that there is an adequate amount of clay binder to coat the sand granules.

Fresh to dry strength

The lack of formwork, which provided stability of fresh mixtures is a major challenge of 3D printed constructions, as the materials' fresh properties need to be engineered to allow layered-based extrusion. For this reason, high-thixotropy and low slump should be developed (Chen, 2020). Exploring the fresh state behavior of printable earth during mixture design should aim for balance between flowability and green strength (Ma, 2017). The mixture design explores the relation between the volume and composition of the binder, the aggregate's particle content, shape and gradation, as well as the water ratio.

Additionally, the presence of admixtures, such as viscosity-modifying admixtures (VMA), accelerators and superplasticizers, could contribute in adjusting the rheological behavior of the mixture (Chen, 2020). These materials have been successfully utilized in manufacturing concrete with specific properties. For example, superplasticizers enhance flowability, without reducing solid ratio. VMAs increase plastic viscosity and cohesion, contributing in extrudability.

At the same time, the dry paste criteria relate to the mechanical properties, as altered by the layering process. The orthotropic behavior exhibited is the outcome of two types of compaction, which results in variations in compressive strength:

- Compaction during extrusion
- Compaction due to the weight of new layers

5 Design by Research

In the traditional process of construction, a design is evaluated on sectors, such as function, structural engineering, material science, et cetera. However, in contemporary practice, a building is progressively viewed as an optimization assignment, where environment, user and legislation are holistically considered. The typical process of design consists of the definition of the shape by the architect, and then it is followed by the structural analysis, dimensioning and construction in collaboration with the engineer. As form is the most significant factor of structural efficiency, this serial process has a major effect in material use (Allen and Zalewski, 2010). This is even more important in free-form architecture, where structural conventions are not sufficient and a more sophisticated method is needed.

Design & prototype a structural clay element using entirely reusable, recyclable materials taken from the local terrain by using the developed workflow as a proof of concept.

5.1 Design Task

The design assignment criteria for the final design and prototype are outlined in *Table 5.1*.

Table 5.1 Design task

Shell design structural optimization	Shape optimization
	Cross section optimization
	Infill optimization
	Support optimization
	Infill as structural core

5.1.1 Digital workflow tools

This chapter introduces the used software and tools for the definition of the digital workflow.

The following software are utilized in this dissertation for the development of the digital workflow. They cover the steps from design to performance evaluation with FEM to robotic simulation and toolpath development.

- **Rhinoceros 6.0:** Robert McNeel & Associates developed Rhinoceros3D, or Rhino as a 3D modeling and computer aided design (CAD). Rhino allows the generation of complex geometries and offers the environment for the scripting editor Grasshopper.
- **Grasshopper:** Grasshopper (also developed by Robert McNeel & Associates) is a plug-in of Rhino for parametric geometry generation. It utilizes visual programming in the form of "component" functions that are wired in sequence, providing a more intuitive algorithmic environment than traditional scripting. The parametric function is enabled by "slider" inputs that can be controlled, affecting the resulting geometry in real-time. The main Grasshopper components are propagation-based and do not include loop functions. This is a restriction for the optimization process that requires iterations. In this case, additional plug-ins and scripting need to be utilized. The Python language was used to facilitate this step, as well as the Large

Deformation component of Karamba3D, which utilizes loops in its script and the Galapagos evolutionary solver.

- **Karamba3D (FEA):** Structural analysis in the form of a finite element method can be integrated in the grasshopper through a number of plug-ins, eliminating the need for manual export of geometry to different software. One of the most widely used is Karamba3D that in the rime of writing this thesis performs linear structural analysis. Developed by Clemens Preisinger, it utilizes the same principle of Grasshopper components, the geometry is translated into a structural model, where material properties, loading cases, boundary conditions are assigned becoming part of the parametric workflow. More specifically for shells, the surface geometry is tessellated into a finite element mesh, the resolution and accuracy of which is determined by the user. It should be noted that the shell elements are triangular with six degrees of freedom per node and in-plane rotational stiffness is not included. Karamba3D adopts the Kirchhoff theory that does not take into account transverse shear deformation for thin plates, and is valid only for a thickness/length relation of: t/L <= 1/10. However, it is deemed adequate for initial form-finding.
- **Galapagos:** The structural optimization of the shape if not specified, can be performed with the assistance of the Galapagos solver, developed by David Rutten. It manifests as a unique Grasshopper component that utilizes an evolutionary genetic algorithm that performs an iterative heuristic research in the form of generations of hundreds of variations for a single objective. More specifically, the solver takes inputs, referred to as gene-pool, from a number of slider variables. Then, the solver adjusts the slider values, generating and evaluating unique genomes in order to minimize or maximize a certain value, called fitness function. In the first generation, random values are assigned and evaluated. The ones with the worst performance are culled and new genomes close to those values are avoided. Therefore, in every subsequent generation the highest performing genomes are utilized, until an acceptable genome is found. The risks entailed with such solvers is that they may be directed to “local” optimums instead of a “global” optimum. In order to eliminate this issue, random genomes are included in every generation to broaden the scope of the research. Moreover, they are significantly slower than other optimization algorithms that utilize machine learning as every genome needs to be fully computed. On the other hand, they allow real-time inspection of the results and the state of the optimization. Finally, they are widely applicable and are able to function even with poor formulation.
- **FUROBOT:** FUROBOT is a free robotic arm programming plug-in by Fab-Union. Its functions include simulation and toolpath generation in the form of G-Code. It is enhanced by the provision of external axes, as well as collision and movement checks. Being integrated in Grasshopper, it facilitates seamless integration in the digital workflow, linking design and fabrication. Although it primarily includes KUKA, ABB & UR robots in its library, it allows custom definition of robotic arms, as well as end effectors. Furthermore, it provides specific components for processes related to typical robotic fabrication methods, such as CnC-milling and 3D printing.
- **HUMAN UI:** HUMAN UI is a Grasshopper3D plug-in developed by Andrew Heumann that allows the creation of apps and user interfaces without the need to code. Its main elements are divided in UI Containers, that are related to the interface design, the UI Elements that provide tools to replicate grasshopper components, such as sliders and B-rep geometries in the interface, and UI Graphs for data visualization.
- **GhPython:** GhPython is a Grasshoper3D component that brings the Python interpreter to define custom scripts utilizing the rhinoscriptsyntax. Its main function is the ability to link Rhino with other software, as well as perform loops functions, which are not available in Grasshopper, which is propagation-based. In this thesis, GhPython is utilized for the infill and toolpath design, as well as the evaluation of the definition of workflow for evaluating the aging material properties.

5.1.2 Function

There are many reasons for constructing an earthen shell structure through additive manufacturing. Possible functions are temporary or permanent constructions, such as:

- Temporary shelter/ housing
- Recyclable pavilions
- Roofing structures
- Shell floors
- Bridge designs
- Warehouses
- Pop-up stores
- Exhibition spaces

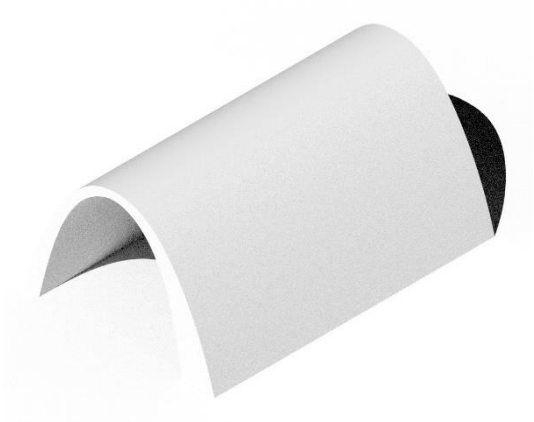

The temporary shelter is chosen as a case study for further development. The concept for the shelter is that it should have a simple rectangular floorplan that offers a temporary housing solution for asylum seekers. The funicular vault was chosen as a typology. It can be used both as roofing structure and functioning building, since it has openings and can be increased in length according to the needs, in contrast to a doubly curved structure. The focus is on the structural stability and efficiency. Therefore, facets, such as architectural appearance, ornamentation, thermal performance or integration of installations is not considered in this study.

5.1.3 Standards

In Civil Engineering practice, Standards have been developed to systematize the execution of structural design. Eurocode is the generally adopted standard for structures regarding material properties and load-cases in Greece.

Snow Load

Snow calculations are done according to EN 1991-1-3 (). The characteristic value for Greece is:

$$s_k = 0.80 \text{ kN/m}^2$$

The snow distribution in a vault is determined by its shape. The Eurocode prescribes no snow accumulation when the roof curve is $\beta > 60°$. For simplification purposes, the load is assumed to be uniform across the entire arch.

Wind Load

Wind load is dependent on shape, size and location of a structure. However, standardized values are assumed based climate and topography. EN 1991-1-4 is the Eurocode for specifying wind calculations. The wind direction chosen for the analysis is assumed to be perpendicular to the eaves and is equal to:

$$q_b = 0{,}46 \text{ kN/m}^2$$

Normally, internal and external pressures should be taken into account. For this thesis, only the external ones are considered. Moreover, there are formulas to calculate the resulting wind pressure based on roof shape as a factor of peak velocity. For simplification purposes, peak velocity is used as the wind pressure.

Construction

There are no standards for 3D printing construction with earth. Moreover, there are no regulations in Greece about load-bearing clay structures. However, regions with similar seismic risks, such as New Zealand have defined building codes and can provide guidelines for the safe constructions.

NZS 4297: 1998 Engineering design of earth buildings

It is applied in adobe and rammed earth structures. It describes the material tests to acquire the mechanical properties as well as the limit values for failure. Generally, it prescribes maximum height of 6,5 m and 600 m2 surface for 1 story (200 m2 for 2 stories).

NZS 4298: 1998 Materials and workmanship for earth buildings

This standard outlines the acceptable material and processing methods for unbaked brick making. Moreover, it includes some notes on cob construction.

NZS 4299: 1998 Earth buildings not requiring specific design

Lastly, this code describes the geometrical properties of constructions that do not fall under standard 4297. Moreover, it provides standard construction details for specific elements, such as foundation, or door-to-floor details.

5.2 Context

Earth is a versatile building material. Due to the variability in soils and water contents, a diverse series of construction methods and techniques have occurred globally. Therefore, it is possible to build both in cold wet climates, as well as hot dry ones. The context chosen for the purposes of the research is Greece due to its abundance of clay and dry climate.

5.2.1 Climate

The structure is located in Greece, where the climate is Mediterranean BSk, according to the Köppen classification (Rubel, 2010). More specifically, it features hot and dry summer seasons, but cold and wet winters. The precipitation is generally low and irregular, averaging annually at around 59.5 cm. The average temperature is 12.2 °C.

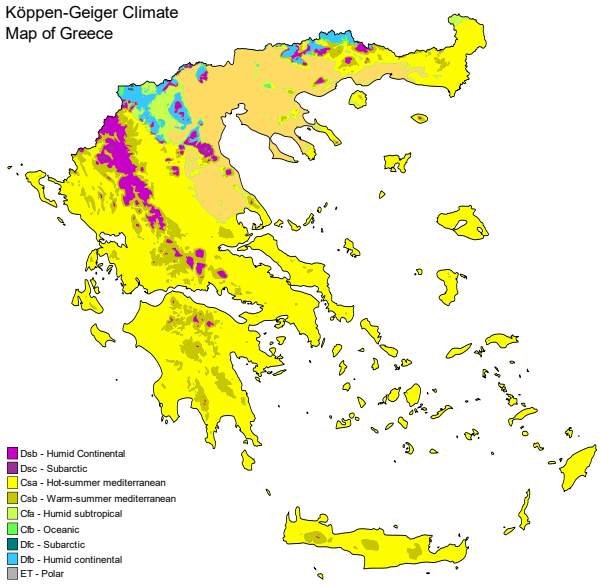

Fig. 5.1 Climate classification of Greece (Beck et al., 2018)

5.3 Digital Workflow Development

Additive manufacturing adopts the Computer-Aided-Manufacturing (CAM) and Computer-Aided-Design (CAD) method which streamlines the construction workflow reducing unnecessary steps and increasing efficiency. The standard process begins with a digital design that is translated into coordinates in space. CAD software is employed to create the design. Then, a slicing process is followed, usually in a different software, which prepares the object for printing. During this procedure, the design is sliced in subsequent layers, which become the coordinates to be traced by the 3D printer. The computed tracing is realized mechanically by employing different mechanisms, such as construction cranes, gantries or robotic arms. At the end of the printer assembly the material extruder end effector is connected with different nozzles that control the geometrical features of the extrusion.

The relationships between material properties and stresses, as described above, require careful consideration in the design phase – even more so for a load-bearing structure. Form and forces are interlinked and can result in reduced stresses when designed properly. Computational design and analysis offer a holistic approach to design that integrates form and forces in order to predict the structural behavior and optimize the performance.

5.3.1 Parametric Model

For the purposes of this research, a funicular shell will be the structural form studied. As previously stated, shells are forms that produce low tensile and bending forces. This allows the utilization of weaker materials, such as earth, compressed waste or stone for load-bearing purposes, as they are strong enough in compression (Rippmann,2016). Moreover, they require less material and can employ the full extent of the potentials of additive manufacturing.

In this chapter, the model setup will be outlined according to the Karamba3D workflow illustrated in *Figure* 5.2. Firstly, the geometrical input, such as point coordinates and curves, must be provided for the construction of the geometry.

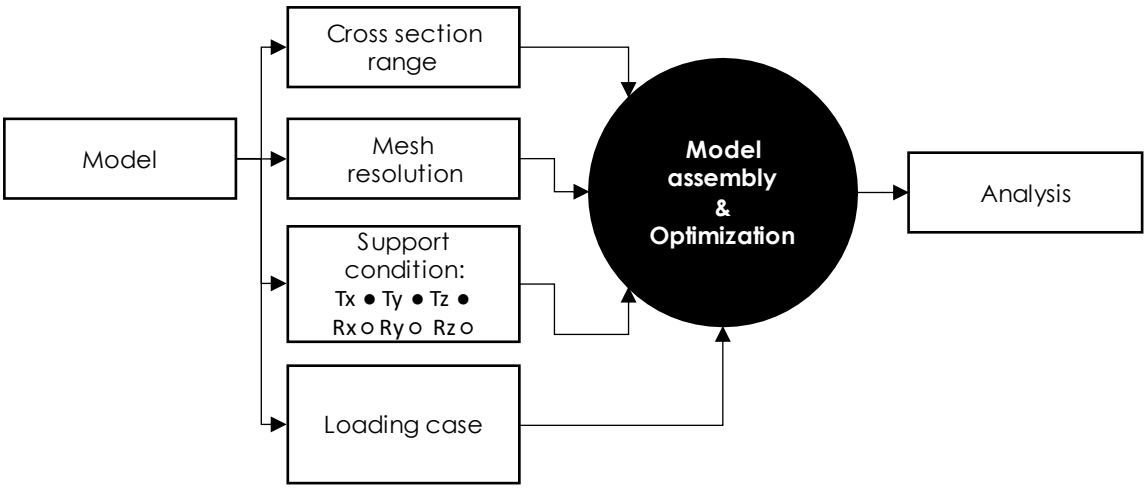

Fig. 5.2 Parametric model diagram

Input of geometry

In order to produce a fully parametric model the geometry is defined directly in Grasshopper. In this way Rhino3D is utilized only for visual representation. The funicular vault is defined by a slider that adjusts the span through main line width, one for the rise, and one for the length. In this way they can be changed independently. A line is produced as a NURBs curve geometry for the definition of the structure width. NURBS curves are used to represent

3D geometries in a mathematical way. In general, they are described by control points, evaluation rule, degree and knots. Further explanation on this type of geometry can be found in the Rhinoceros 3D site.

Figures 5.3.a) & 5.3.b) illustrate the script of the line creation and conversion into a Karamba3D element.

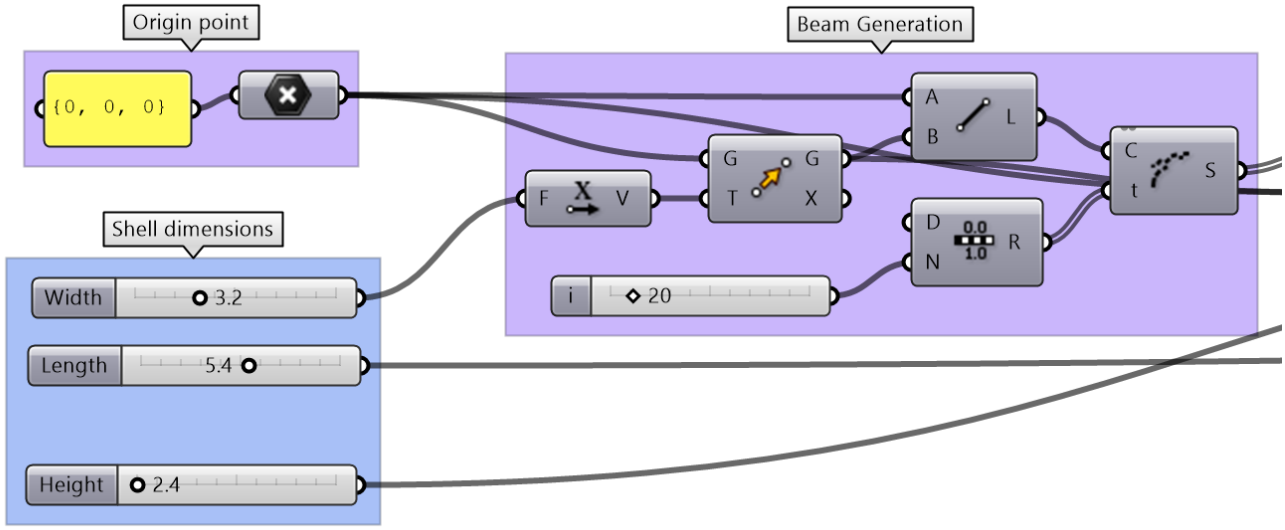

Fig. 5.3.a) Baseline for arch generation

Thrust line definition

The proposed method involves the definition of a flat line, in the case of arches, or a surface that corresponds to the footprint of the structure. Form-finding a 2D arch compared to a 3D mesh saves processing power. This geometry is relaxed to the optimal arch or doubly-curved surface where static equilibrium for pre-defined loading conditions occurs, otherwise known as thrust line. As explained in chapter 3.2, the form-finding process employs the particle-spring method of the Large Deformation Component of Karamba3D, a plug-in of grasshopper3D (Daniel Piker, 2006). This part of the script is displayed in *Figure* 5.4.

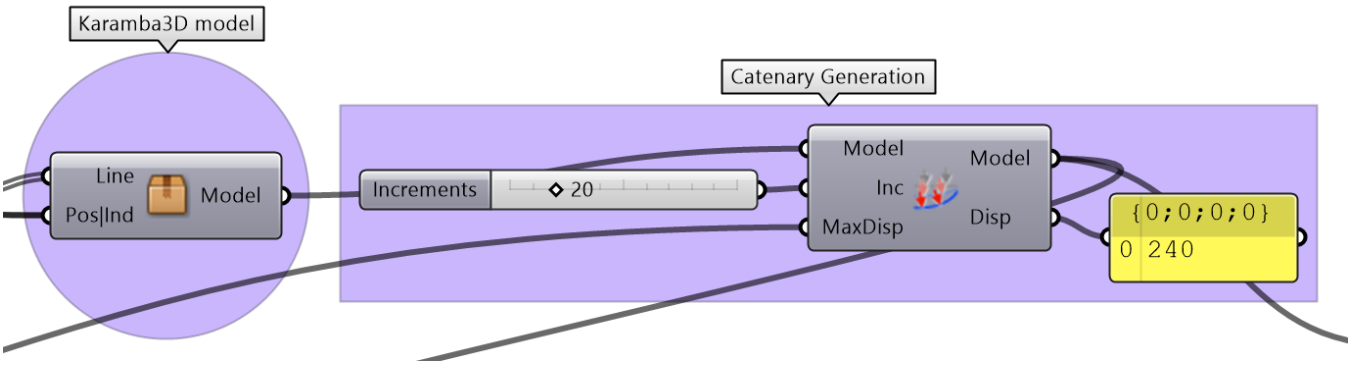

Fig. 5.3.b) Catenary generation

With this method, the final form is the outcome of applied loads and spring stiffness as described by the eq. 3.1.

$$SF_{ratio} = \frac{kspring}{Uforce} \text{ (eq. 3.1)}$$

where:

k_{spring}: spring stiffness of the discretized springs

U_{force}: unary force [dimensionless load]

Arch analysis

The form-finding and analysis results can be viewed through the *Model View* (Karamba3D), *Shell View* (Karamba3D) and *Result Vectors on Shell* (Karamba3D) components.

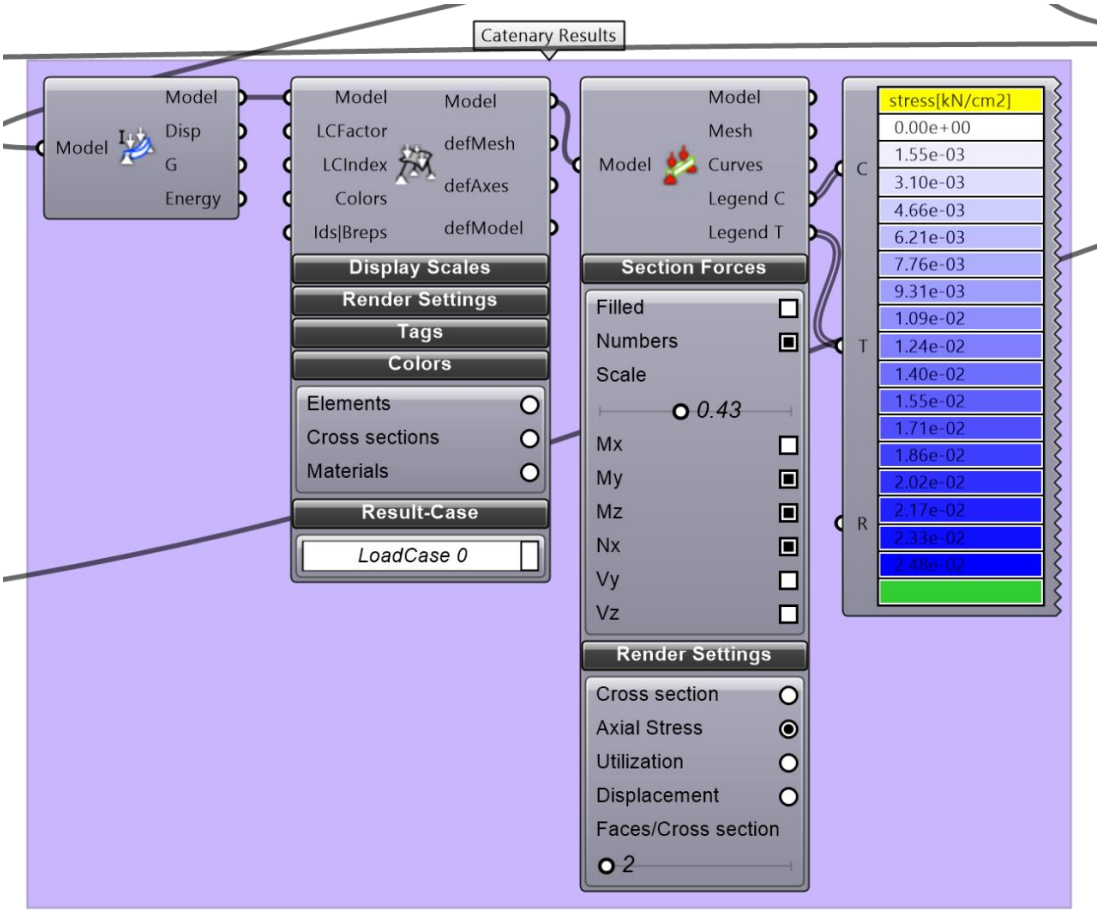

Fig. 5.4 Catenary arch analysis

Funicular vault generation

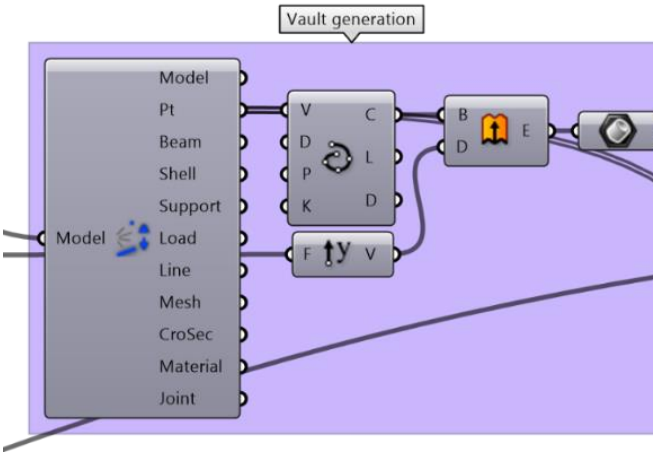

Fig. 5.5 Funicular barrel vault

Next step in the form generation is the vault shape. After the catenary arch is formed, a straight extrusion is performed to generate the funicular barrel vault, as shown in Figure 5.5. The slider illustrated in Figure 5.1 is used to control the vault length.

Input of material properties

Karamba3D has a limited selection of materials in its library. Therefore, a new one needs to be defined with the assistance of the Material Properties (Karamba3D) component. Newer versions of Karamba3D allow the assignment of orthotropic materials through the drop-down menu. When defining orthotropic materials in Karamba3D the local x-axis determines the first material direction. Strains by temperature changes indicated by alphaT1 & T2 are not taken into account, Finally, the yield stresses fy1 & 2 indicate the strengths of the material. In the current version of Karamba3D, the yield strength of the second direction is not used. *Figure* 5.6 shows the material properties defined in Karamba3D.

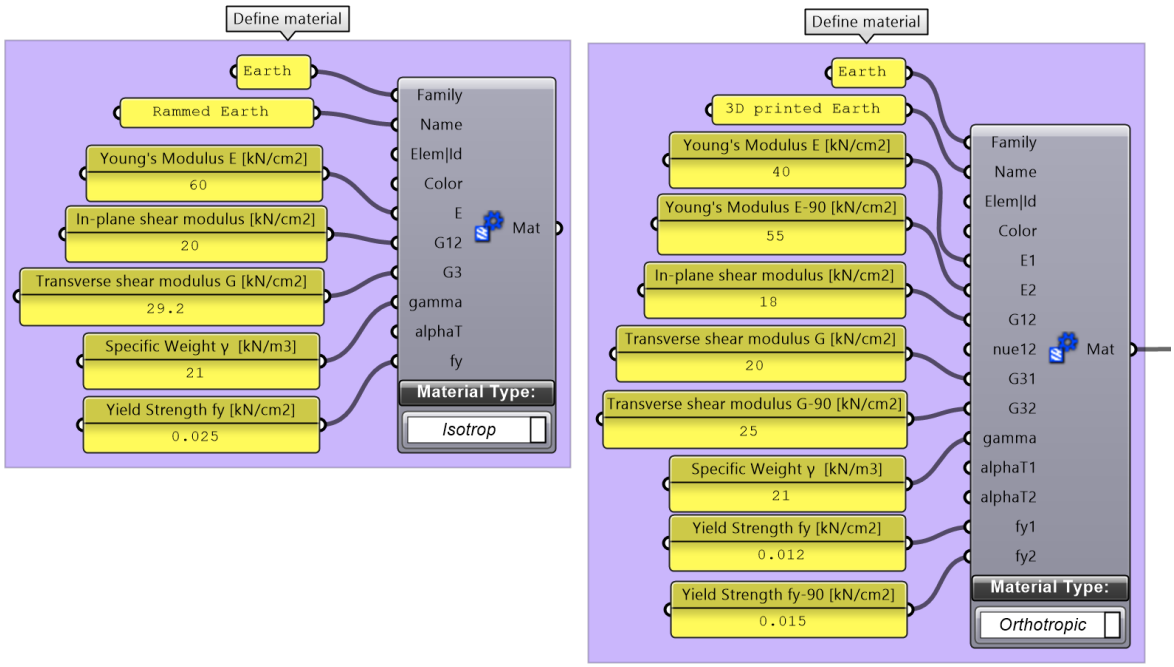

Fig. 5.6 Karamba3D Materials definition

Definition of Support conditions

Next to material, the necessary boundary conditions need to be defined. The edge curves of the vault are appointed as supports in the Support (Karamba3D) component. There are six available degrees of freedom (dofs), three for translation and three for rotation. A pinned support condition is chosen, meaning that the three dofs of translation need to be fixed. *Figure* 5.7 illustrates this part of the script.

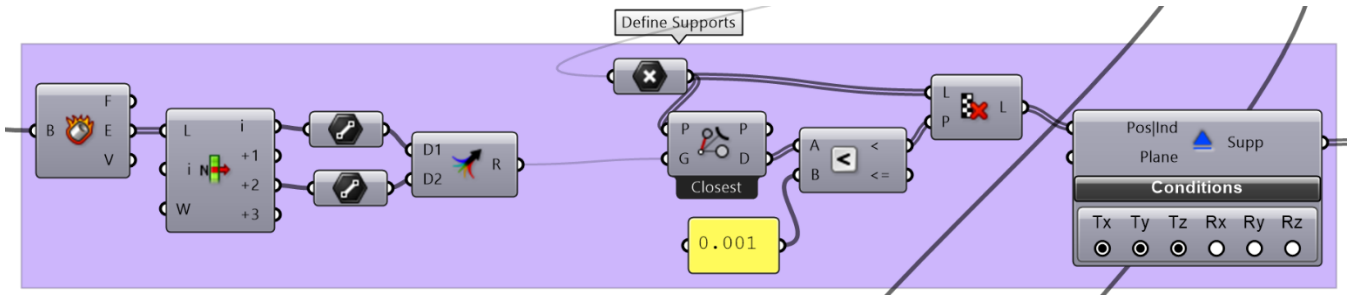

Fig. 5.7 Karamba3D Support

Definition of loads

Loading on structure is categorized by their time variation in different actions:

- Permanent (G), such as the self-weight
- Variable (Q), such as wind or snow
- Accidental (A), such as explosion

For the analysis, the self-weight, the applied snow load and wind load are taken into account, according to the Eurocode standards for Greece, as described in chapter 5.1.3. Due to the experimental nature of the project, the safety factor is 2. Accidental actions are not taken into account. For simplification purposes the snow load is projected in the total surface of the arch. Using the *Loads (Karamba3D) component* with a "Mesh Load" type. The load definition part of the script is illustrated in *Figure* 5.8

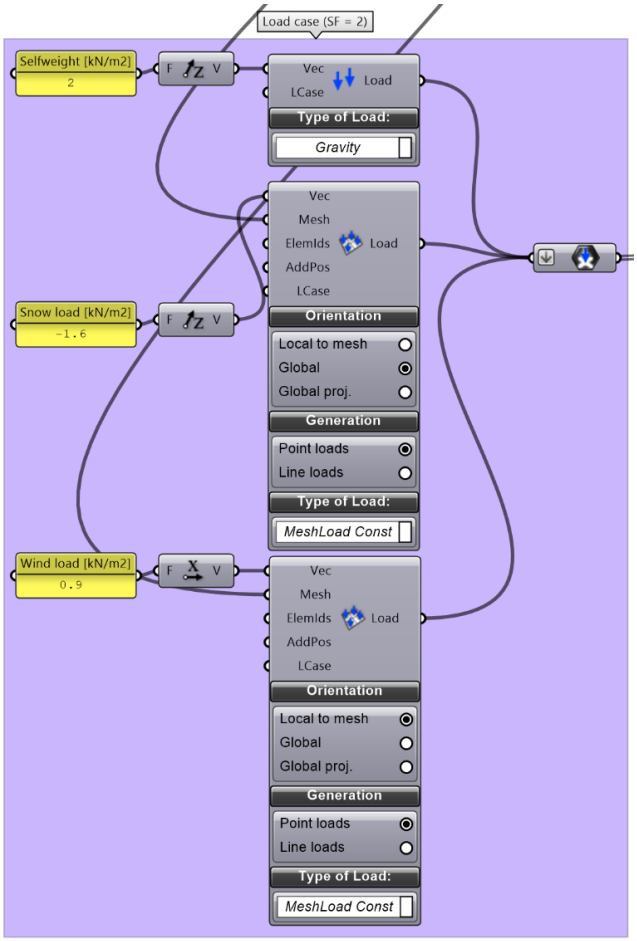

Fig. 5.8 Karamba3D Load case

Cross section definition & Optimization

Sole membrane function is difficult to ensure, as it is dependent on support conditions. Therefore, cross section optimization is crucial to prevent failure, especially at the boundary conditions where tensile stresses are more likely. According to the Karamba3D developers, the cross-section optimization component takes into account local buckling when deciding on a cross section height. The range of values for the cross section are determined by the user, as displayed in *Figure* 5.9, and the assembled model is input to the Karamba3D Cross-section optimization component.

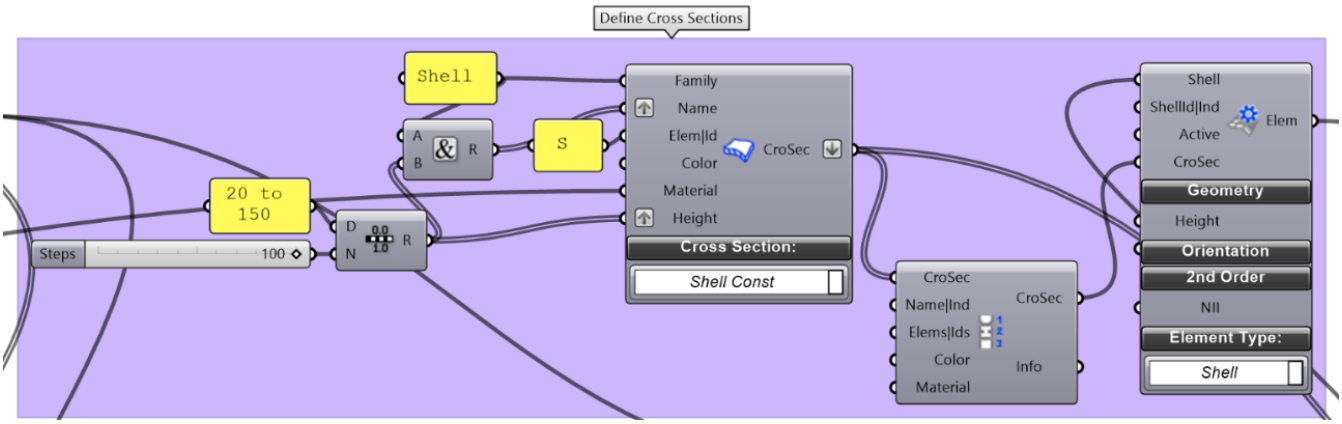

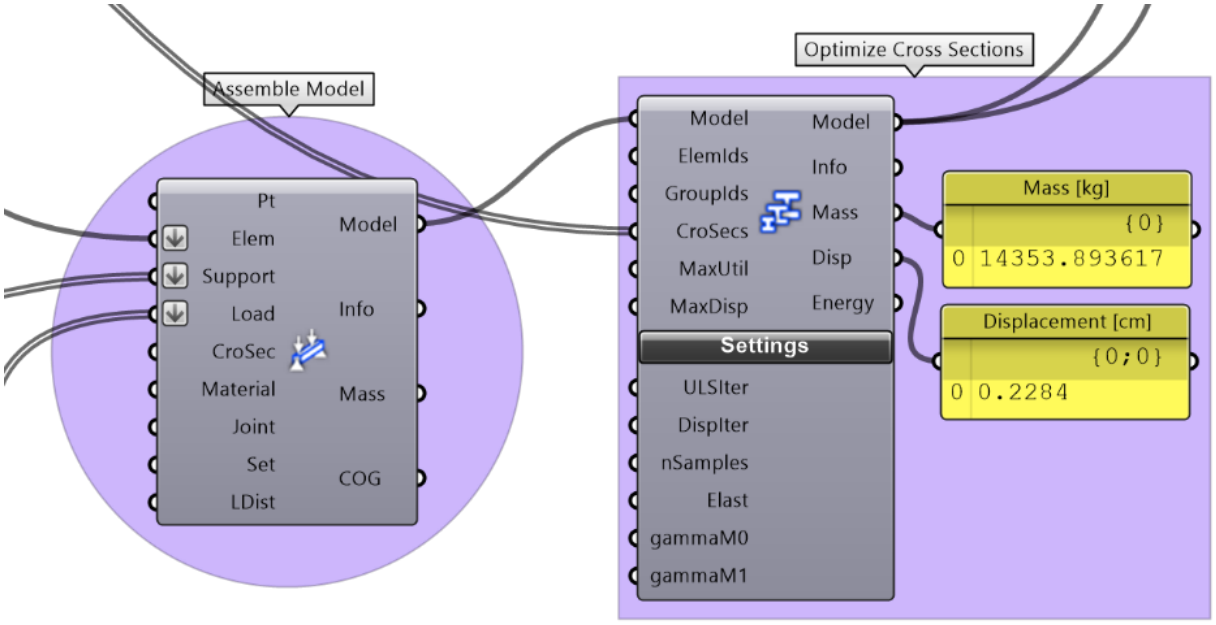

Fig. 5.9 Karamba3D Cross-section range & Optimization

Model details

In order to increase the accuracy of the data, the minimum mesh resolution of 0.03 [m] is chosen, as shown *in Figure 5.10.*

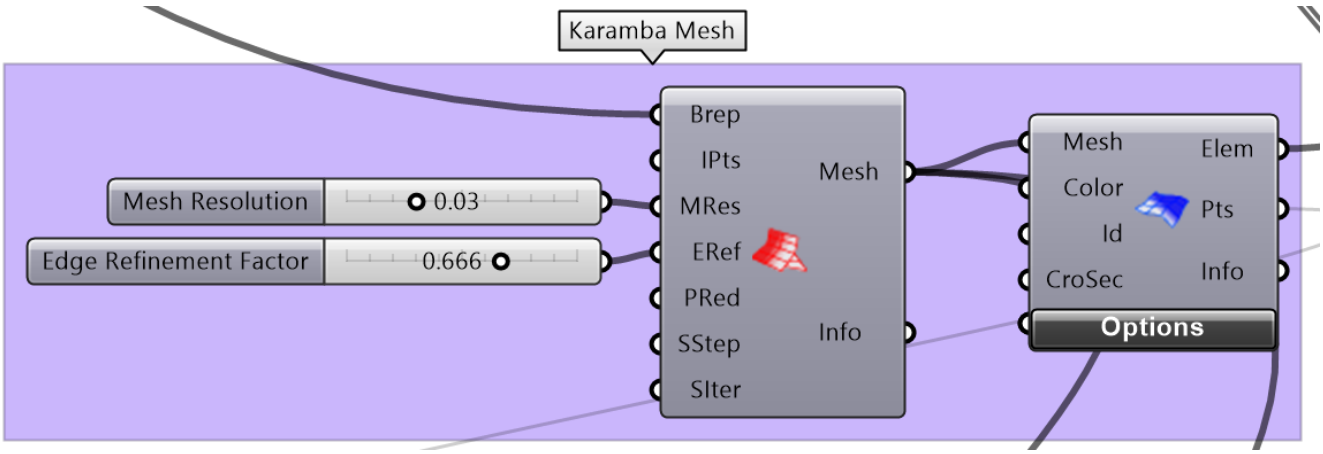

Fig. 5.10 Karamba3D Mesh resolution

Preliminary Vault Results

The resulting mesh geometry is displayed in *Figure 5.11*. It is comprised of 74544 triangular faces.

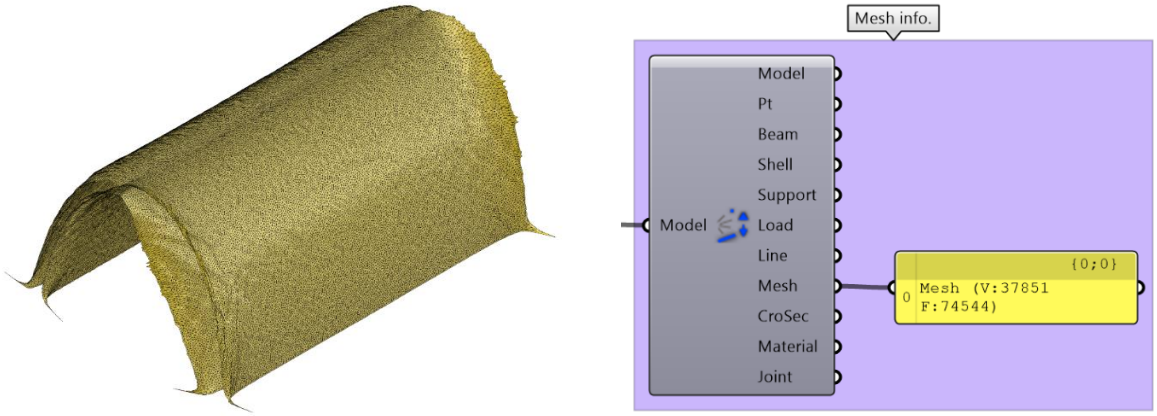

Fig. 5.11 Karamba3D Resulting vault mesh & information

The vault analysis yields information on the principal normal forces and moments, as well as the optimized cross section thicknesses. The minimum and maximum values are visualized in *Figures 5.12 & 5.13*.

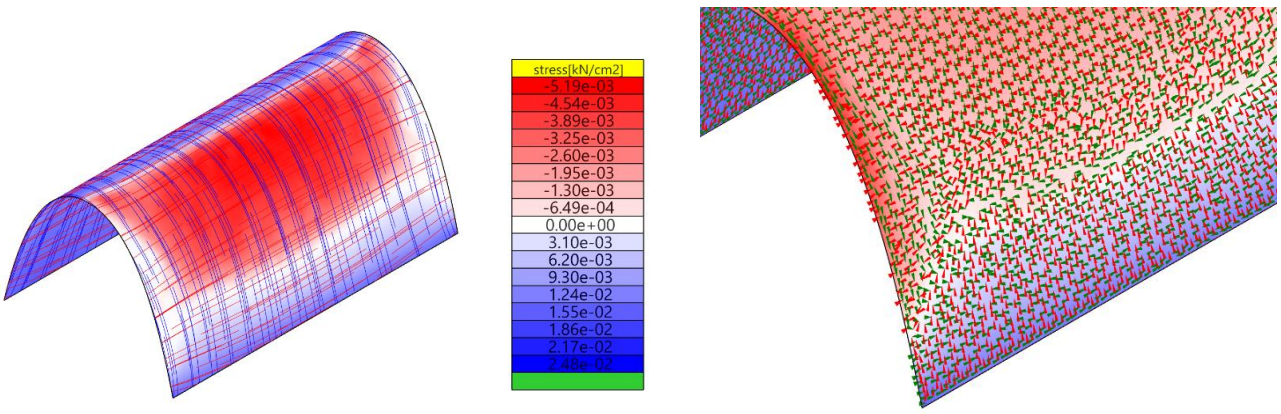

Fig. 5.12 Karamba3D Principal stresses & trajectories

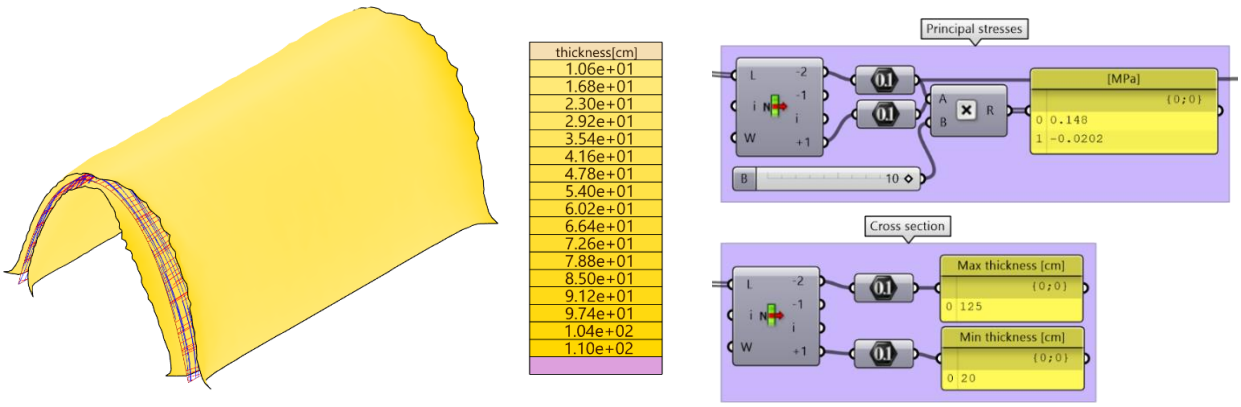

Fig. 5.13 Karamba3D Cross-section thicknesses

5.3.2 FEM Integration

FEM software will be incorporated in the workflow for calculations, resulting in an integrated and iterative process between form and forces. As stated previously, even though the material is isotropic, the production method results in orthotropic behavior due to the air gaps between layers. Newer versions of ANSYS Workbench software support analysis of 3D printed materials. TU Delft offers ANSYS Workbench through an educational license. The FEM software will assess the structure in accordance with a non-linear pushover analysis. Until the mechanical properties are derived from the laboratory tests, preliminary material properties gathered throughout the literature will be used for the development of the model.

Limitations of structural analysis

The goal of Finite Element Analysis, using Karamba3D and ANSYS is the reproduction of experimental results. It should be mentioned that the simulation will inevitably deviate from the actual behavior, since factors like printing imperfections and inconsistencies are not modelled. Instead, a continuous printing is assumed, even though in real situations the process will pause and resume. For this reason, comparing a simulated model analysis with an actual print test, would yield more reliable results and give information on the deviation between them. This was not achieved due to the discontinued access to the robotic arm for manufacturing a prototype for testing. To predict this novel material of printable earth, the FEA model should be able to include non-linear elastic behavior. Earth has very low tensile strength. The integration of reinforcement during the printing process could improve ductility and tensile strength by increasing the allowable deformation post-cracking. This is possible in Sofistik through the assignment of a Mohr-Coulomb material type and setting up a non-linear analysis. However, as the goal of the structure is to avoid exceeding the linear-elastic limit and for simplification purposes, linear elastic behavior is assumed.

However, significant effort was made to approximate a real situation with maximum precision. This was accomplished by the incremental increase in model detail and boundary conditions complexity. Firstly, the integration of Karamba3D in the form-finding process, allows the shape optimization. However, the Karamba3D analysis is based on metal plasticity theory and uses Mises yield surfaces. In other words, a simple isotropic Elastic-plastic material is used to model the 3D printed earth. Due to these limitations in the material characteristics, the ANSYS Workbench analysis is introduced in order to validate the resulting form. In this way, a more realistic design can be achieved and safer conclusions can be drawn. Therefore, even though the qualitative validity of the results could be improved, the quantitative failure behavior is assured.

Moreover, it should be noted that this process conducts a macro-modelling study, for which the sample was defined as a homogenous mixture, without distinguishing the inconsistencies due to layering. Even though visual inspection of sawed samples exhibited a monolithic view, previous studies and a micro scoping investigation reveal the presence of pores along the interfaces between layers. This inevitably alters the mechanical characteristics of the material. These changes will be factored in the material properties assigned in the simulation. Therefore, instead of detecting crack initiations and propagations, this study focuses on predicting the structural behavior, such as forces, stresses and deformations.

The approach followed in this thesis for the structural validation is the permissible stress design that focuses on ensuring that the exhibited stresses do not exceed the elastic limit and the buckling load does not exceed the critical load. This is a limitation, as contemporary civil engineering has adopted limit state design, which applies Magnification Factors to the loads and Reduction Factors to the resistances while fulfilling two conditions: the ultimate limit state (ULS and the serviceability limit state (SLS) (McCormac, 2008). For this reason, a general safety factor of 2.0 is chosen for the loading case.

FEA Geometry definition

The surface-based geometry of Rhino3D and Karamba3D is not compatible with ANSYS Workbench, which requires solid geometries. Therefore, a Grasshopper3D script is defined to generate a solid vault. It achieves this by assigning specified thicknesses in the two edge curves and the top. In the end, the earth object modelled in Rhino3D as a solid is baked and exported in ANSYS Workbench as an iges model. This process is illustrated in *Figure 5.14*.

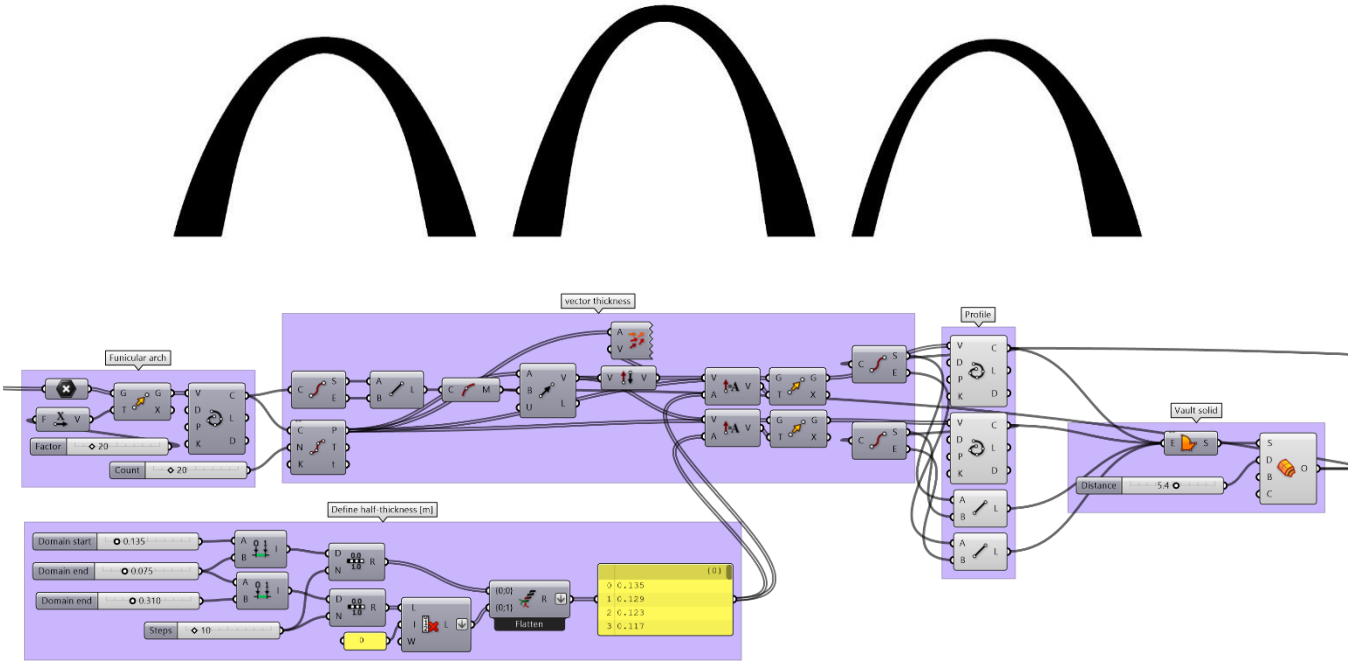

Fig. 5.14 Solid vault generation

FEA Model Details

In order to analyze the parts of the Finite Element Model (FEM), they underwent a process of discretization into 3D 8-node linear brick elements. The earth sample was transformed into a FE mesh with a resolution of 0.08 [m], as exhibited in *Figure 5.15*.

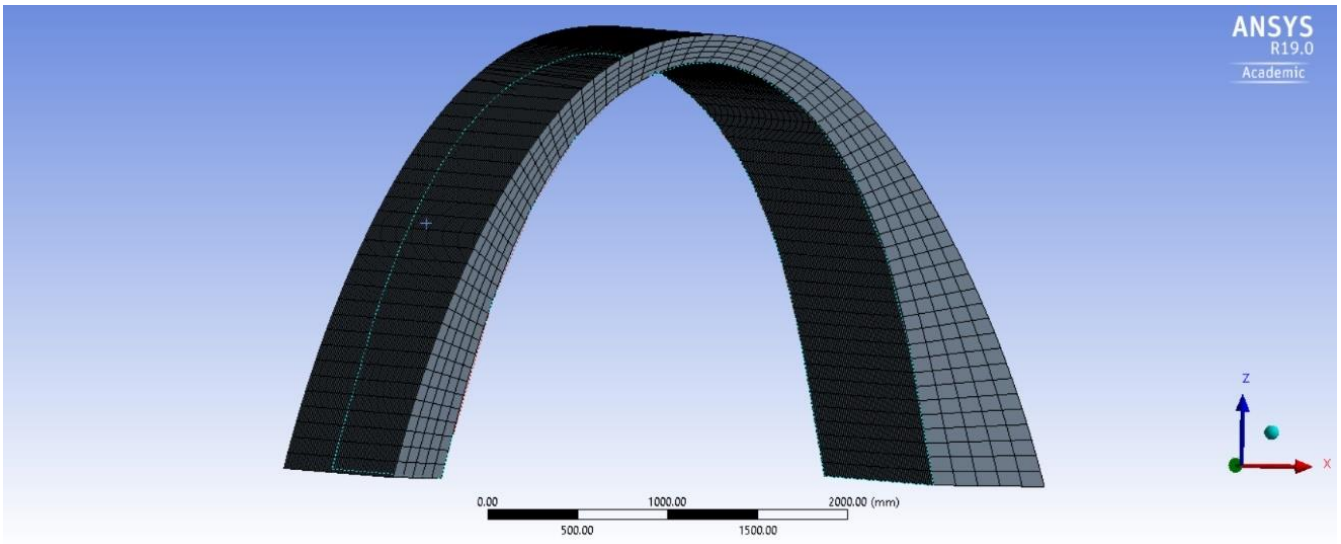

Fig. 5.15 Ansys workbench mesh resolution

Material Data

The aging behavior of the material is very important in guaranteeing desirable printing conditions in terms of layer adhesion and printability. It is possible to simulate this time-dependent property as part of the printing process to define the optimal printing speed and time. However, ss the structural analysis in ANSYS Workbench is performed on the final structure, the optimal material properties are assumed.

The parameters used in the FE model for the material simulation are based on literature regarding earth blocks (Illampas et al., 2011) and modified according to research on the orthotropic behavior of additive manufactured mixtures. The material properties of the mixture are illustrated in *Table* 5.2. The density, as well as the Poisson ratio were derived from literature on transversal and axial strains, while the Young's Modulus was calculated by the stress-strain curve of a similar test, namely the Adobe brick-making workshop of the 2019-20 Earthy course and compared with references. The value is determined by the average of the slopes of the linear parts of the curves. A very low yield stress is assumed due to the low elasticity of clay. The failure stress was decided based on previous results of monotonic uniaxial compression tests. These assumptions are made to compensate for the lack of actual tests. The properties of steel are well documented and are derived from relevant literature (Illampas et al., 2011).

Table 5.2 Earth material properties

Property	Value	Unit
Density	1900	kg/m3
Orthotropic Elasticity		
Young's Modulus X direction	400	MPa
Young's Modulus Y direction	550	MPa
Young's Modulus Z direction	400	MPa
Poisson's Ratio XY	0.3	MPa
Poisson's Ratio YZ	0.3	MPa
Poisson's Ratio XZ	0.16	MPa
Shear Modulus XY	180	MPa
Shear Modulus YZ	200	MPa
Shear Modulus XZ	180	MPa
Tensile Yield Strength	0.12	MPa
Compressive Yield Strength	4	MPa
Tensile Ultimate Strength	0.37	MPa
Compressive Ultimate Strength	5	MPa

Support Conditions & Load Case definition

The support conditions are defined as pinned supports using displacement boundaries. In order to define the load case with the determined load factor of 2, all loads should be multiplied by a factor of two. To replicate this effect for the gravitational load of the self-weight, an acceleration load with the same value is designated at the object's center of mass. Moreover, the wind load is defined as pressure, instead of the surface load defined in Karamba3D. These settings are shown in *Figure* 5.16.

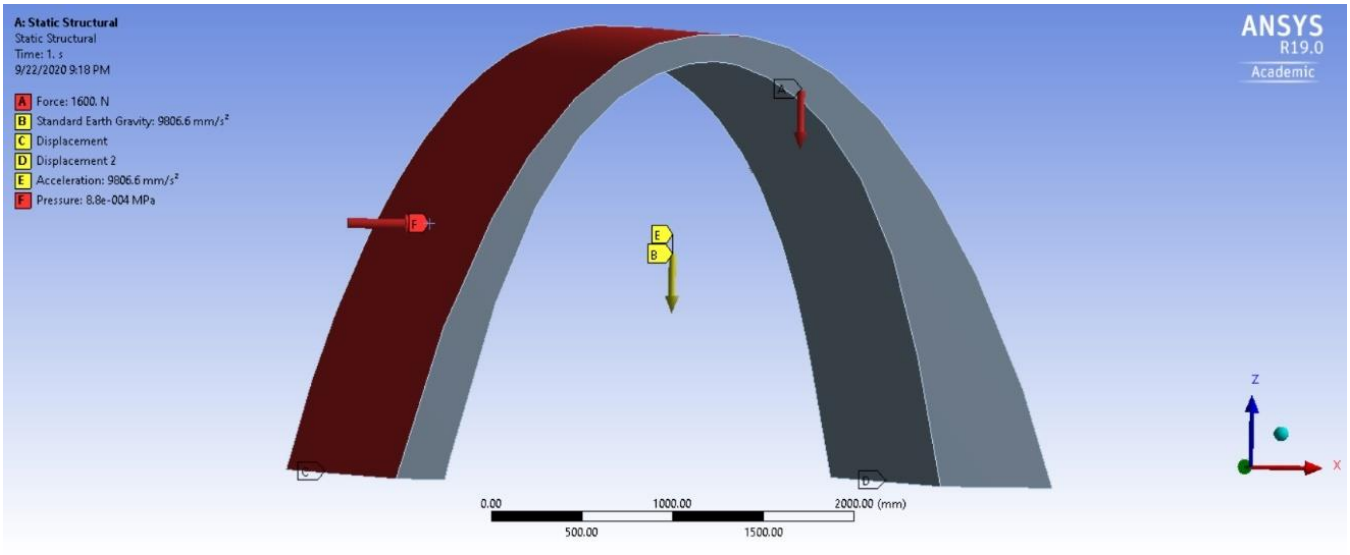

Fig. 5.16 Ansys workbench load case

Static Analysis

Figure 5.17 presents the Maximum Principal Stresses. The simulation shows a maximum stress of 0.11602 MPa < 0.12 MPa (yield strength). This means that according to the analysis, the structural stability is verified. These results should be compared with physical tests in terms of deviation to ascertain their validity.

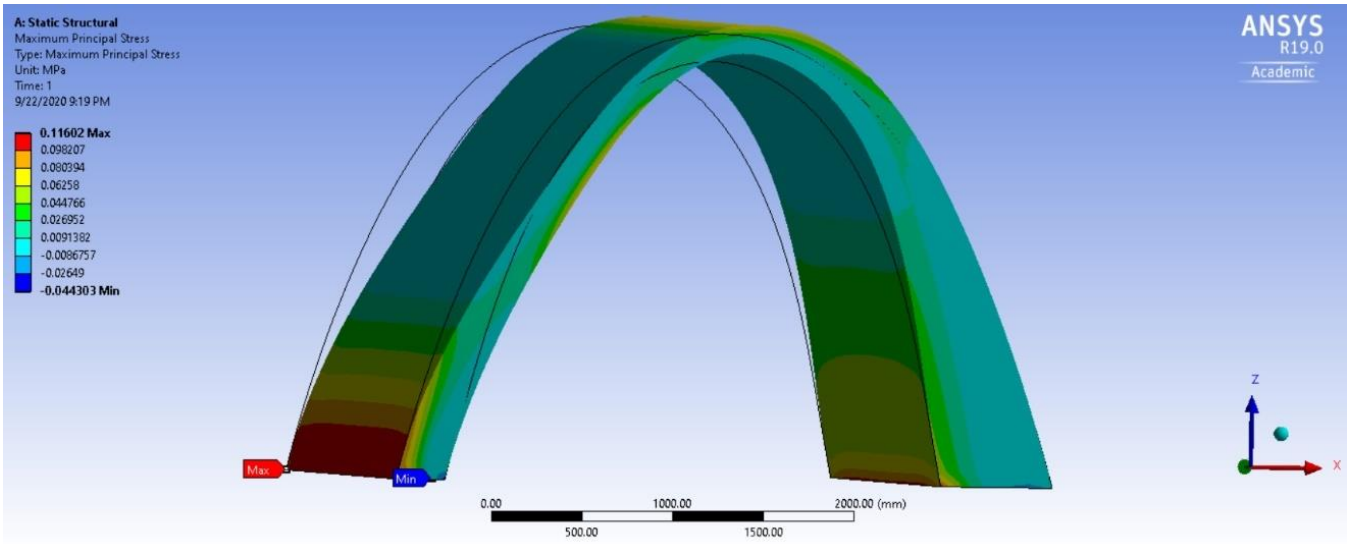

Fig. 5.17 Ansys workbench Maximum Principal Stresses

Buckling Analysis

As mentioned before, shell structures are sensitive to buckling. With ANSYS Workbench it is possible to perform a buckling analysis on the shell structure, according to the linear eigenvalue problem: The buckling deformation for the first positive buckling mode is illustrated in *Figure 5.18*.

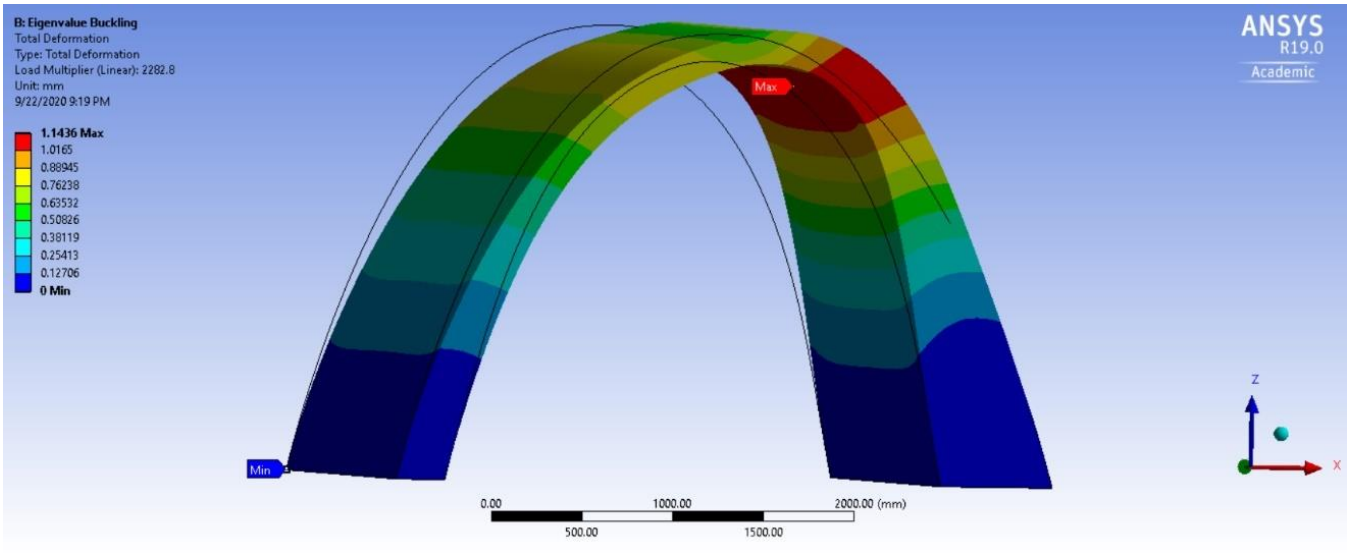

Fig. 5.18 Ansys workbench Linear eigenvalue Buckling analysis

In order to validate the results of the numerical analysis, an analytical one is advised. Even though there is no simple equation d is a way to perform an analytical calculation of buckling for columns. Slender columns are also prone to buckling before the stresses reach the maximum shear strength. Therefore, we can approximate the shell with a slender column, which can be calculated with the Euler formula. To take into account the difference in geometries and structural systems, the column will have the total height of the shell, while the resulting force value will be halved for the comparison, as displayed in *Figure 5.19*.

The Euler formula is given by the equation:

$$P_{cr} = \frac{\pi^2 EI}{(KL)^2}$$

where

P_{cr}: Euler's critical load (longitudinal compression load on column),

E: Young's modulus of investigated material

I: 2nd moment of area of the column cross section,

L: unsupported column height,

K: effective length factor of column

Fig. 5.19 Buckling analysis approximation

Approximating the wall with a slender column, the 2nd moment of area is calculated by the equation:

$$I = bh^3/12$$

The buckling check is integrated in the digital workflow, as part of the Grasshopper3D script. This process is illustrated in *Figure* 5.20.

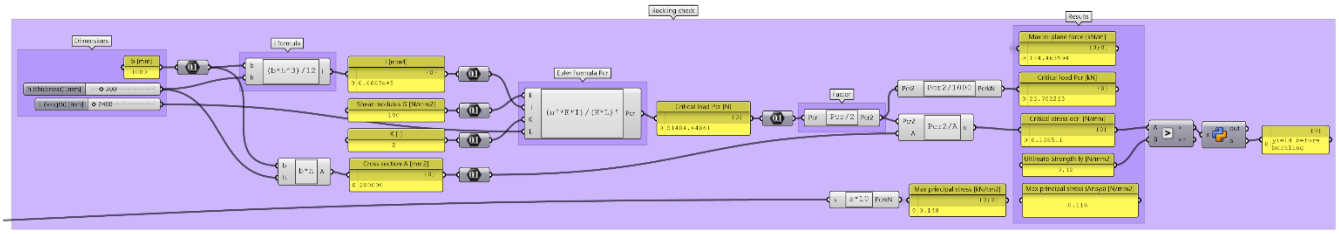

Fig. 5.20 Ansys workbench Linear eigenvalue Buckling analysis

Even before performing the calculations it can be noticed that the critical load is inversely proportional to the height. This means that reducing the height of the shell will improve buckling resistance, while reducing amount of material. On the other hand, the critical load is proportional to the 2nd moment of area which is proportional to the thickness. This means that increasing thickness, will result in improved buckling resistance, while increasing amount of material.

5.3.3 Slicing strategy

In this chapter, the slicing strategy is described that addresses the subject of cantilever printing. Firstly, a process is defined based on inspiration from historic examples of masonry construction. Then, the specific fabrication constraints of the adaptation to additive manufacturing process are outlined, resulting in permissible forms. Finally, an assessment method is suggested.

Additive manufacturing of cementitious pastes, such as earth, give rise to significant possibilities in constructing free-form digitally produced designs. The material properties, especially in their fresh state have limited the realization of such geometries to simple, and often standard forms. However, their yield strength is not zero, allowing a degree of cantilevering. Part of this research attempts to explore and extend the variety of feasible shapes without supports, by utilizing established principles from history for cantilever structures. This decision was made to avoid the complexity of fabrication and high cost of precise formworks, as well as their subsequent construction waste.

"Nubian" printing

The typical strategy for preparing an object for 3D printing is the horizontal slicing with a vertical translation which is employed by common 3-axis 3D printers. In this case the overhangs are formed through corbels of filament. This causes bending stresses. On the opposite perspective, in order to ensure mainly shear stress in the printing should aim at maximizing contact area between layer faces. This thesis proposes a "Nubian vault" inspired slicing of a constant 40-degree angle printing where the extruder is normal to the surface, as exhibited in *Figure* 5.21. Ducoulombier and Carneau (2019) have performed a successful scaled experiment following this process. In the script, this process is defined by the slicing parameters of angle and layer height, as illustrated in *Figure* 5.22.

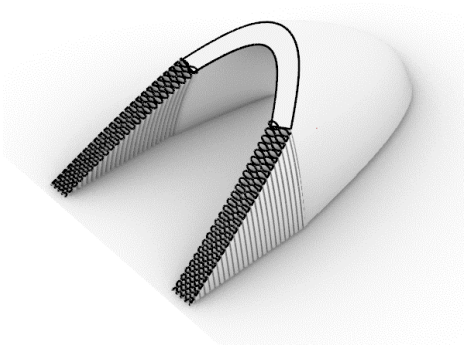

Fig. 5.21 "Nubian" inspired slicing

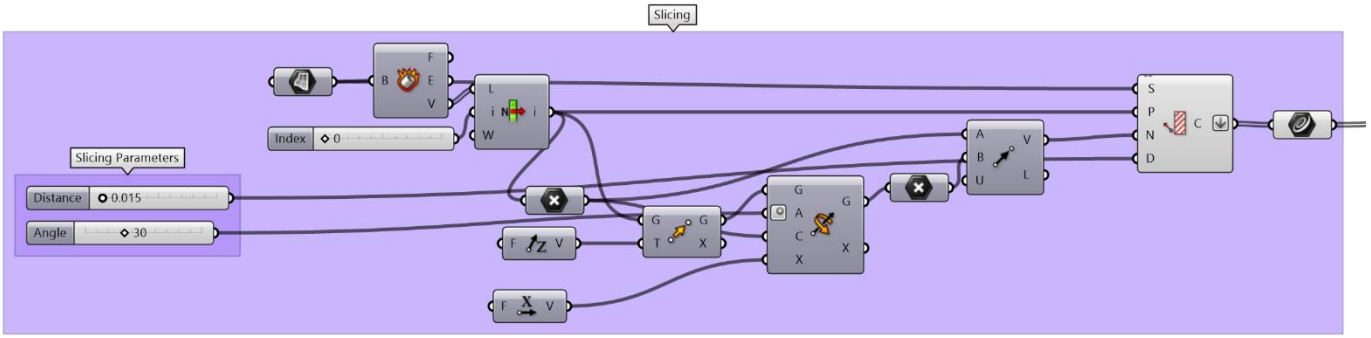

Fig. 5.22 Grasshopper3D slicing process

5.3.4 Infill Design

This section describes the development of the infill strategy of the design. The aim is to produce a parametric tool that gives full control of the infill density in a fabrication-aware manner. This expands the possibilities of use of the digital tool beyond structural optimization, to other types of performance-based design.

Goals

The material is deposited according to instructions, referred to as g-code. The g-code pattern influences the void shapes and volumes between, the layer adhesion, altering the mechanical properties of the material. Moreover, infill gaps contribute positively to the drying and firing times and reduce thermal gradients in the product.

Even though the original material is isotropic, through the additive manufacturing process, orthotropic behavior emerges. The aim of toolpath development and g-code generation is to ensure that the pattern geometry and orientation contributes to structural integrity.

The main considerations of the toolpath design goals are:

- ensure constant speed for optimal deposition (through gradual transitions in corners)
- continuous lines with optimal overlapping (taking into account the nozzle dimensions)
- increase layer adhesion and overhang angle through toolpath height and orientation

Infill percentage

The interior structure of a 3D printed object is called *infill*. Typically, the infill structure is regular and selected by the user in terms of volume percentage and infill pattern in the slicing software. Naturally, the infill has a major effect in the material use, printing process, as well as the mechanical properties of the object. A higher volume percentage improves the resistance to external loading, at an increase in material use (Wu et al., 2018). However, by using structural analysis and optimization, a mechanically strong and relatively lightweight structure can be produced. Due to the poor strength of the material, an infill percentage of 75% is chosen.

Stress-Line Additive Manufacturing (SLAM)

Principal stress lines are curves that illustrate the paths of internal forces for defined boundary and loading conditions. In structural design, they can indicate the optimal topology for material distribution, as well as segmentation (Michalatos, Kajima, .2015). The idea of utilizing stress lines in the design originate in the work of Michell (1904). Plug-ins such as Karamba3D and Millipede have contributed to the emergence of stress- line based ideas in common design software, such as Rhinoceros3D. However, Commercial slicing software do not take into account stress lines. Instead they compute a grid-based infill. Aligning material deposition to stress lines has the potential to increase structural efficiency and performance. The script follows the trajectories of the stress lines in any geometry assigned for a funicular barrel vault, as illustrated in *Figure* 5.23.

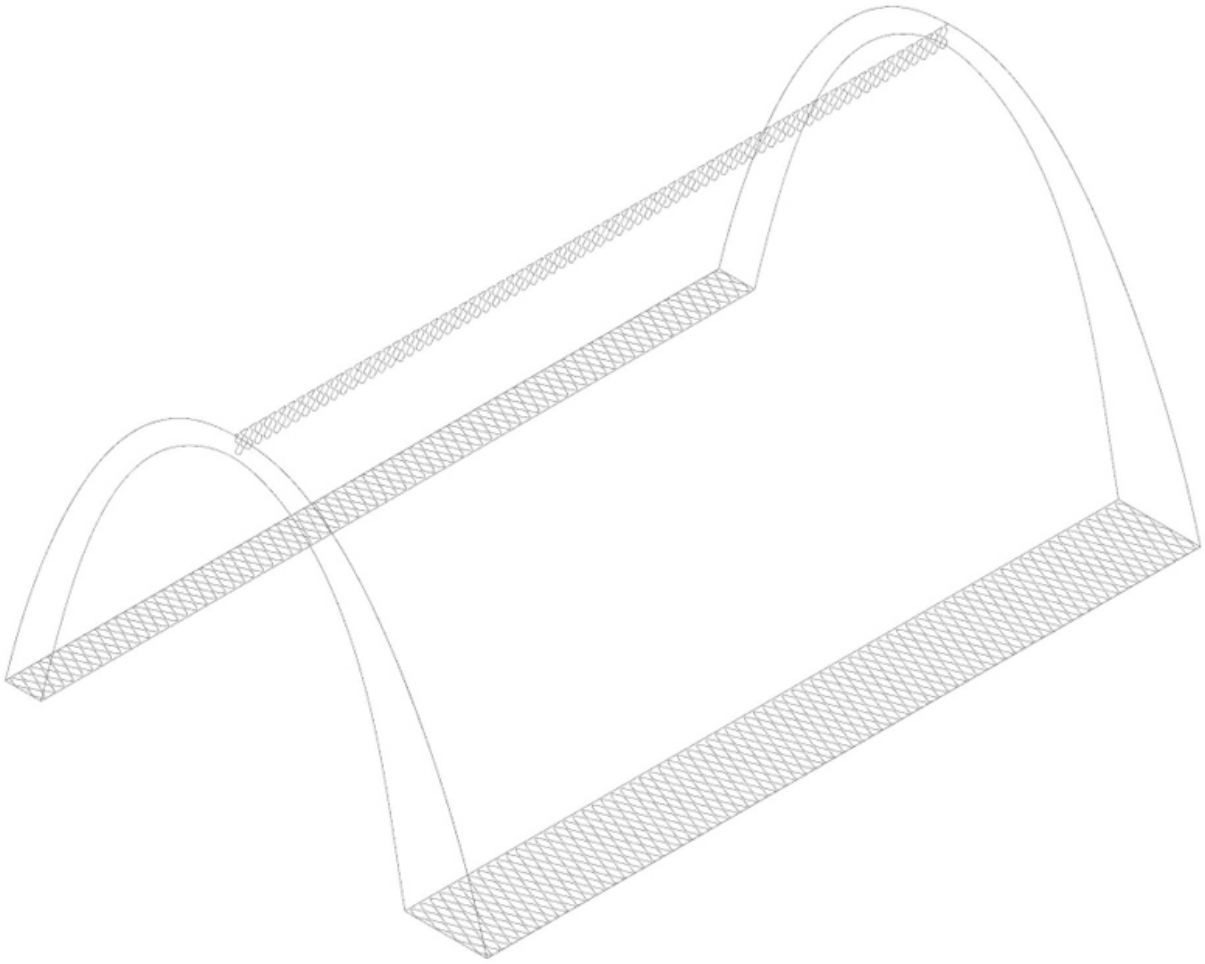

Fig. 5.23 Stress-line Infill alignment

Modular Infill Approach

Typically, structural optimization workflows are based on a voxel-based geometry, where resolution is the only parameter. Though these processes result in theoretically optimized results in terms of material reduction, the end forms usually require excessive redrawing and re-topologizing to be adapted into a geometry that can be manufactured. Moreover, their algorithms are still limited in terms of realistic material behavior as well as other types of constrains. This process leads in single objective, sub-optimal results.

The modular infill approach, shown in *Figure* 5.24, was conceived due to the fabrication aware nature of the project. In this way, feasibility constrains can be considered from the conception of the design. Those are not only limited to structural performance, but can involve reinforcement integration, services and other performance criteria.

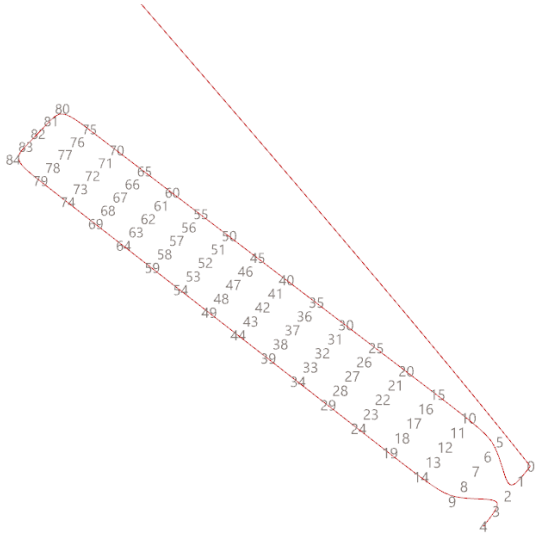

Fig. 5.24 Modular infill concept

A script is developed that defines a number of different feasible infill patterns, leaving the decision to the user requirements through a drop-down list. Currently, six different patterns, exhibited in *Figure* 5.25 are stored. The list can be expanded until an infill library is formed, achieving modularity in a local scale.

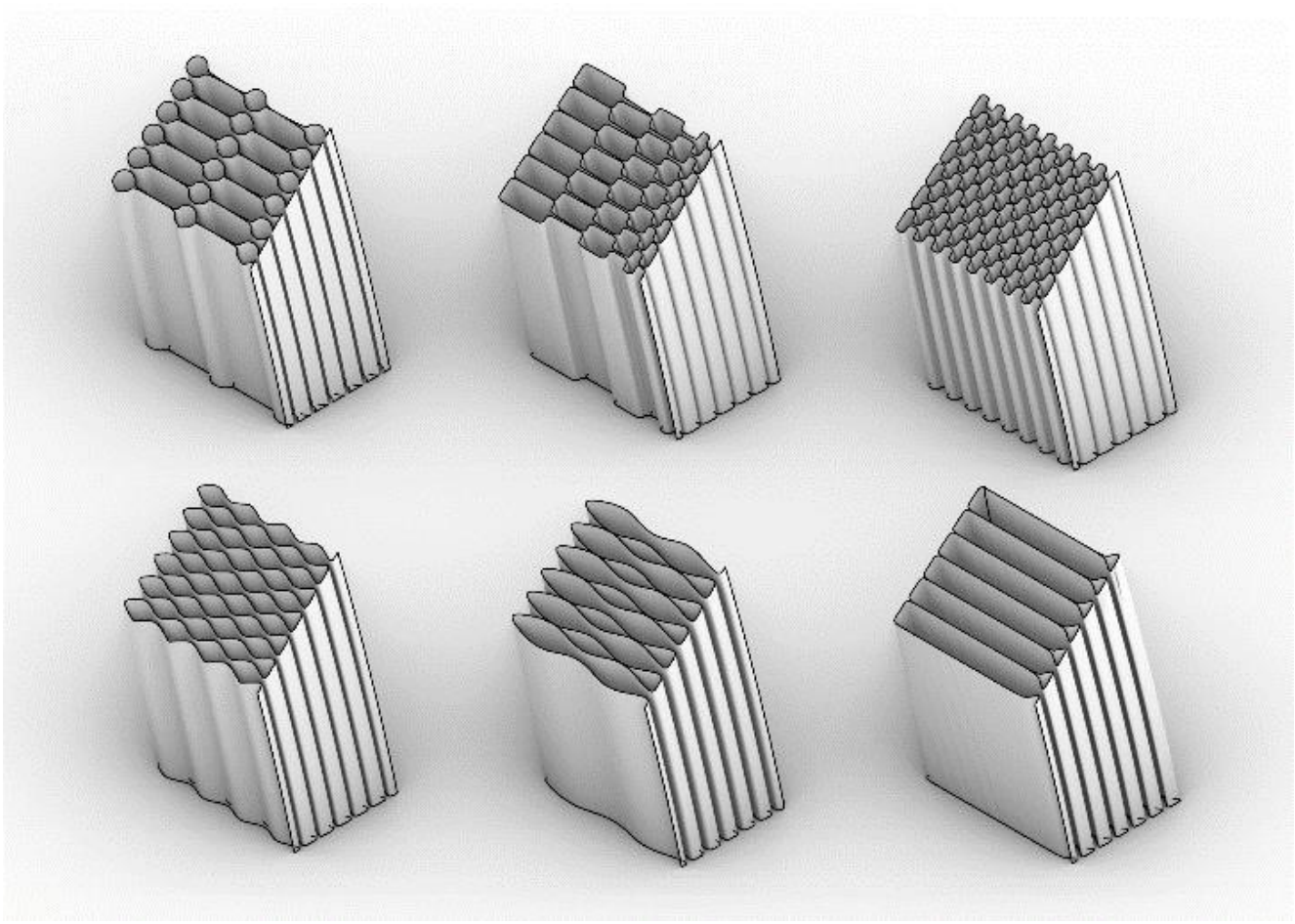

Fig. 5.25 Infill library

The goal of the script is the generation of the overall geometry from the chosen infill pattern. The process is illustrated in *Figure* 5.26. This is achieved by segmenting and populating the general form finding parameters, in this case the two base surfaces and the top one. The surfaces are segmenting by the variable that affects the infill percentage. The sub-surfaces formed are rebuilded into a grid of points based on their dimensions. Then, any infill pattern can be formed as a curve interpolation of a selection of the grid points. A GhPython script was defined to integrate the infill generation with the drop-down list, as shown in *Figure* 5.27. In the end, all the infill curves are joined on their respective surfaces and sweeped, generating the final form.

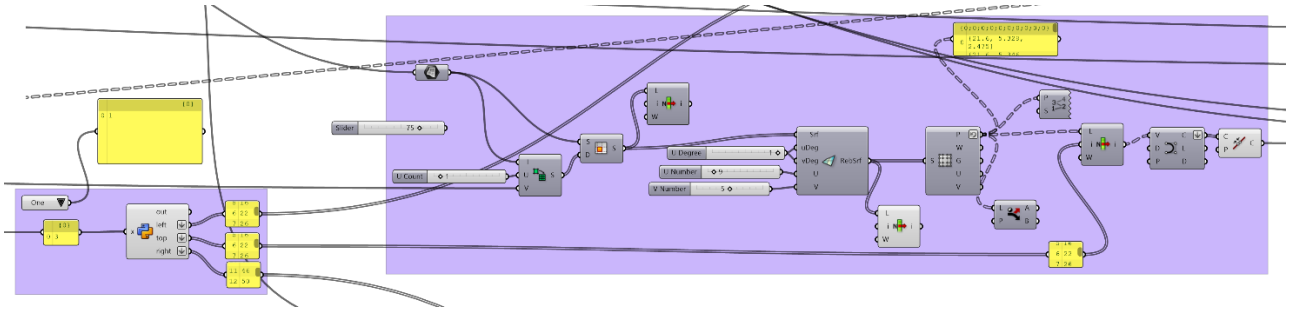

Fig. 5.26 Infill pattern definition

```
1.  import rhinoscriptsyntax as rs
2.  left = 1
3.  top = 1
4.  right = 1
5.  if x == "1":
6.      left = 0,1,2,5,10,35,40,41,42,43,44,39,14,9,2,3,4
7.      top = 0,1,2,5,10,35,40,41,42,43,44,39,14,9,2,3,4
8.      right = 0,1,2,5,10,70,75,80,81,82,83,84,79,74,14,9,2,3,4
9.  elif x == "2":
10.     left = 0,1,2,15,20,25,36,42,38,29,24,19,2,3,4
11.     top = 0,1,2,15,20,25,36,42,38,29,24,19,2,3,4
12.     right = 0,1,2,15,20,25,42,55,60,65,76,82,78,69,64,59,42,29,24,19,2,3,4
13. elif x == "3":
14.     left = 0,1,2,6,10,16,22,26,30,36,42,38,34,28,22,18,14,8,2,3,4
15.     top = 0,1,2,6,10,16,22,26,30,36,42,38,34,28,22,18,14,8,2,3,4
16.     right =
    0,1,2,6,10,16,22,26,30,36,42,46,50,56,62,66,70,76,82,78,74,68,62,58,54,48,42,38,34,28,22,18,14,8,2,3,4
17. elif x == "4":
18.     left =
    0,1,2,7,6,5,10,11,12,17,16,15,20,21,22,27,26,25,30,31,32,37,36,35,40,41,42,43,44,39,38,37,32,33,34,29,28,27
    ,22,23,24,19,18,17,12,13,14,9,8,7,2,3,4
19.     top =
    0,1,2,7,6,5,10,11,12,17,16,15,20,21,22,27,26,25,30,31,32,37,36,35,40,41,42,43,44,39,38,37,32,33,34,29,28,27
    ,22,23,24,19,18,17,12,13,14,9,8,7,2,3,4
20.     right =
    0,1,2,7,6,5,10,11,12,17,16,15,20,21,22,27,26,25,30,31,32,37,36,35,40,41,42,47,46,45,50,51,52,57,56,55,60,61
    ,62,67,66,65,70,71,72,77,76,75,80,81,82,83,84,79,78,77,72,73,74,69,68,67,62,63,64,59,58,57,52,53,54,49,48,4
    7,42,43,44,39,38,37,32,33,34,29,28,27,22,23,24,19,18,17,12,13,14,9,8,7,2,3,4
21. elif x == "5":
22.     left =
    0,1,2,7,6,5,10,11,12,17,22,21,20,25,30,35,40,41,42,43,44,39,34,29,24,23,22,17,12,13,14,9,8,7,2,3,4
23.     top =
    0,1,2,7,6,5,10,11,12,17,22,21,20,25,30,35,40,41,42,43,44,39,34,29,24,23,22,17,12,13,14,9,8,7,2,3,4
24.     right =
    0,1,2,7,6,5,10,11,12,17,22,21,20,25,30,35,36,37,42,47,52,57,56,55,60,65,70,75,80,81,82,83,84,79,74,69,64,59
    ,58,57,52,47,42,37,38,39,34,29,24,23,22,17,12,13,14,9,8,7,2,3,4
25. elif x == "6":
26.     left = 0,1,2,1,5,11,12,17,16,20,26,27,32,31,35,41,42,43,39,33,32,27,28,24,18,17,12,13,9,3,2,3,4
27.     top = 0,1,2,1,5,11,12,17,16,20,26,27,32,31,35,41,42,43,39,33,32,27,28,24,18,17,12,13,9,3,2,3,4
28.     right =
    0,1,2,1,5,11,12,17,22,27,32,37,36,40,46,47,52,57,62,67,72,71,75,81,82,83,79,73,72,67,62,57,52,47,48,44,38,3
    7,32,27,22,17,12,13,9,3,2,3,4
```

Fig. 5.27 Infill grid pattern

Gradient Infill

An evolution of the modular infill is the Gradient Infill strategy based on the principles of topology optimization (TO). Typical TO methodologies cull elements below certain densities, resulting in the characteristic fibrous geometries.

Instead, Hermann (2015) applied the same algorithms in beams while incorporating material stiffnesses and densities. Topology Optimization is a computational method that optimizes material distribution for structural performance. The inputs are the boundary conditions and geometric constraints, defined by the user. It can be a valuable tool in the early design process of structural form-finding. The local-scale modular infill opens the path for local-scale agency and solutions by the designer integrated in the overall fabrication concept in a bottom-up way, as showcased in *Figure 5.28*. In a future iteration, multiple performance criteria where services could be color-coded and communicated to the script through a graph mapper, assigning the available modular patterns to their respective positions, forming a complex gradient overall pattern that is still fabrication aware.

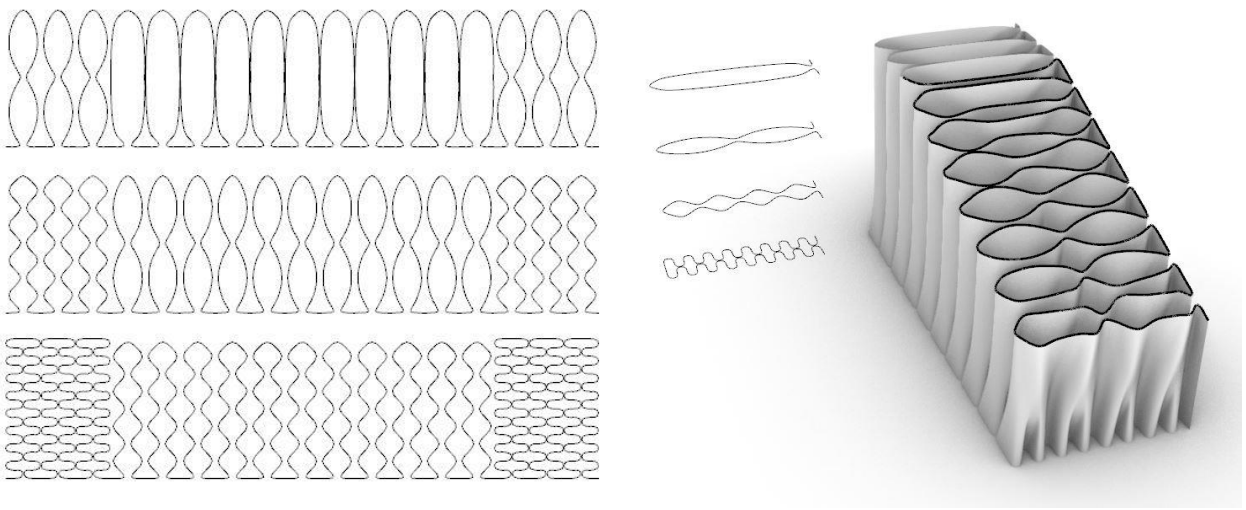

Fig. 5.28 Gradient infill possibility

5.3.5 Robotic Simulation

Limitations

Due to the addition of an external axis, the simulation allows the robot to move and rotate freely around the toolpath of each layer. This may cause the arm to collide with previous already printed layers as they are not considered when a new toolpath is assigned and there are no tools to avoid them currently in FURobot. This limitation is possible to be overcome by adjusting the starting position and the external axis domain through the corresponding sliders. By limiting the movement on the external axis, it is possible to ensure that the robotic arm will only perform the necessary movements and will not collide with previous layers.

Method

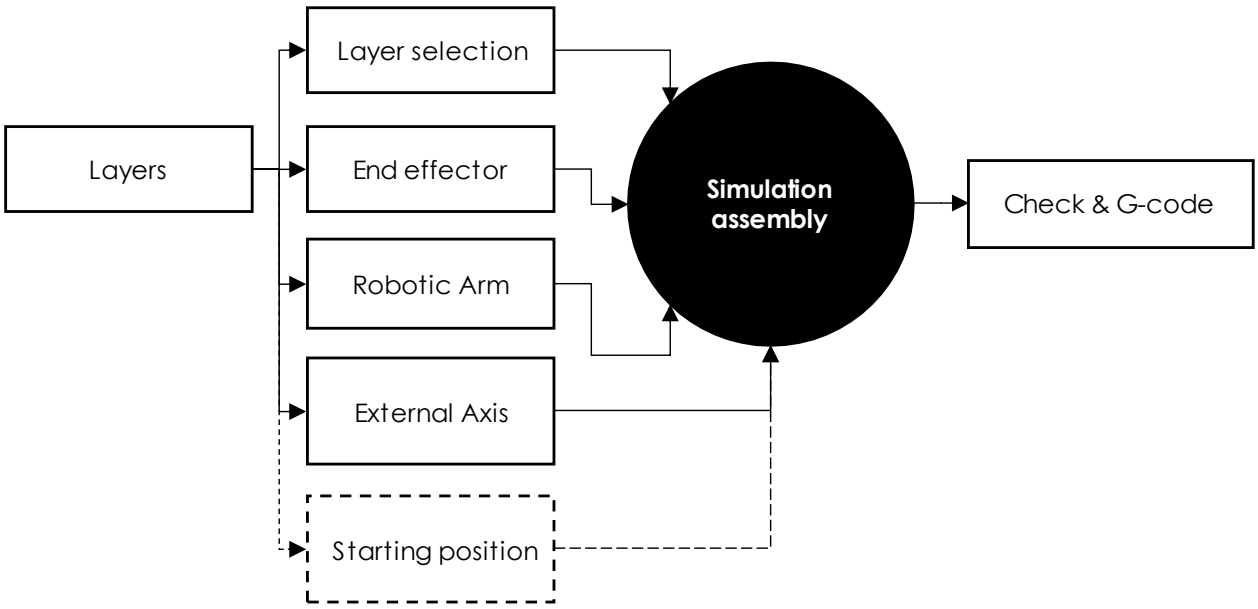

Fig. 5.29 Robotic simulation diagram

Layer choice

The layer choice is performed through a python script where the total amount of layers is stored. Though a GhPython scripted button and a Grasshopper3D pipeline, described in *Figures 5.30.a) & 5.30.b)* the user can go back and forth in order to select the preferred layer for printing.

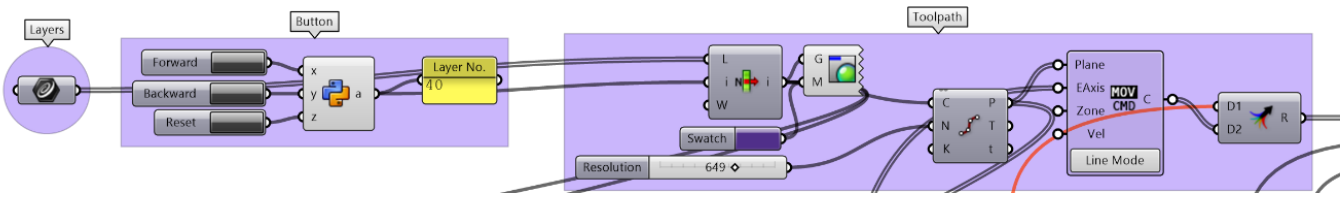

Fig. 5.30. a) Robotic simulation layer choice

```
1. import rhinoscriptsyntax as rs
2. import scriptcontext as sc
3. if x:
4.     sc.sticky["step"] = sc.sticky["step"] +1
5. if y:
6.     sc.sticky["step"] = sc.sticky["step"] -1
7. if z:
8.     sc.sticky["step"] = 0
9.
10.  a = sc.sticky["step"]
```

Fig. 5.30. b) Layer selection button

End effector definition

The plug-in allows the definition and calibration of a user-defined end effector. This is made possible by the custom end-effector component that takes as input the end effector mesh geometry, as well as a component that uses sliders to position the end effector on the robotic arm, as shown in *Figure* 5.31.

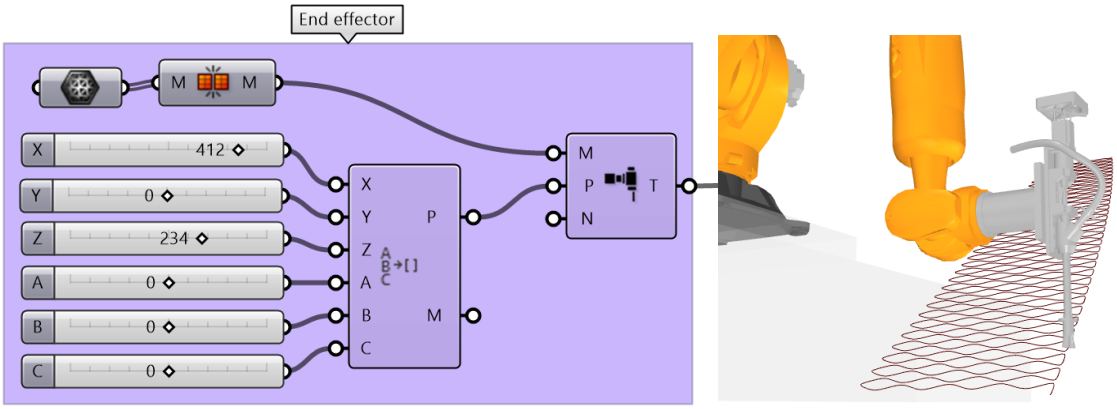

Fig. 5.31 Custom end-effector definition

Robotic arm & External Axis definition

FURobot offers an extensive library of commercially available robotic arms, as well as a tool to define a custom model. The main requirement of the robotic arm is to have sufficient reach. Kuka 4343 was chosen as a robotic arm that fulfilled this requirement. However, there are cases, such as the topic of the thesis, when the reach of the robot is insufficient. To print a larger object, an external axis is used. In FURobot, there is a pipeline for defining a custom external axis.

The main issue is that the robotic arm needs to move back and forth, while printing a single layer. To achieve this motion, a list of values as positions is generated, according to the Y coordinate of the start, middle and endpoint of each toolpath. In this way, the motion can by only alternating or consistent, depending on each toolpath. This part of the script is showcased in *Figure* 5.32.

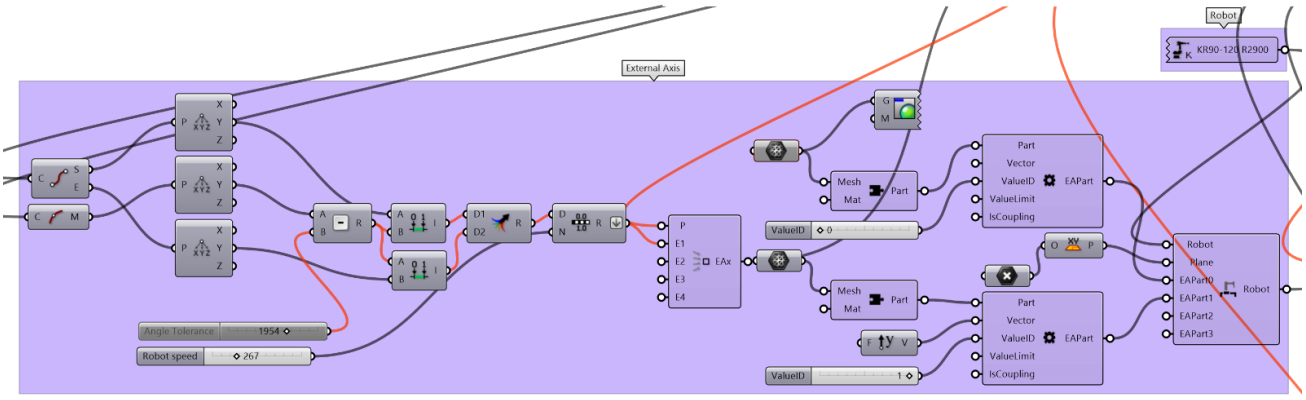

Fig. 5.32 Robotic arm & External axis definition

Simulation Check & G-code generation

All the above functions are essential in defining a working G-code. When they are completed, they are assembled into the main component of FURobot. The simulation output is visualized and checked in real-time on the Rhino 3D interface. If there are any issues or errors that might come up during the assembly and check, they can be

pinpointed and resolved. When the final check is successful, the G-code of the specified layer is output and can be copied and transferred to the robotic arm controller in text form. This process is illustrated in *Figure* 5.33.

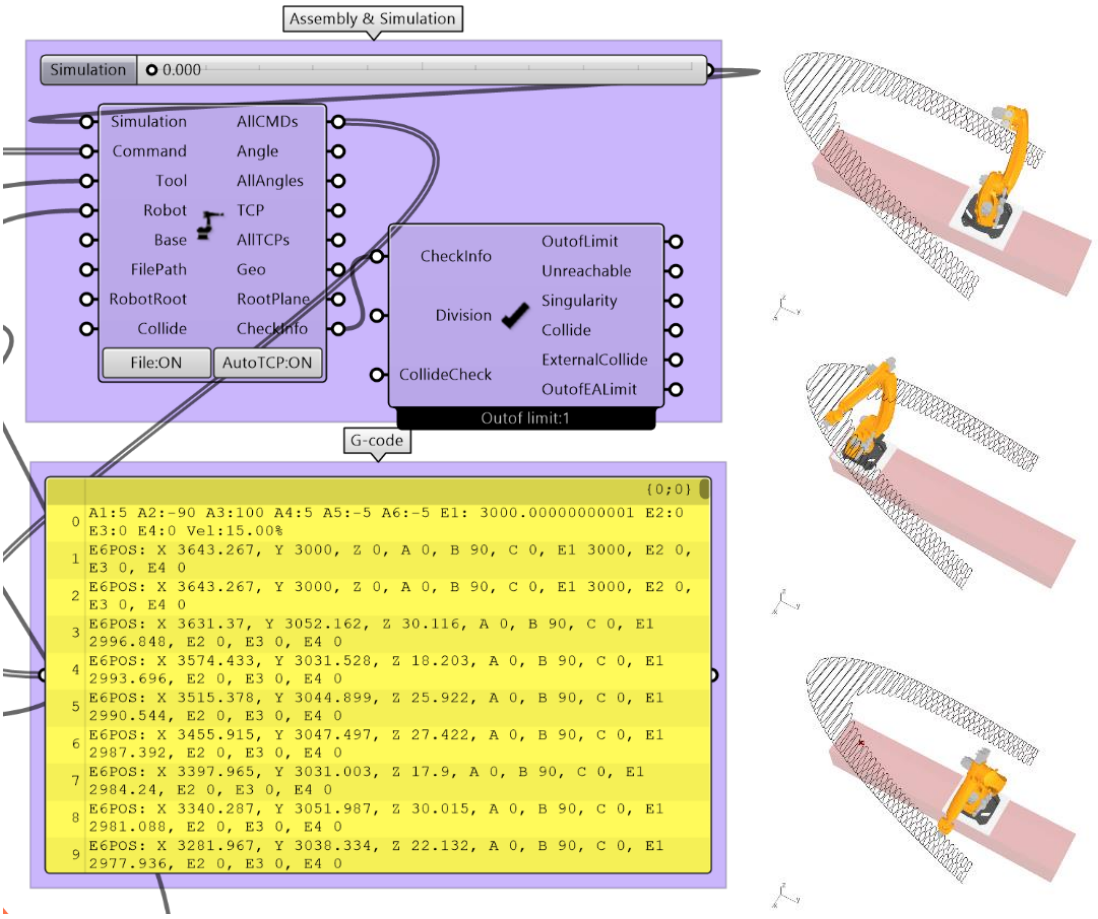

Fig. 5.33 Simulation check & G-code

5.3.6 LCA integration

Life cycle analysis [LCA] is an impact (environmental, economic) estimation methodology over the entire lifetime, from cradle to grave. LCAs are very beneficial when a series of options is considered, in order to determine the optimal one. In addition, they can be used as benchmarks for products in terms of efficiency and cost. They are typically completed through spreadsheets.

Grasshopper can perform spreadsheet functions, such as the ones normally utilized by Life Cycle & Cost Analyses. The advantage by integrating them in the parametric model is the processing of data and visualization of results in real-time, assisting in evaluation and decision-making.

Methodology

Due to the lack of available datasets, a thorough LCA that takes into account the complete lifetime from “cradle to grave” is not possible. In its place, a literature review is conducted on case studies with similar characteristics, in order to make a comparative assessment. However, when possible, calculations are made.

In the case of housing structures, a useful way of organizing the total lifecycle impact is dividing it in two parts, as shown in Figure 5.34:

- Embodied Energy
- Operational Energy

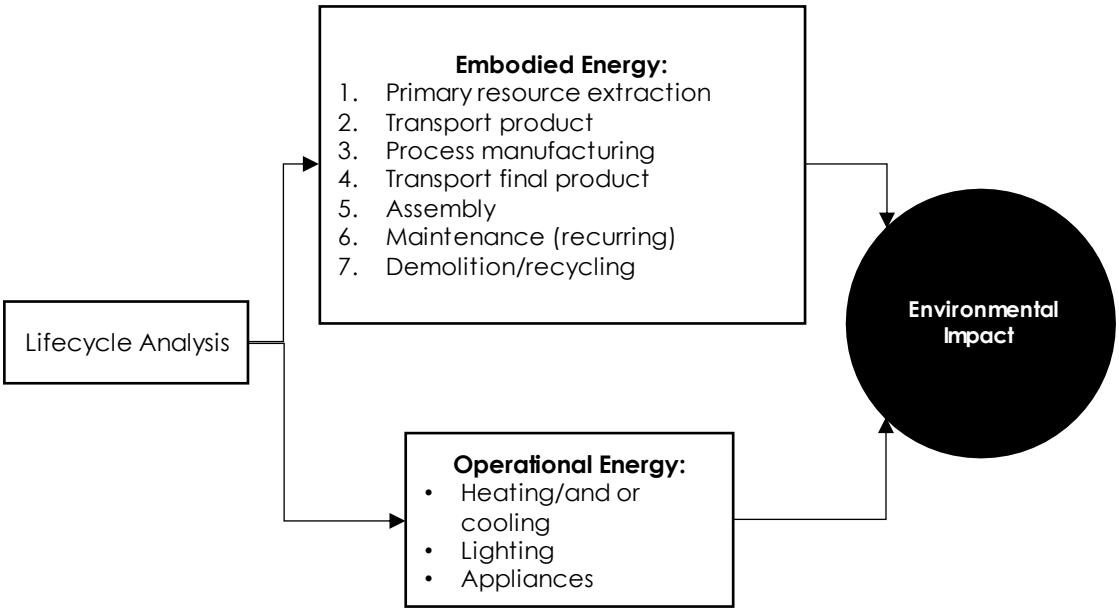

Fig. 5.34 LCA scheme

Embodied Energy

In order to estimate the viability and impact of earth construction, the supply of the required materials needs to be addressed. The embodied energy is the sum of energy requirements during the phases of material production, transportation to site, construction & maintenance of the final structure, demolition & recycling (McMullan, 1983) as illustrated in *Table* 5.3. Naturally, using local soils results in lower embodied energy due to less transportation and processing costs than technical materials (Zabalza et al., 2010). A common indicator to quantify the embodied impact per unit floor area is [MJ/m2]. Therefore, the most energy intensive process is the additive manufacturing process, which is dependent mostly on the robotic arm energy demand of 3 kW. This calculation is integrated in the parametric tool, as it is directly related to the geometry. By powering the extrusion using solar panels the Embodied Carbon of the electricity is minimized, as they have the least impact.

Table 5.3 Embodied impact of Earthen structure

Embodied Energy	[kWh/m2]	[KgCO2]
Primary Resource Extraction	16	0.93
Transport unfinished product	0	0
Processing & Manufacturing	800 - 1000	46.4 - 58
Transport Final Product	0	0
Assembly	0	0
Maintenance (Recurring)	0	0
Demolition/Recycling	0	0
Total	873	52

Operational Energy

The use phase is evaluated by the operational energy required and is related to comfort. It involves the heating and cooling demand, domestic hot water and appliances, as well as lighting. It should be noted that the impact of renovations or maintenance is not included in this component.

The operational energy is interrelated to the thermal performance of the construction, which is not studied in this research. Moreover, it is highly dependent on the climate aspects of the location. Therefore, assumptions are made from literature. These are comparatively shown in *Table* 5.4. More specifically, the research of Lidia Rincon (2019) on the thermal behavior of an earthbag dome shelter in a Mediterranean climate is taken as a reference. The research confirms the low insulation of earthen constructions measuring a thermal conductivity λ as high as 2.18 W/mK.

The design integrates passive environmental design strategies to achieve thermal comfort during winter and summer, such as direct solar heat gain combined with the heat storage capacity of the high thermal mass, as well as cross ventilation. Though the form studied in the literature is not identical to the case study, the same strategies can be directly applied to improve thermal performance. In the end, as concluded by the research, an energy demand of 1.3 kWh/m2 per day for the heating season is assumed. However, there is high variation in the geographical distribution in the length of the heating period in Greece. It ranges from 140 days in the south to 220 days in north. A favorable location should be preferred.

Regarding the typical construction, the research of Chastas et al. (2017) is used for a single-family house in northern Greece. As a heating season of 181 is assumed in this case, the same will be used for calculations on the earthen construction.

Table 5.4 Operational Energy comparison

Energy Demand	Typical construction	3D printed earth
Heating [kWh/m2a*]	53.59	235.3
Cooling [kWh/m2a*]	33.27	0
Domestic Hot Water [kWh/m2a*]	30.30	30.30
Total	117.16	265.6

a: annually.

Results

In order to provide a more comparative assessment, the estimated values will be compared with the ones of a typical concrete dwelling structure in a similar climate. They are tabulated in *Table* 5.5. In this case, the research case of Sabnis & Pranesh (2017) will be used as a reference for the embodied energy and carbon values

In order to estimate whether the overall impact of a construction is larger, the expected lifetime of the building needs to be specified by the user. The workflow calculates and compares both the impact of the earthen construction and a typical concrete one. Then, according to the need, the best option, as well as its projected impact is highlighted. According to these assumptions, if the lifetime of the construction is above 9 years, the typical construction has less impact in terms of overall kWh, as shown in *Figure* 5.35.

Table 5.5 comparison data

	Embodied Energy [kWh/m2]	Embodied Carbon [kgCO2e/m2]	Operational Energy [kWh/m2 per year]
Typical construction	1440.5	486.77	117.16
3D printed earth	873	52	265.6

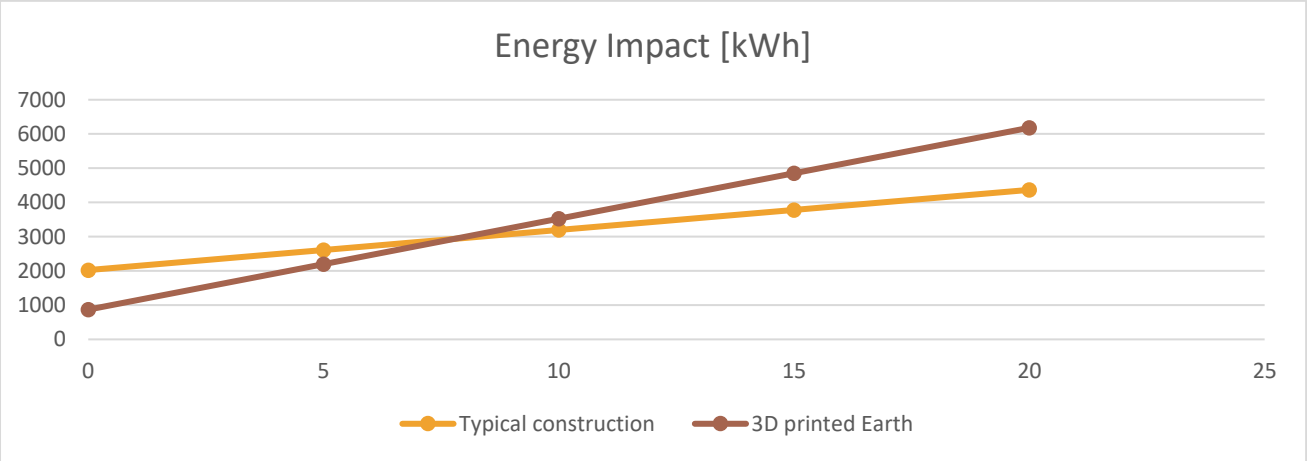

Fig. 5.35 LCA scheme

5.3.7 User interface

The digital design workflow utilizes the HUMAN UI plug-in to provide a user-friendly interface for accessing the digital workflow tool for people that are not familiar with Grasshopper3D.

Interface design

The interface is organized in 4 columns. In the first one, the design decisions are organized in discrete panels according to the form finding steps. The user inputs the required information, from geometrical constraints to mix design and lifetime.

The second one corresponds the specific design decisions the user has made into geometrical thumbnails, providing real time feedback. In the third one, all design decisions are integrated and the end design is showcased. Finally, in the fourth column the impact of the proposed structure is illustrated in terms of material use and Life cycle Assessment, taking embodied and operational energy into account and comparing it to a typical concrete construction in the same climate. In this way, the user can directly know whether the proposed solution meets sustainability criteria for the determined lifetime.

Interface screen

A snapshot of the developed user interface is depicted in Figure 5.36. Additionally, a short demonstration of the interface workflow was recorder and can be accessed at: https://youtu.be/1ataE-AWpAA

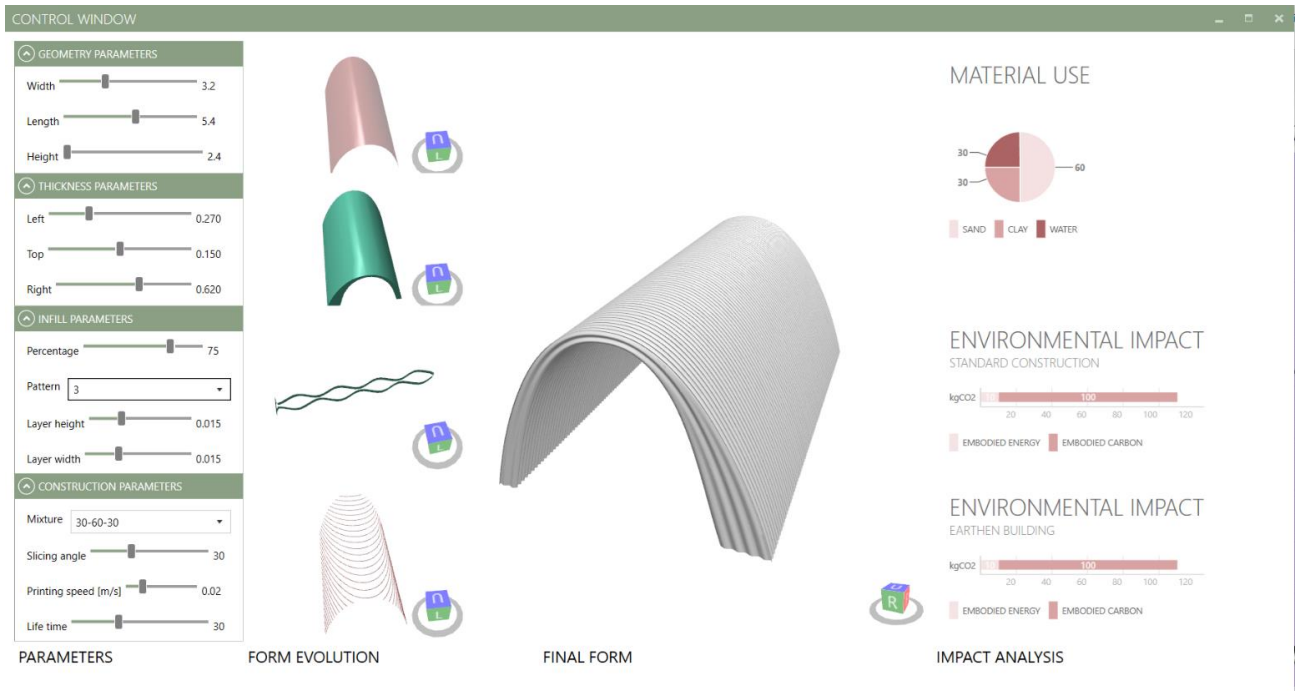

Fig. 5.36 HUMAN UI User interface

5.4 Prototype

Unfortunately, the manufacturing of an actual prototype was not possible due to the current pandemic. In its place, scale models shown in Figures 5.37.a) & 5.37.b) respectively were fabricated. The prototypes were printed using PLA in a private-owned Prusa Mini. The intention was not only to show a visual of the proposed solution, but to showcase the design as a byproduct of its manufacturing process. Both of the prototypes have a 0.2 mm layer height. The filament width for the 1:20 prototype is to scale. Therefore, in the 1:100 prototype, the inclined slicing concept is showcased, which resulted in no need for supports. The object is printed as a solid with a predefined infill as the scale was too small to showcase the design.

Fig. 5.37.a) "Nubian" printed 1:100 prototype

On the contrary, in the 1:20 section the infill is not predetermined by the slicer software, but adopts the design. It should be mentioned that the Nubian printing technique is not used in this case, as only an arch is printed and not a full vault. Therefore, as can be seen in the sliced image, supports were required. The arch is segmented in 3 parts to show the fabrication-aware constant infill density, despite the cross-section optimization

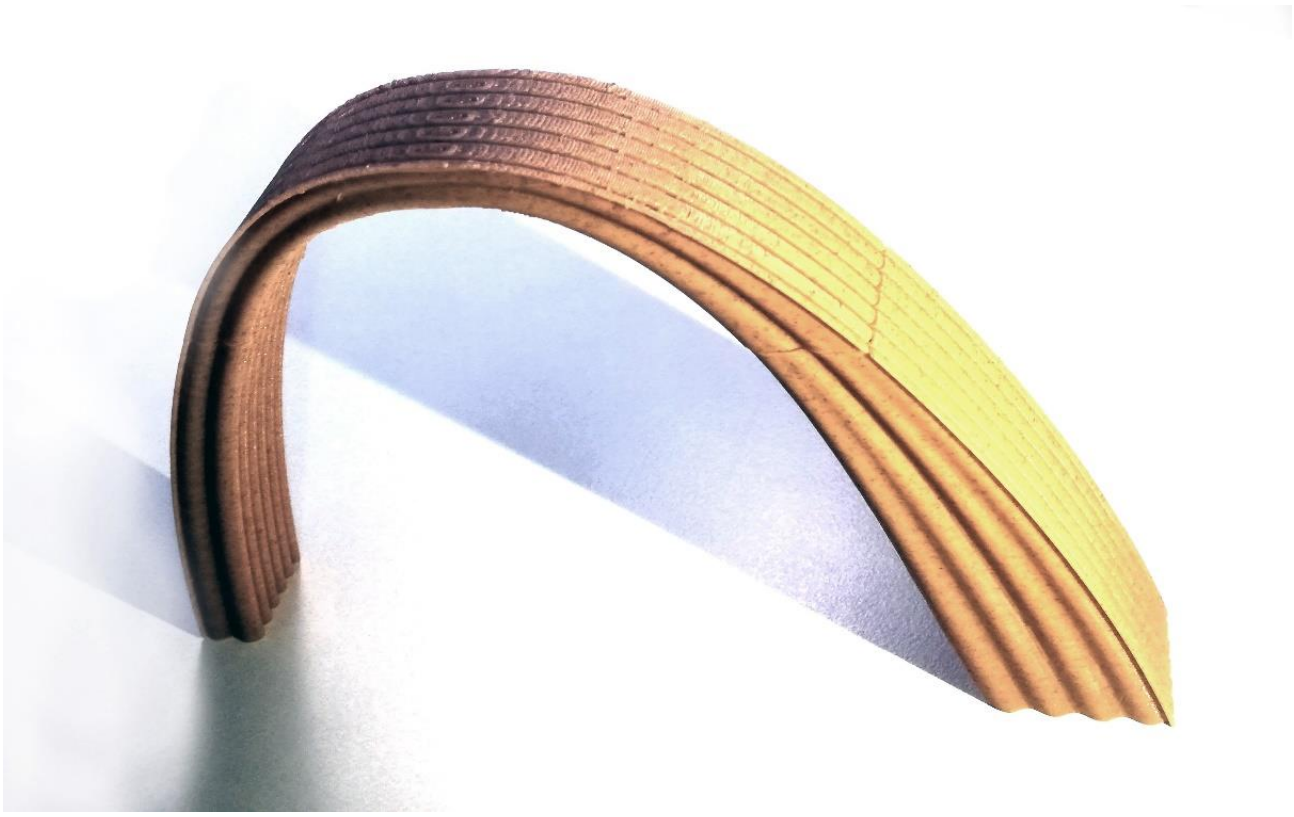

Fig. 5.37.b) 1:20 section prototype

5.5 Results

5.5.1 Framework for on-site resource utilization FOR 3D printing

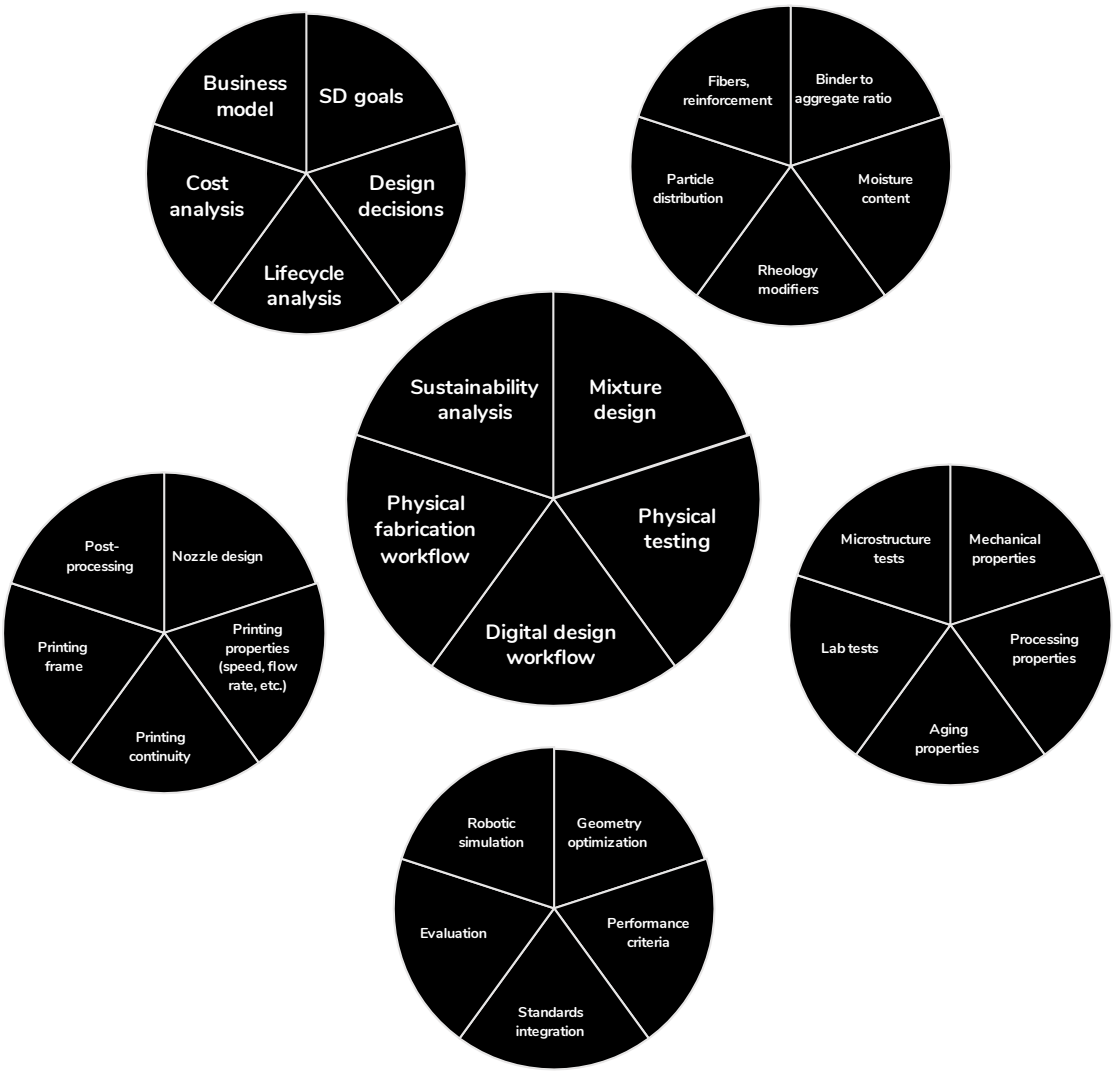

Fig. 5.38 5.5.1 Framework for on-site resource utilization FOR 3D printing

5.5.2 Physical Workflow

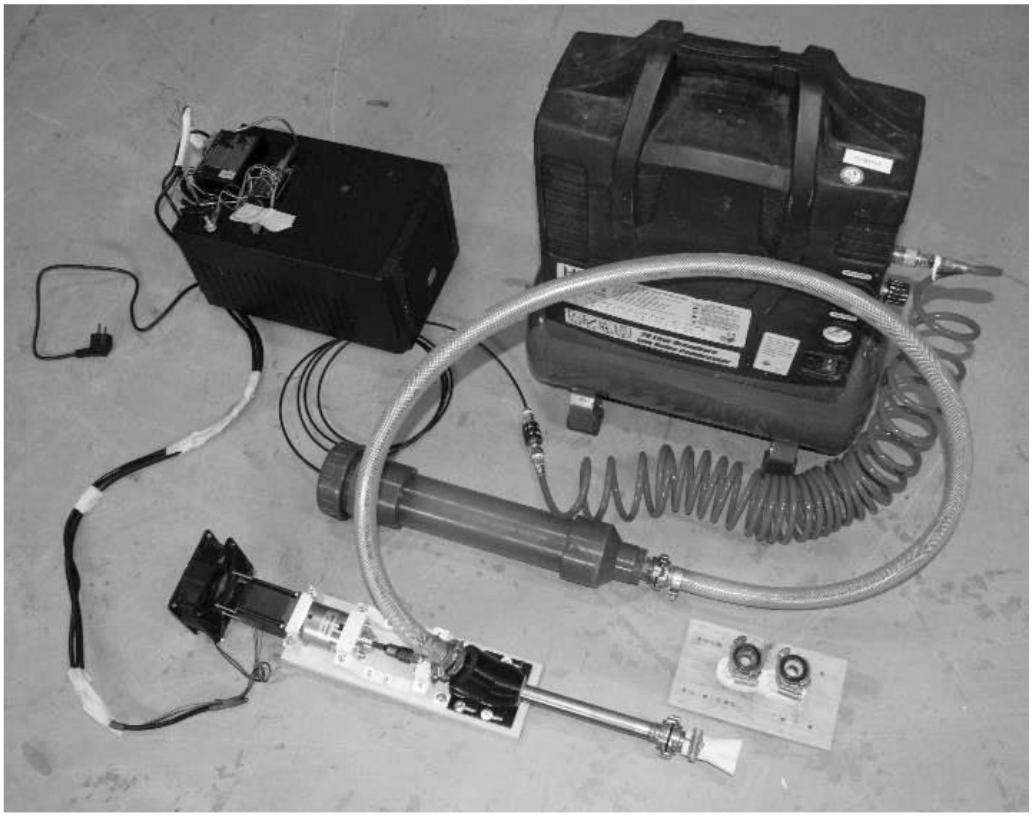

Fig. 5.39.a) Physical setup

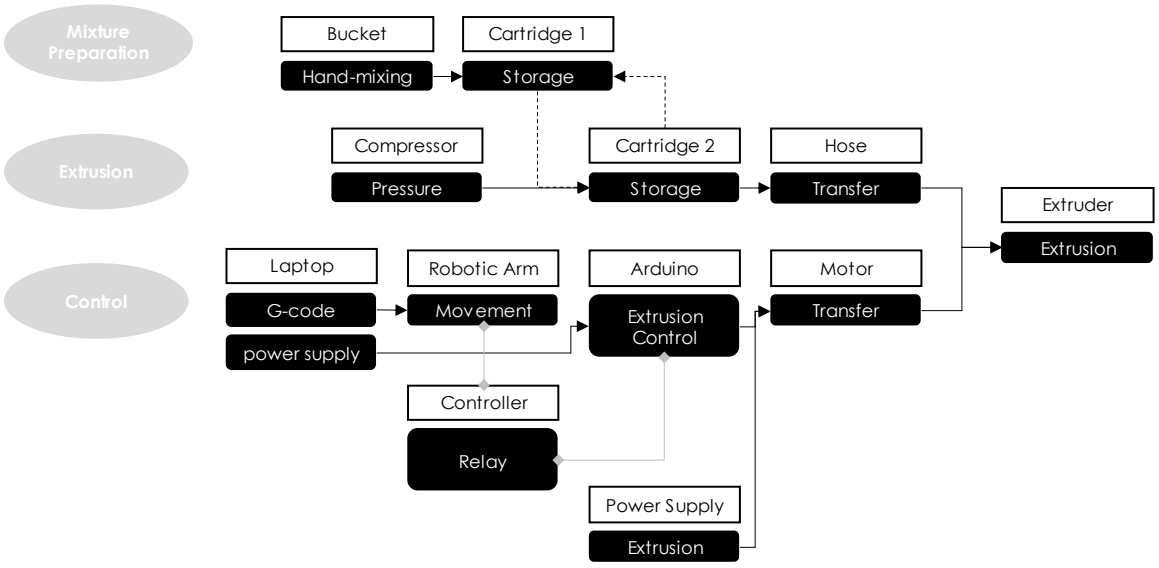

Fig. 5.39.b) Physical setup diagram

5.5.3 Digital workflow

Current workflow

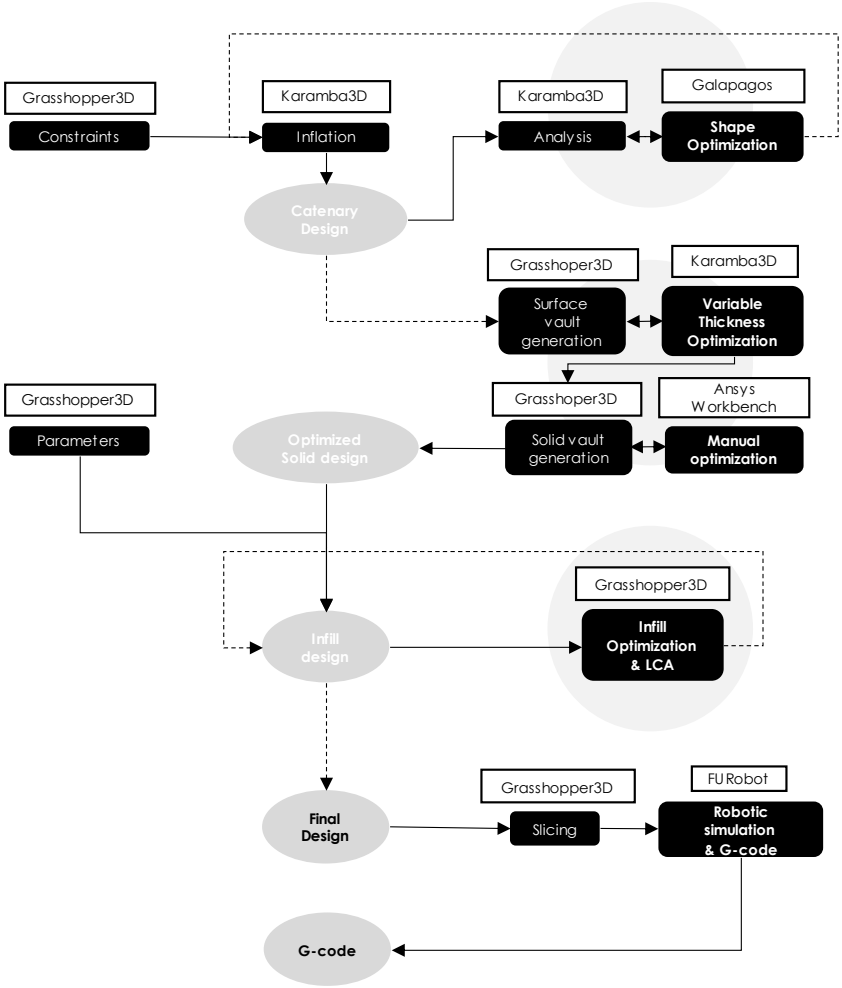

Fig. 5.40.a) Digital design to fabrication to LCA workflow

Ideal workflow

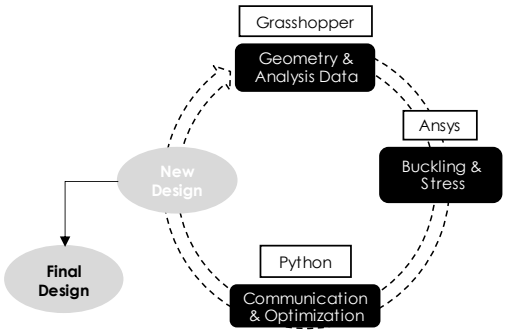

Fig. 5.40.b) Ideal digital workflow

5.5.4 Case study

Typically, a Nubian vault is a solid structure with a cross section of 60cm. Through the proposed workflow, a theoretical material reduction of 56% is possible.

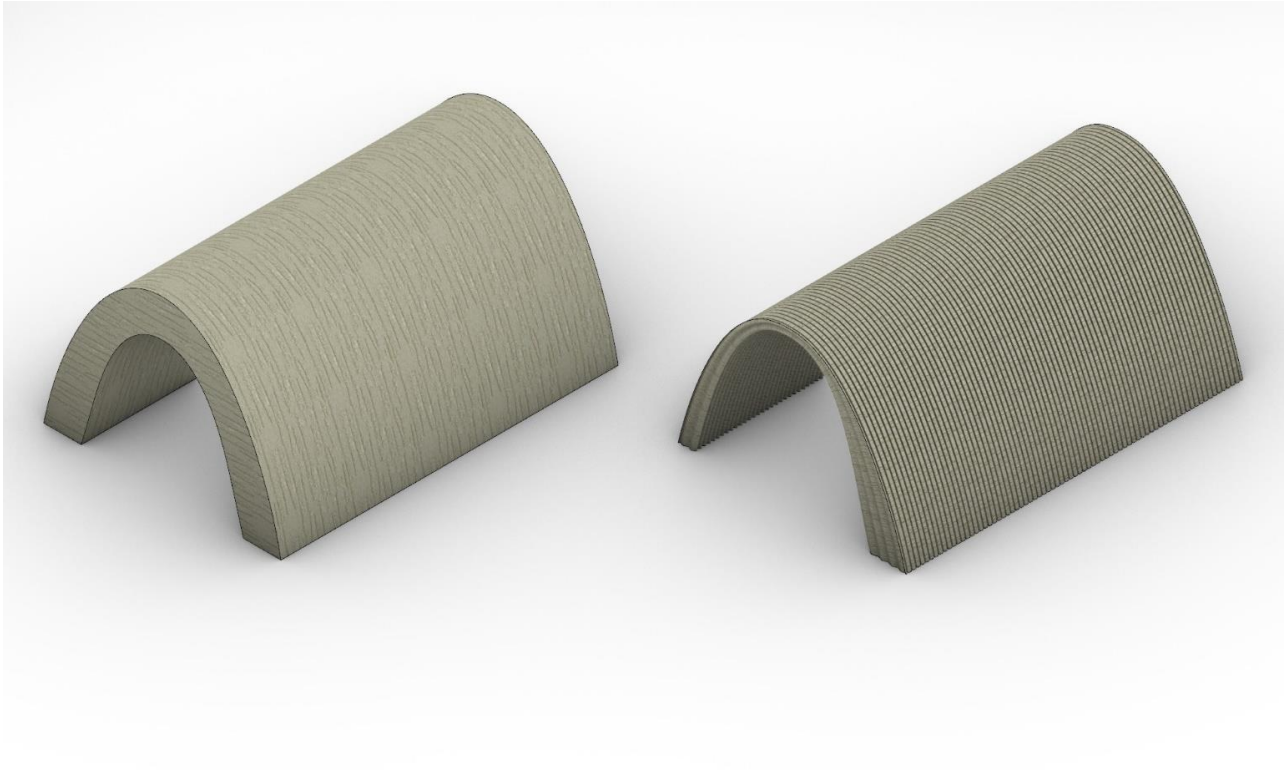

Mass before optimization: 39410.8 [kg]

Mass after optimization: 16970.8 [kg]

Reduction: 56%

Fig. 5.41 Material optimization result

5.6 Final Design

5.6.1 Sliced Layers

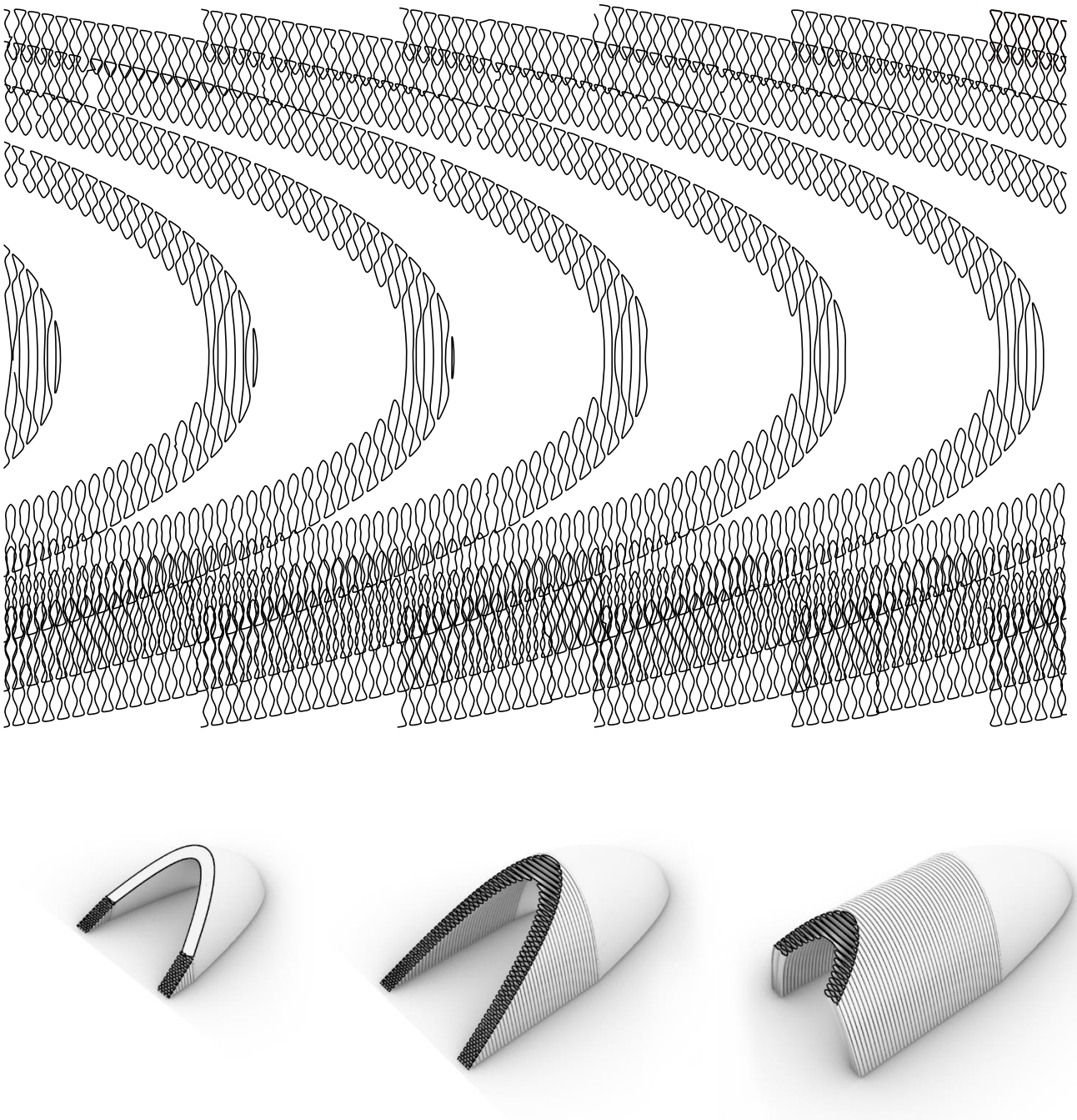

Fig. 5.42 Examples of toolpaths & fabrication sequence

5.6.2 3D Visualizations

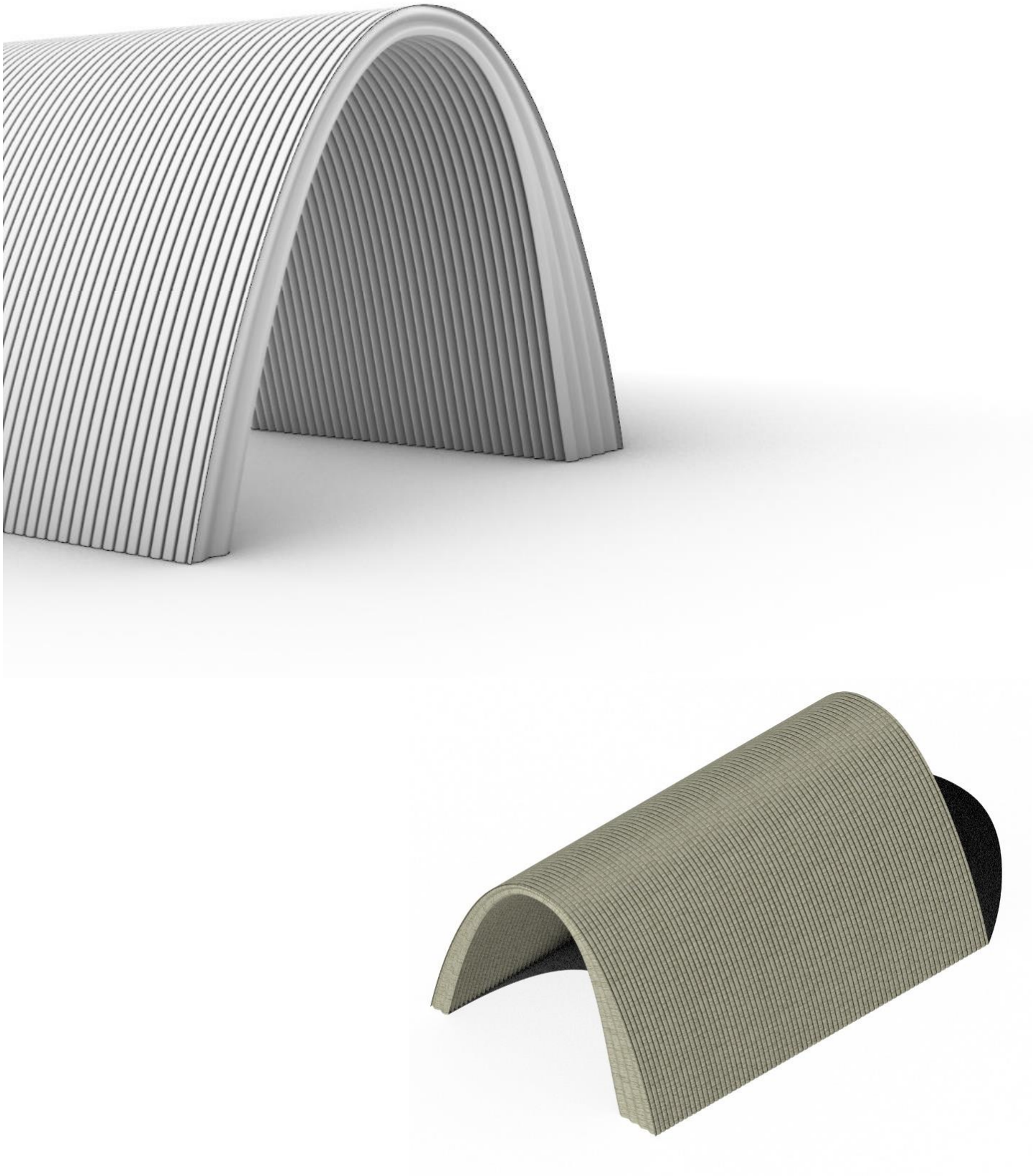

Fig. 5.43 3D visualizations

6 Discussion

This dissertation recorded the definition of a physical and digital pipeline on designing and fabricating a structurally optimized 3D-printed shell out of earth. In this chapter the limitations of the approach will be discussed and recommendations for their improvement will be made. Essentially, the development of a functioning workflow was just the first step in introducing this field of research. A starting point on which future research can build upon by reducing the steps, optimizing the workflow or by developing a step further, increasing the depth of the research and validity. The limitations are divided in two categories; the ones related to the physical workflow and the ones related to the digital workflow.

6.1 Physical Workflow discussion

6.1.1 Printing continuity

RAM has the potential of continuous and autonomous fabrication from start to completion of a structure. However, the current setup limits the potentials of paste extrusion due to the use of manually replaced cartridges for refilling. This requirement for human intervention results in a discontinuous process. This will inevitably cause cold joints and inconsistencies in layer bonding, compromising structural stability. Though the cartridge replacement process could potentially be automated, this type of imperfection due to the finite nature of the setup is hard to model and account in FEA software, reducing their reliability. Moreover, additional steps of calibration need to be introduced, increasing construction time and risks for error. For these reasons, a continuous setup should be developed.

6.1.2 Printing speed

The current printing speed achieved by the extruder is around 1-2 cm/s. This is mainly caused by the use of sand to the mixture. Its addition as aggregate significantly reduced the need for clay and eliminated shrinkage, while increasing compressive strength. However, some particles managed to drift between the pipe interior and the snail, clogging the machine. To overcome this issue, a gearbox was installed to increase torque strength, as the stepper motor was not able to overcome the frictional forces inside the snail pipe. This reduced the maximum speed exponentially, without actually solving the issue of clogging. The main component that is responsible is the concrete drill bit utilized as a snail. Being a commercial product designed for a different cause, it did not function as intended due to its geometrical properties. Compared to professional Teflon snails for clay extrusion, the flank thickness was much higher, increasing the contact area with the inner surface of the pipe, as well as the helix angle. A different drill bit could be tested or developed that is similar to commercial ones, such as the one sold by WASP or Lutum, or purchased directly. Another direction could be the exploration of a different extrusion principle, in the form of pump extrusion through a syringe logic. The same stepper motor can be reused, as well as most of the parts of the existing setup.

6.1.3 Material limitations

Due to the natural and on-site soil approach of this thesis, the material exploration was limited to a broad exploration and understanding of the processing parameters of a readily available and sufficient mixture for extrusion. As a result, the final mixture properties have a wide range of values in terms of strength. On the other

hand, there is a very limited number of options to control these properties after the mixture is prepared. Development of concrete paste relies on an extended backdrop of research in fine-tuning its properties through additives, such as hardeners and re-plasticizers, as well as the current unsustainable network of material flows. For the specific case study, this condition was deemed acceptable due to the temporary nature of the construction. In order to develop earthen construction for more permanent functions without considerable increase in environmental impact, locally available hardeners, such as lime can be considered, as well as hybrid systems with timber as load bearing structure and earth as fill.

Next step for the material exploration could be the integration of performance criteria beyond structural optimization. Through the deposition of different materials, properties tailored to the application can be achieved. A multi-head printer or the synchronization of multiple robotic extruders will allow the simultaneous printing of materials with light-weight, self-healing, load-bearing, acoustic or insulating properties.

6.1.4 Standards development

3D printed materials are the product of their printing processes. Therefore, main limitations related to standards development is the establishment and agreement on a specific workflow as well as the printing condition. Currently, there is a lot of research in understanding and modifying the material properties in a laboratory setting. However, one of the main arguments for 3D printing is on-site construction. It would be an interesting avenue to explore the control of printing conditions despite changes in the environment, for example with the assistance of sensors to adjust moisture according humidity.

6.2 Digital workflow discussion

6.2.1 Form discussion

This form was chosen due to its easily extendable area, its openings that allow it to function both as roofing area and usable space, as well as its compatibility with “Nubian inspired” printing to avoid sub-structure. However, as a single-curved geometry is a less rigid structure than a doubly-curved one, it required a substantial surplus of material to achieve structural safety to the point that it could be contested whether it can be considered a shell structure due to its high thickness in places. This thickness could be reduced further if the structure was oriented in parallel to the prevailing wind, as stiffness is higher on that axis. However, the worst load-case scenario was assumed for research purposes.

6.2.2 Infill design

The method accounted the impact of the infill design as a percentage reduction of the mechanical properties. Though, such correlations have been experimentally noticed, their effect may not be directly equivalent in practice. Physical tests should be performed to validate these assumptions. Moreover, the infill pattern is chosen based only on structural criteria. Other types of performance or ornamentation were not considered. However, they are possible to integrate in a multi-objective optimization process.

6.2.3 Robotic simulation

As the infill generation is integrated in the overall form volume and does not need to be generated in a different process, the simulation for the robot movement was a fairly easy process. Slicing was performed with simple Grasshopper3D components and toolpath G-code generation utilized the free plug-in FURobot. The integration of an external axis extends the useable reach area in one axis, which is compatible with the investigated geometry. It would be interesting to develop a mobile robot arm setup that can be driven in an area domain. This is also possible with FURobot, though it wasn't required for the specified structure. However, what was not considered in the simulation process was the synchronization of the robotic arm movement with the extrusion printing. Currently, the robotic arm and the stepper motor have separate controllers. Developing a connection through a relay switch was part of the ambition for the project, but it was not possible due to the Covid-19 and closing of the facilities.

6.2.4 Structural evaluation

Karamba3D has the potential to integrate form-finding and evaluation in its setup. However, its validity is currently limited to linear isotropic materials, such as steel and corresponding structures, such as beams, space frames and reinforced shell structures. Moreover, its reliance on triangular finite elements results on an overestimation of the stiffness of a structure. That is why external professional software, such as ANSYS or Sofistik are required to validate the results.

Sofistik provides tools to integrate Rhino generated NURBs geometry, as well as Grasshopper components to set up a structural analysis. However, it currently supports shell elements with constant thickness. This should normally not be an issue as shells are typically thin. In that case, shells utilizing timber or steel rebar can easily be considered for that setup.

In the case of mono-material earthen shells where there is high thickness variation, a solid based analysis software is needed, such as Ansys. Ansys currently does not provide tools for Grasshopper3d integration and Karamba3D does not generate solid forms. Therefore, an intermediate step to translate the generated values to a solid geometry was developed in Grasshopper3D. Though it allows easy generation of different thicknesses on the shell, the export is still done manually. An external script utilizing Python and machine learning to facilitate an automated "loop" process to link Grasshooper3D and Ansys and lead to a more optimized result is possible and has been achieved by researchers. However, it was beyond the scripting skills of the author.

6.2.5 Impact & Cost analysis

Standard construction materials, such as steel, concrete, fired bricks, even timber have been developed in the sector of civil engineering, and extensively researched in universities (Schroeder, 2015). Lifecycle analyses can benefit from a number of different datasets that quantify the impact of those constructions. On the contrary, earthen construction science is still in its early stages. Therefore, there is no elaborate database for Additively manufactured earthen buildings. The limited amount of prototype pavilions is fairly new and are still being monitored for their performance. Therefore, the impact and cost analysis system boundary are limited to the information on the needed material and time of fabrication. Moreover, even when there is relevant literature, comparisons are difficult due to the variations in scopes and system boundaries.

7 Conclusion

This section presents an overview of the research findings towards RAM of earthen structures as a concrete alternative. In the beginning, the research methodology and questions are addressed. Then, the arguments for the adoption of the proposed method to architecture will be highlighted. Finally, suggestions for future research on aspects of the project that require further investigation will be made.

7.1 Conclusions

The main research question: "*How to develop a design to fabrication workflow for a structurally optimized shell towards robotic additive manufacturing by earth*?" captures the research agenda and avenues as the intersection of the following words and phrases:

1. *Design workflow development* with
    a. *Structural optimization*, as performance criterion
    b. *Shell structure*, as the investigated geometry
2. *Robotic fabrication workflow development* with
    a. *Additive manufacturing*, as a construction method
    b. *Earth, as a structural material*

This intersection is only made possible through current digital tools that allow efficient control and exchange of information among the different disciplines involved and physical tests to provide the data not available in literature.

However, the above avenues are not independent and should not be investigated separately. For example, additive manufacturing alters the material properties of earth, and the investigated geometry is limited by the robot reach. Therefore, another approach is needed to be adopted to organize the above key concepts into new interdisciplinary clusters. The approach chosen is the design by research and research by design methodology.

The *research by design* part integrates the material exploration and extruder design and manufacturing with the end goal of developing guidelines for an earthen paste that is suitable for structural applications and at the same time extrudable from the prototype physical setup, pushing the limits of both. Therefore, it mostly involves the physical setup. From this direction, the first sub-question was formed as: What are the advantages and limitations of using earth in RAM? What is the effect of material parameters (mixture design /kiln /drying time) in the mechanical properties of the component and what are the required material qualities for the proposed setup?

This question is mostly addressed in the literature review and the design by research section. The main advantages of earth as a construction material are its global availability, recyclability, sufficient mechanical strength with high thermal mass, and its compatibility with Additive Manufacturing. On the other hand, its main disadvantages are its water resistance, its limited mechanical strength, its lack of standardization and the prejudice associated with a non-technical material.

Considering strength as the investigated criterion there are some guidelines that should be followed. To begin with, the moisture content should be close to the Plastic Limit of the clay-based mixture, while allowing sufficient flowability and extrudability. Regarding the dry elements, a higher clay content improves cohesion and surface bonding, increasing shear strength, plasticity and surface finish. At the same time, it enlarges the effects of drying

shrinkage. On the other hand, higher aggregate content, such as sand, improves compressive strength and shrinkage behavior. However, even more important than the aggregate content for the mechanical strength is the accomplishment of mixture homogeneity that assures proper coating of the aggregate particles with clay. The use of kiln to take advantage of the vitrification process of ceramics is a proven method to increase strength. However, the kiln size becomes a limiting factor for the size of the structure. Therefore, there is need for segmentation, redundancy and assembly strategies. In addition, the sustainability-related arguments of earthen construction are essentially negated, as current firing processes are more energy intensive than construction with concrete. Lastly, drying time in on-site printing is difficult to control in this setup. Assuming the integration of sensors to control moisture, the drying time should be long enough to ensure adequate layer bonding, while being short enough to expedite the transition from green to dry strength.

In addition, the main limitations of additive manufacturing as a construction method still apply. Some of those are printing frame, overhangs and certification issues. These are currently being addressed by researchers worldwide, such as Skitmore & Perkins (2015), Bos et al. (2016), Baarsen et al. (2015) and Galiaard et al. (2015). To overcome size limitations, researchers Shepperd P. & Williams C. (2017) are developing a swarm of UAVs in order to 3d print structures of any geometry. In terms of overhangs, the ultimate goal would be the 3d printing of overhanging or horizontal structures at-place without supports. This is an issue of material properties over time, as well as printing angle. Projects, such as the "Apis cor impossible printing" utilize a "Nubian" inspired printing technique, as well as fast-setting concrete to develop a workflow for addressing the next frontier in 3D printing in construction. In terms of certification, currently contractors need to provide their own warrantees for a 3D printed building, as there in no universal code that applies. This is normal for novel building techniques and is expected to stay like this for the near future. However, as with previous technological innovations, such as reinforcement, the building codes will eventually catch up. Pioneer projects like the two-story residential building erected in Germany by the Danish manufacturer COBOD and the PERI GmbH construction company showcase that 3D printed buildings can obtain regulatory approval (Peri, 2020).

The design by research part combines the literature review and the results of the previous part to form the digital workflow that bridges the immaterial aspect of the form-finding, evaluation and simulation, with the material aspect of robotic control and fabrication. From this endeavor, the second sub-question is formed as: "What are the design and performance criteria involved in designing a robotically 3D printed component out of earth? What is the effect of printing parameters (infill percentage & pattern, layer height & direction, extrusion speed)?" To communicate these criteria, a new terminology for additively manufactured materials is currently being formulated. These novel criteria consist of buildability, extrudability, flowability, open time, as well as traditional ones such as compressive and shear strength. Printing parameters are crucial in the resulting mechanical properties of a component. As the resulting geometries are porous, they are consequently hard to model and predict accurately at the moment. Therefore, physical tests are required to quantify them. However, their effects can be observed.

In principle, infill pattern should be aligned to the principle stresses to provide lateral stability. Moreover, there is a correlation of infill percentage and mechanical properties. Adjusting them according to the infill percentage is a common practice to factor its effect to the overall strength. However, that is mostly applicable for the Young's modulus E and the maximum stress σ. For the other values, the lowest recorded limits were used.

Regarding filament properties, an increase in layer height has a positive effect on the maximum stress. This can be attributed to the reduction of the total number of contact interfaces between layers, which are the cause of pores and insufficient layer bonding. However, as the amount of material extruder is constant, an increase in layer height is naturally accompanied by a reduction in layer width. This affects negatively the buckling resistance of the element, which in the case of shells has the highest risk of failure. Printing direction results in orthotropic material properties. Therefore, as with other orthotropic materials the axis aligned to the filaments exhibits higher strength and should be aligned with the principal stress directions. In practice this is difficult to achieve without formwork. Therefore, a "Nubian" inspired printing direction was assumed as it takes advantage of the maximum allowable overhang angle, without causing plastic buckling failure. Finally, extrusion speed is related not only to printing time, but also to layer width and interlayer bonding. With a lower extrusion speed, it is possible to push more filament increasing its width and layer adhesion.

The end result of the proposed method should be evaluated based on its merits and its contribution to architecture. Though the cultural aspect of computational design and digital fabrication as an architectural style is present and can be debated, it is undeniable that contemporary and future architecture is becoming more and more environmentally conscious and in line with sustainable development goals. The degree to which the aforementioned methods and tools can contribute towards this is evaluated by the last sub-question as: "What is the projected cost and environmental impact of the proposed construction?" A complete answer to this question would require the consideration of a building's whole lifecycle from "cradle to grave". In this system boundary, comfort conditions and energy demand calculations, as well as energy reduction measures constitute a significant section of a building' s carbon footprint. One, that contemporary technical materials excel at. However, these performance criteria were beyond the scope of this research.

As this research focuses only on the structural performance of construction, it can not reliably be compared to an actual building envelope, though some general material properties are mentioned. Available indicators, such as Primary Energy Intensity and production costs can only offer comparative information on the impact of the construction, with a system boundary "from cradle to gate". Therefore, in this view this question was answered to the extent that the energy & cost reduction potential of the construction is high enough to offer a promising alternative to concrete due to earth's high recyclability, local availability and compatibility with RAM. Moreover, the material use reduction achieved by the process is noteworthy as despite the abundance of sand, clay is an important material in many fields of human activity.

7.2 Recommendations

This section covers recommendations for future research avenues that the author thinks are most important. Although some have already been hinted at during the discussion points or they were beyond the scope of the current project, they require special mention.

7.2.1 Multi-storey construction

For the successful implementation of 3D printing in construction, it will eventually need to compete with established methods in an automated way. For that, multi-storey construction is the next frontier. The most significant obstacle towards this is reinforcement integration. Steel printing or robotic steel rod welding during printing are some of the ideas that are currently being researched. Another avenue could be the use of timber from proximal sustainably harvested forests for load bearing function, utilizing the 3D printing materials as fill. Therefore, future research should be aimed at manufacturing code compliant building elements.

7.2.2 Multi-objective optimization

The added value of 3D printing is its potential to integrate different material properties as well as services by design through programmable material behavior. Therefore, all related building elements and the indoor conditions they achieve should be investigated and tested according to their respective performance criteria in different climates. In this way, a toolkit system can be formed that ensures high quality, comfort conditions and safety.

7.2.3 Sustainability Analysis

As lifecycle and carbon footprint analyses become an increasing requirement of buildings, in-situ resource utilization becomes an attractive option to mitigate construction impact. Therefore, a quantitative assessment of each stage of a building's lifecycle should be made and compared with typical construction.

Furthermore, the sustainability analysis should be accompanied by a business model and marketing strategy. This option could be

7.3 Reflection

In this chapter, a final reflection is composed on the graduation process and topic.

7.3.1 Graduation Process

Relationship between graduation topic & studio theme/method

The thesis assignment is carried out within the Sustainable Graduation Studio. The graduation topic introduces a computationally-driven workflow for a structurally optimized building element, with a focus on shell geometries using earth as a construction material. It combines parametric design and robotic additive manufacturing in order to minimize the impact of the construction industry in the environment. It achieves this through efficient use of energy and resources using a recyclable and environmentally friendly material.

The topic is related to ongoing TU Delft research regarding 3D printing with clay as a construction material. It serves as a follow-up of Ammar Ibrahim's thesis on 3D printed clay facades that integrate ventilation systems and Tommaso Venturini' s research on earth extrusion. The main focus in this case is on Design Informatics and Structural Design, two fundamental directions of the Building Technology and Sustainable Graduation studio. Structural design and optimization processes have been limited by rationalization processes of typical construction methods, namely the cost of formwork. With the assistance of computational tools and digital fabrication methods, structural design can be freed from these constraints, resulting in a structurally optimal result. In this way, Design Informatics is very complimentary to Structural Design.

Relationship between research method & design

The main objective was to define an integrated pipeline for the successful design and fabrication using the methods mentioned above. The project follows the Design by Research & Research by Design approach. This was elaborated into four sub-objectives.

Firstly, critical examination was dealt on the state-of-the-art and best practices. This was important to define the design and performance criteria of the manufacturing process and the structure. The limited documentation and standards meant that the research was based on successful precedents and ongoing tests.

Secondly, a research by design process was carried out in the mixture exploration and extruder development. Literature on clay as a construction material provided a base for the material properties of earth. However, due to their alteration because of the manufacturing process, physical tests were deemed necessary as the basis of the design. Therefore, the project is dependent on the development of the extrusion system, especially the extruder. A non-linear process ensued where material requirements and extruder abilities were tested against each other. The completion of the extruder required a significant amount of time and alterations from the initial plan, as factors such as the availability of delivered parts, the insufficient motor strength and subsequent unsuccessful print tests

inhibited the expected progress. Nonetheless, successful and consistent extrusion is paramount for the realization of the project as the mechanical properties of additively manufactured earth are unknown. In the end, a working extruder was manufactured. However, due to the Covid-19 pandemic and closing of the University facilities, no samples were able to be printed and tested for strength. Assumptions for the material properties were made according to literature and ongoing research in agreement with the mentors. Though the decided values are reasonable, their accuracy can be contested due to the lack of physical tests.

Thirdly, a design by research exploration into the formal possibilities, informed by material and manufacturing process constraints ensued. On the definition and development of the necessary steps and tools, both physical and digital workflows were defined according to the available apparatus and the technical skills of the student. While this thesis developed an optimized shell, the use of grasshopper, which is a propagation-based system and its plug-ins, resulted in a linear process, which is not as effective as a fully parametric optimization model. Though the grasshopper and scripting skills of the author were sufficiently developed during the thesis process, in the end the computational skills to link grasshopper to the evaluation software, as well as advanced structural knowledge on non-linear FEA analysis, due to the lack of available material data were unfortunately beyond the current abilities of the author and the time scope of this thesis.

Finally, a prototyping process not only for the extruder, but also for the design task was intended. However, it was not possible to be performed due to the lack of access to a robotic arm or a clay extruder. Instead, scaled PLA samples were printed by a cartesian 3D printer to investigate infill overlapping and showcase the printing process. It is still the ambition of the author to find a way to manufacture a prototype section by clay until the final submission of the thesis.

A SWOT diagram analysis of the method is composed below. In general, the research approach led to a successful definition of a workflow that covers all the necessary steps from design to fabrication, which was the main aim of the research. Parts of this workflow that depended on external factors were not able to be realized. However, they constitute an essential part of decision making during the design, as an experimental & innovative way of construction.

	Helpful	Harmful
Internal origin	**Strengths** • Technical skills • Prototyping / Testing • Tool/workspace availability • Potential partnership	**Weaknesses** • Time/budgetary limitations • Insufficient literature • Broad nature of research • Limited scripting skills
External origin	**Opportunities** • Innovation contribution • Emerging topic • Database development • Evaluative method	**Threats** • External factor dependence • Sub-optimal design • Unreliable results

SWOT analysis of methodology

7.3.2 Societal impact

The thesis introduces an automated workflow for the practice of construction. It is currently limited by the adoption of robotic fabrication by construction companies and legal standards. However, more and more companies, especially the ones interested in prefabrication have integrated robotic arms in their processes, as well as a considerable number of startups develop robotically fabricated structures. In terms of standards development, universities and researchers already produce research aimed at providing standards for 3D printed materials,

especially in the case of concrete. Therefore, the results of this thesis will be very useful and applicable in present and future practice.

The project is aligned to sustainable development goals. The presented method achieves a significant amount of material and cost reduction, as proven by the structural evaluations, while utilizing a globally available recyclable material. Moreover, this process of construction creates significantly less waste than typical construction where formwork as well as installation work, and end of life demolition cause an immense amount of waste. Therefore, the projected innovation is realized to the extent of delivering an efficient stable structure to provide shelter and safety conditions through a responsible consumption of resources. Additional performance criteria should be developed further to ensure acceptable comfort conditions and waterproofing methods in order to extend the construction's lifespan and improve the wellbeing of inhabitants. The adoption of the proposed technologies has the potential to create new jobs, while utilizing electric energy. The repeatability offered by the setup due to its adaptive and parametric capabilities contributes to the promotion and expansion of a sustainable built environment, that inhibits climate degradation. The multidisciplinary nature of the process enhances collaboration and partnerships between all related stakeholders, facilitating local economies due to the ubiquitousness of the main material.

Social impact is embedded to all the design decisions and ambitions, especially for areas where there is no lack of space. Currently, multistorey construction is inhibited by the low strength of the material. However, part of the workflow is applicable to 3D printing with stronger materials, such as concrete, where the benefit of material use reduction is even more impactful. Concrete replacement with earth, where it is applicable, will affect lifestyles, due to different construction properties (low insulation, odor, need for maintenance). However, by utilizing local on-site materials, the unsustainable network of material transportation is addressed, while the distinctive character of each location and culture is showcased.

The use of robots in the construction industry is expected to have a significant impact in reducing the need in human labor. Moreover, this process should be gradual enough that society adapts to these changes without major issues. As these digital tools become an integral part of design to construction workflows, the boundaries between disciplines are blurred and new transdisciplinary professions emerge. The basic goal of these tools is to construct a more sustainable, safe and comfortable environment. More and more engineers educate themselves in these tools and become interested in computational design, while having more expert knowledge in their respective fields than architects. This may eventually pose a risk to architecture. However, it can also be an opportunity. As this approach integrates design and performance, architects need to find a way to take agency and penetrate these new fields, by bringing their own expertise, sensibilities and way of thinking.

8 References

The main research avenues are:

[1] Addis, B. (2014). *"Physical modelling and form finding," in Shell Structures For Architecture*. New York: Routledge.

[2] Adriaenssens, S., P. Block, D. Veenendaal, and C. Williams (2014). Shell Structures for Architecture: Form Finding and Optimization. New York: Routledge

[3] Alghamdi, H., Nair, S. A. O., & Neithalath, N. (2019, February 2). Insights into material design, extrusion rheology, and properties of 3D-printable alkali-activated fly ash-based binders. Retrieved from https://www.sciencedirect.com/science/article/pii/S0264127519300711

[4] Allen, E. and W. Zalewski (2010). *Form and Forces: Designing Efficient, Expressive Structures*. Hoboken, New Jersey: John Wiley & Sons.

[5] Baarsen, S.B., Schönwälder, J., Houtman, R., Veen, A. C., Vermeulen, H. & Haan, S. (2015). The 3D Printed Canal House. IASS Symposium 2015: Future Visions. Paper#528213.

[6] Bagrianski, S., & Halpern, A. B. (2013, December 05). Form-finding of compressive structures using Prescriptive Dynamic Relaxation. Retrieved from https://www.sciencedirect.com/science/article/pii/S0045794913002976?via=ihub

[7] Barnes, M. (1988). Form-finding and analysis of prestressed nets and membranes. *Computers & Structures*, *30*(3), 685-695. doi:10.1016/0045-7949(88)90304-5

[8] Beck, H. E., E. Zimmermann, N., McVicar, T. R., Vergopolan, N., Berg, A., & Wood, E. F.. (2018). *Present and future Köppen-Geiger climate classification maps at 1-km resolution* (Version 1). figshare. https://doi.org/10.6084/m9.figshare.6396959.v1

[9] Bianchi, L., Dorigo, M., Gambardella, L. M., & Gutjahr, W. J. (2008). A survey on metaheuristics for stochastic combinatorial optimization. *Natural Computing*, *8*(2), 239–287. doi: 10.1007/s11047-008-9098-4

[10] *Blum, C.; Roli, A. (2003). "Metaheuristics in combinatorial optimization: Overview and conceptual comparison". 35 (3). ACM Computing Surveys: 268–308.*

[11] Bommes, D., Zimmer, H., Kobbelt, L. (2009). Mixed-integer quadrangulation. ACM Transactions on Graphics (TOG) 28, 3, 77.

[12] Bos, F., Wolfs, R., Ahmed, Z. and Salet, T. (2016). Additive manufacturing of concrete in construction: potentials and challenges of 3D concrete printing. Virtual and Physical Prototyping. 11(3), pp209-225. doi:10.1080/17452759.2016.1209867

[13] Boswell, P. G. H. (1948). A preliminary examination of the thixotropy of some sedimentary rocks. *Quarterly Journal of the Geological Society*, *104*(1-4), 499-526.

[14] Carneau, P., Mesnil, R., Roussel, N., & Baverel, O. (2020, April 23). Additive manufacturing of cantilever - From masonry to concrete 3D printing. Retrieved from https://www.sciencedirect.com/science/article/pii/S0926580519308568#f0015.

[15] Chastas, P., Theodosiou, T., Kontoleon, K. J., & Bikas, D. (2017). The effect of embodied impact on the cost-optimal levels of Nearly Zero energy buildings: A case study of a residential building in Thessaloniki, Greece.

[16] Chen, Y., Figueiredo, S. C., Li, Z., Chang, Z., Jansen, K., Çopuroğlu, O., & Schlangen, E. (2020, March 19). Improving printability of limestone-calcined clay-based cementitious materials by using viscosity-

modifying admixture. Retrieved from https://www.sciencedirect.com/science/article/pii/S0008884619315911?fbclid=IwAR2vIM_ykJob9EEkrJBXs__9Z8RDkYZlY_IZ6vizA4k4tyJVuHhASeFHiGA

[17] Day, A. (1965). An introduction to dynamic relaxation. *The Engineer, 219*(5688), 218-221.

[18] De Wit, S. (2016), Parametric Segmental Timber Shell Structures Using Form-Finding: In combination with structural analysis and digital fabrication, Eindhoven, The Netherlands

[19] Dethier, J. (1982). Down to Earth. Mud Architecture: An Old Idea, a New Future. Thames & Hudson, London.

[20] Dobson, S. (2000). Continuity of Tradition: New Earth Building. In: Terra 2000: Eighth International Conference on the Study and Conservation of Earthen Architecture. James & James, London.

[21] Duballet, R., Baverel, O., & Dirrenberger, J. (2017, August 17). Classification of building systems for concrete 3D printing. Retrieved from https://www.sciencedirect.com/science/article/pii/S0926580516302977?via=ihub

[22] Ducoulombier, Nicolas, & Carneau, Paul. (2019). Formwork-free 3d printing of a barrel vault with cementitious material. Zenodo. http://doi.org/10.5281/zenodo.3496964

[23] Flügge W. (1972) Theory of Shells. In: Tensor Analysis and Continuum Mechanics. Springer, Berlin, Heidelberg. https://doi.org/10.1007/978-3-642-88382-8_9

[24] Galiaard, S., Hofman, S., Perry, N. & Ren, S. (2015). Optimizing Structural Building Elements in Metal by using Additive Manufacturing. IASS Symposium 2015: Future Visions. Paper#501821.

[25] *Gerry Bye, Paul Livesey, Leslie Struble (2011). "Admixtures and Special Cements". Portland Cement: Third edition.* doi:10.1680/pc.36116.185

[26] Herrmann, M. (2015, January 01). Gradientenbeton - Untersuchungen zur Gewichtsoptimierung einachsiger biege- und querkraftbeanspruchter Bauteile. http://dx.doi.org/10.18419/opus-634

[27] Illampas, R., et al. "A Study Of The Mechanical Behaviour Of Adobe Masonry." *WIT Transactions on The Built Environment*, WIT Press, 23 Aug. 2011, www.witpress.com/elibrary/wit-transactions-on-the-built-environment/118/22755.

[28] Kazemian, A., Yuan, X., Cochran, E., & Khoshnevis, B. (2017, April 20). Cementitious materials for construction-scale 3D printing: Laboratory testing of fresh printing mixture. Retrieved from https://www.sciencedirect.com/science/article/pii/S0950061817306657

[29] Kezdi, A. (1969). Handbuch der Bodenmechanik, Bd. 1 Bodenphysik. VEB Verlag f. Bauwesen, Berlin

[30] Kilian, A., & Ochsendorf, J. (2005). Particle-spring systems for structural form finding. *J.-Int. Assoc. SHELL Spat. Struct, 148*, 77.

[31] Kontovourkis, O., Tryfonos, G., & Georgiou, C. (2019). Robotic additive manufacturing (RAM) with clay using topology optimization principles for toolpath planning: the example of a building element. Architectural Science Review, 1–14. doi: 10.1080/00038628.2019.1620170

[32] Linkwitz, K. (2014). Force density method: Design of a timber shell. *Shell Structures for Architecture. Form Find and Optimization*, 59-71.

[33] Ma, G., Li, Z., & Wang, L. (2017, December 15). Printable properties of cementitious material containing copper tailings for extrusion based 3D printing. Retrieved from https://www.sciencedirect.com/science/article/pii/S0950061817324546

[34] Mandat, M. (2020). Robotic 3DPrinting Earth: Earthen additive manufacturing with customized nozzles to create gradient material for on-demand performance. Retrieved from https://repository.tudelft.nl/islandora/object/uuid:cf78d7d6-bc5f-4143-a6c7-9a112ab69f2b?collection=education

[35] Mariette Moevus, Yves Jorand, Christian Olagnon, Sandrine Maximilien, Romain Anger, et al.. Earthen construction: an increase of the mechanical strength by optimizing the dispersion of the binder phase. Materials and Structures, Springer Verlag, 2015, pp.1--14. ⟨10.1617/s11527-015-0595-5⟩. ⟨hal-01159955⟩

[36] McCormac, Jack C. (2008). Structural Steel Design (4th ed.). Upper Saddle River, NJ: Pearson Prentice Hall. ISBN 978-0-13-221816-0 – via Google Books (preview).

[37] McMullan R., (1983), "Environmental science in building", 6th edition, UK, England: Palgrave Macmillan

[38] Minke. G. (2000). Earth Construction Handbook. WIT Press, Southampton, UK.

[39] Minke, G. (2012). Building with Earth. New York: Birkhũser Publishers for Architecture.

[40] Mitchell, J. K. (1961). Fundamental aspects of thixotropy in soils. *Transactions of the American Society of Civil Engineers*, *126*(1), 1586-1620.

[41] Nerella, V. N., Näther, M., Iqbal, A., Butler, M., & Mechtcherine, V. (2018, September 24). Inline quantification of extrudability of cementitious materials for digital construction. Retrieved from https://www.sciencedirect.com/science/article/pii/S0958946518302956

[42] Ngo, T. D., Kashani, A., Imbalzano, G., Nguyen, K. T. Q., & Hui, D. (2018, February 13). Additive manufacturing (3D printing): A review of materials, methods, applications and challenges. Retrieved from https://www.sciencedirect.com/science/article/pii/S1359836817342944?via=ihub.

[43] O.O. Akinkurolere, Cangru Jiang, A.T. Oyediran, O.I. Dele- Salawu and A.K. Elensinnla, 2006. Engineering Properties of Cob as a Building Material. Journal of Applied Sciences, 6: 1882-1885.

[44] Panda, B., Paul, S. C., & Tan, M. J. (2017, July 27). Anisotropic mechanical performance of 3D printed fiber reinforced sustainable construction material. Retrieved from https://www.sciencedirect.com/science/article/pii/S0167577X17311679#f0020.

[45] Panda, B., Singh, G. V. P. B., Unluer, C., & Tan, M. J. (2019, February 19). Synthesis and characterization of one-part geopolymers for extrusion based 3D concrete printing. Retrieved from https://www.sciencedirect.com/science/article/pii/S0959652619305840

[46] Panda, B., Unluer, C., & Tan, M. J. (2019, August 13). Extrusion and rheology characterization of geopolymer nanocomposites used in 3D printing. Retrieved from https://www.sciencedirect.com/science/article/pii/S1359836819331579

[47] Peri. (2020, August 13). Retrieved from https://www.peri.com/en/business-segments/3d-construction-printing.html

[48] Perkins, I. & Skitmore,M. (2015). Three-dimensional Printing in the Construction Industry: A Review. International Journal of Construction Management. pp1-9. doi:10.1080/15623599.2015.1012136

[49] Perrot, A., Rangeard, D., & Courteille, E. (2018, April 6). 3D printing of earth-based materials: Processing aspects. Retrieved from https://www.sciencedirect.com/science/article/pii/S0950061818308079.

[50] Piker, D. (2013), Kangaroo: Form Finding with Computational Physics. Architectural Design 83, no. 2.

[51] Pusch, R. (2007, September 4). Chapter 6 Mechanical Properties of Clays and Clay Minerals. Retrieved from https://www.sciencedirect.com/science/article/pii/S1572435205010068.

[52] Rael, R. and San Fratello, V., 2018. *Printing Architecture*. New York: Princeton Architectural Press.

[53] Rahul, A. V., Santhanam, M., Meena, H., & Ghani, Z. (2019, August 21). Mechanical characterization of 3D printable concrete. Retrieved from https://www.sciencedirect.com/science/article/pii/S0950061819321282?via=ihub.

[54] Reeves, G. M, Sims, I. & Cripps, J. C. (eds) (2006). Clay Materials Used in Construction. Geological Society, London, Engineering Geology Special Publication, 21.

[55] Reiter, L., Wangler, T., Roussel, N., & Flatt, R. J. (2018, June 12). The role of early age structural build-up in digital fabrication with concrete. Retrieved from https://www.sciencedirect.com/science/article/pii/S0008884617312930

[56] Rippmann, M., Block, P., & Sobek, W. (2016). *Funicular Shell Design: Geometric approaches to form finding and fabrication of discrete funicular structures*. Zürich: ETH-Zürich.

[57] Roussel, N., Ovarlez, G., Garrault, S., & Brumaud, C. (2011, October 13). The origins of thixotropy of fresh cement pastes. Retrieved from https://www.sciencedirect.com/science/article/pii/S0008884611002353

[58] Rubel, F.; Kottek, M. (2010). Observed and projected climate shifts 1901–2100 depicted by world maps of the Köppen-Geiger climate classification. Meteorol. 135–141.

[59] Schroeder, H. (2009). Konstruktion und Ausführung von Mauerwerk aus Lehmsteinen. In: Mauerwerkkalender, pp. 271–290. W. Ernst & Sohn, Berlin

[60] Scopigno R., Cignoni P., Pietroni N., Callieri M., Dellepiane M. (2017). "Digital Fabrication Techniques for Cultural Heritage: A Survey". *Computer Graphics Forum* 36 (1): 6–21. DOI:10.1111/cgf.12781.

[61] Shaeffer, M. (2009). Concrete Forms – A Formwork Formula: Tips for success. Construction. Last modified January 21, 2009. www.forconstructionpros.com/concrete/equipment-products/forms/article/10302640/concrete-forms-a-formwork-formula-tips-for-success.

[62] Shepherd, P., & Williams, C. (2017). Shell Design Considerations for 3D Printing with Drones. *Proceedings of the IASS Annual Symposium 2017*. Retrieved October 27, 2020.

[63] Shibam Hadramawt. (2020, September 11). Retrieved from https://en.wikipedia.org/wiki/Shibam_Hadramawt

[64] "Soliquid Is the Startup Doing Large-Scale 3D Printing in Suspension." *3Dnatives*, 3 July 2019, www.3dnatives.com/en/soliquid-3d-printing-suspension-090720194/.

[65] Srivastana, P. K., Simant, & Shuckla, S. (2017). Structural Optimization Methods: A General Review. IJIRSET, 6(9).

[66] Sutcu, M., Alptekin, H., Erdogmus, E., Er, Y., & Gencel, O. (2015, March 3). Characteristics of fired clay bricks with waste marble powder addition as building materials. Retrieved from https://www.sciencedirect.com/science/article/pii/S0950061815002020.

[67] Thurm C (2001) Analyse der Möglichkeiten der ökologisch verträglichen Modifizierung von Baulehmen mit Zuschlägen und Zusatzstoffen. Bauhaus-Universität, Fak. Bauingenieurwesen, unpublished diploma thesis, Weimar

[68] Underwood, P. (1983). DYNAMIC RELAXATION. *Comput methods for transient anal* (pp. 245-265) Retrieved from www.scopus.com

[69] United Nations Organization. (1987). Report of the World Commission on Environment and Development: Our Common Future (Brundtland Report). UNO. New York.

[70] Valente, M., Sibai, A., & Sambucci, M. (2019). Extrusion-Based Additive Manufacturing of Concrete Products: Revolutionizing and Remodeling the Construction Industry. Journal of Composites Science, 3(3), 88. MDPI AG. Retrieved from http://dx.doi.org/10.3390/jcs3030088

[71] Yunliang Ding. (1986). Shape optimization of structures: a literature survey, Department of Aeronautical, Structures and Materials, computers & Structures Vol. 24. No. 6. pp. 985-1004.

[72] Williams, C. (2014). What is a shell? In Shell Structures for Architecture: Form Finding and Optimization, pp. 21–31. London: Taylor & Francis - Routledge.

[73] Wolfs, R. J. M., Bos, F. P., & Salet, T. A. M. (2018, February 9). Early age mechanical behaviour of 3D printed concrete: Numerical modelling and experimental testing. Retrieved from https://www.sciencedirect.com/science/article/pii/S000888461730532X

[74] Wu, J., Aage, N., Westermann, R., & Sigmund, O. (2018). Infill Optimization for Additive Manufacturing—Approaching Bone-Like Porous Structures. *IEEE Transactions on Visualization and Computer Graphics*, 24, 1127-1140.

[75] Zabalza Bribián, I., Valero Capilla, A., Aranda Usón, A. (2011). Life cycle assessment of building materials: comparative analysis of energy and environmental impacts and evaluation of the eco-efficiency improvement potential. Build. Environ. 46,1133–1140.https://doi.org/10.1016/j.buildenv.2010.12.002.

[76] Zhang, X. W., Kong, L. W., Yang, A. W., & Sayem, H. M. (2017, February 16). Thixotropic mechanism of clay: A microstructural investigation. Retrieved from https://www.sciencedirect.com/science/article/pii/S0038080617300021#b0135

[77] Zuo, Z., Gong, J., Huang, Y., Zhan, Y., Gong, M., & Zhang, L. (2019, March 8). Experimental research on transition from scale 3D printing to full-size printing in construction. Retrieved from https://www.sciencedirect.com/science/article/pii/S0950061819304660.

[78] **Υ.ΠΕ.ΧΩ.Δ.Ε**. (2000), "**Ελληνικός Αντισεισμικός Κανονισμός**, ΕΑΚ 2000", **Αθήνα**

9 Appendix

Digital Grasshopper3D Workflow

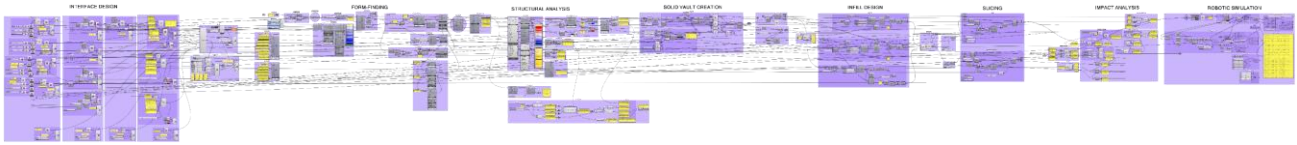

Fig. 9.1 Workflow definition

Interface

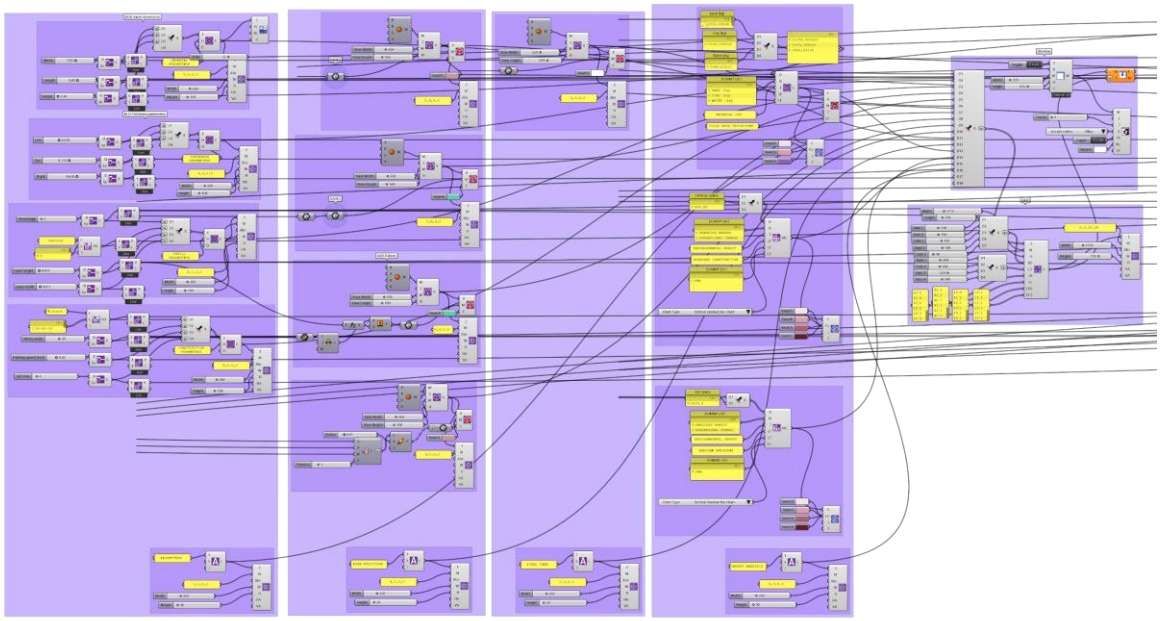

Fig. 9.2 Interface definition

Form-finding

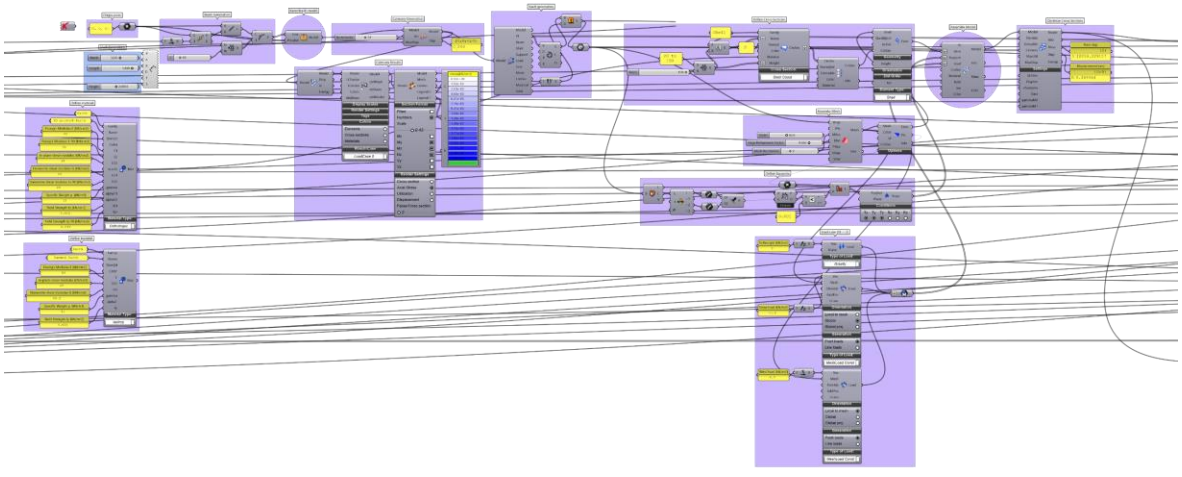

Fig. 9.3 Form-finding definition

Structural analysis (Karamba3D)

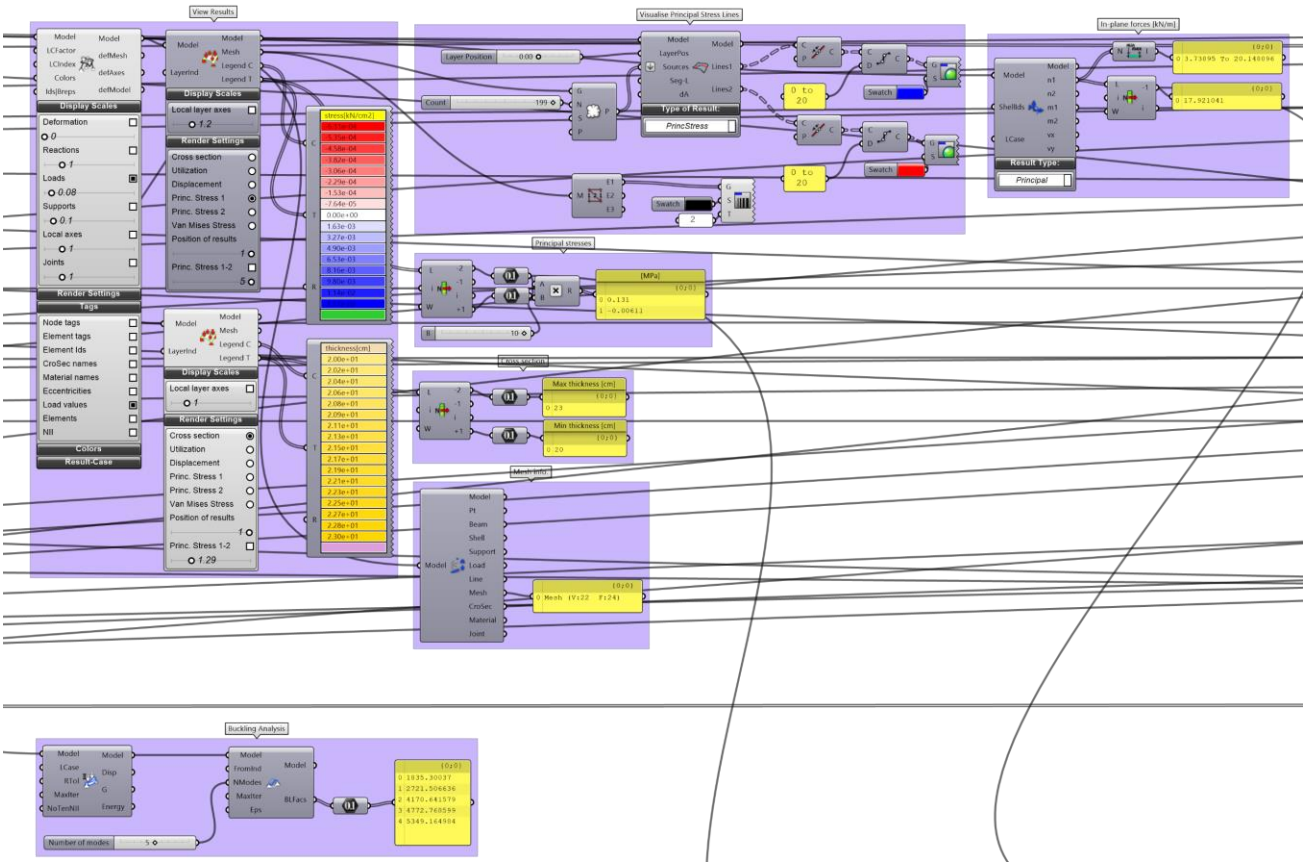

Fig. 9.4 Structural analysis definition

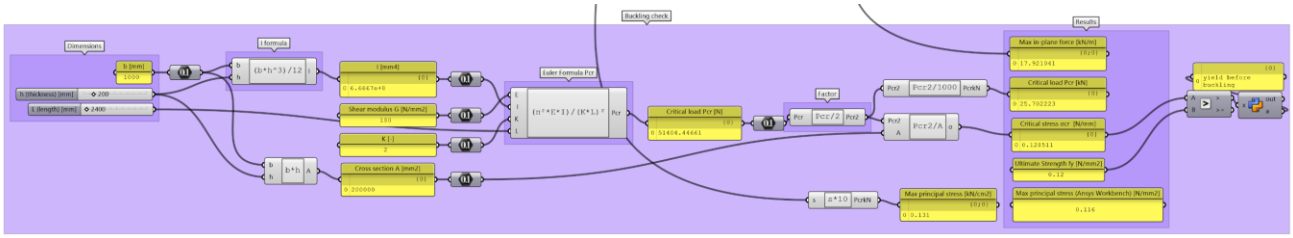

Fig. 9.5 Buckling check

Structural analysis plots

Fig. 9.6 Karamba3D Resulting vault mesh

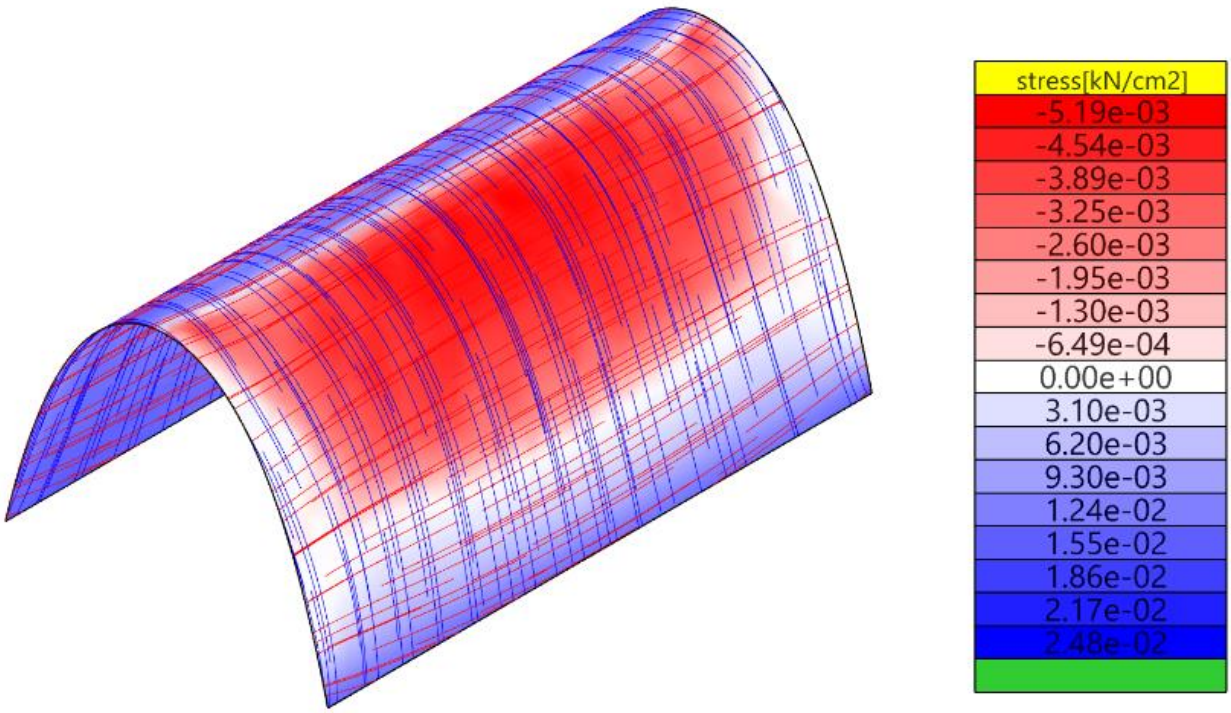

Fig. 9.7 Principal stresses

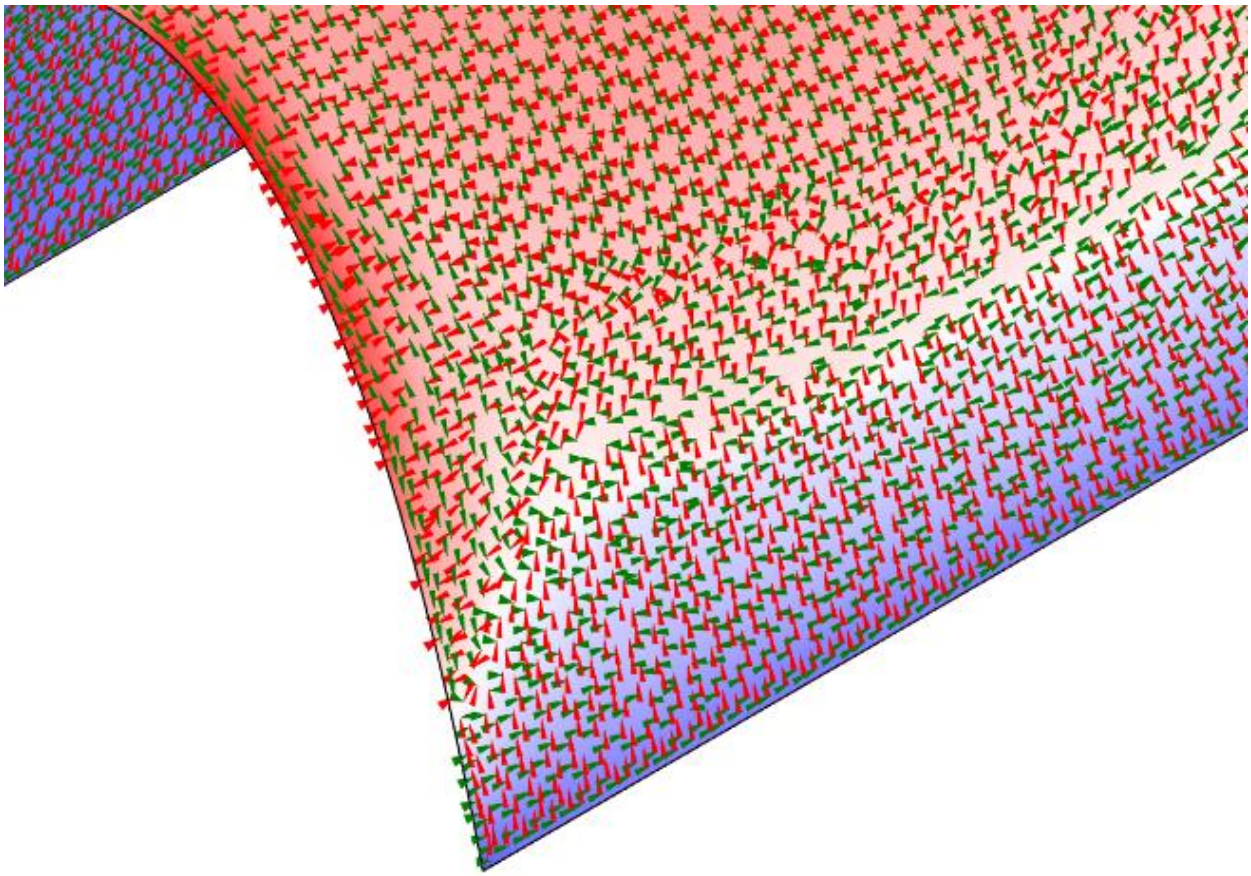

Fig. 9.8 Karamba3D Principal stress trajectories

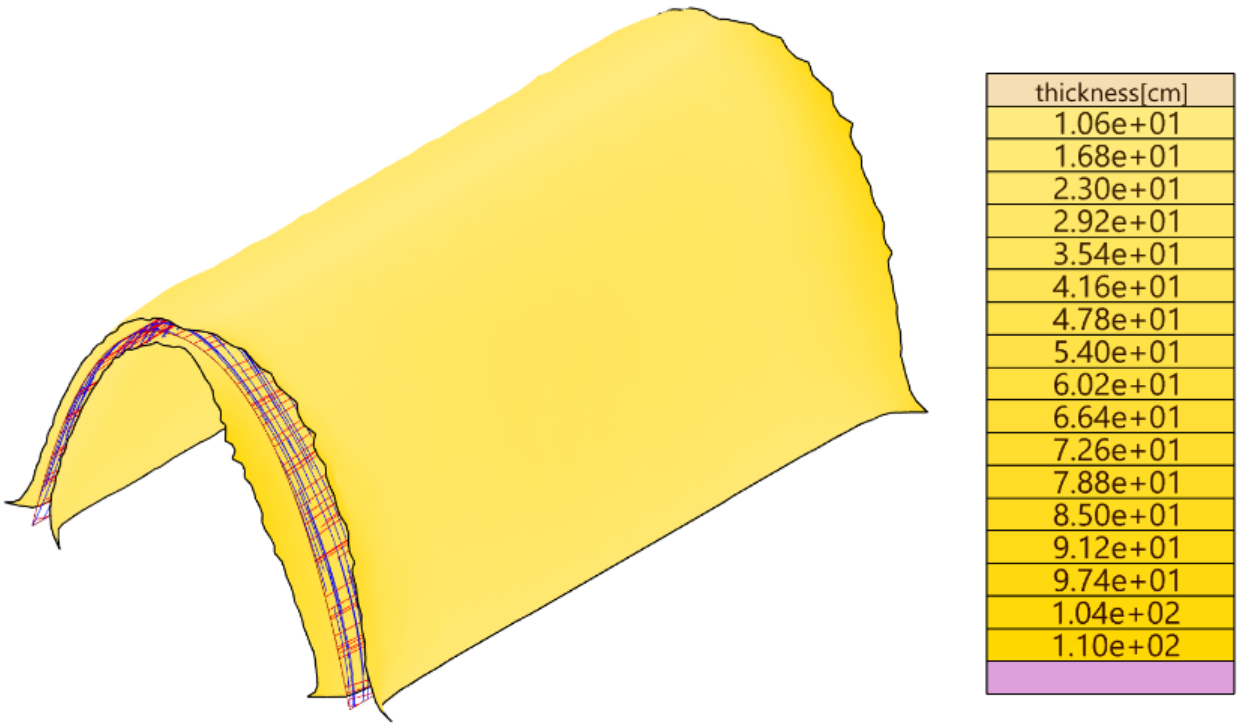

Fig. 9.9 Karamba3D Cross-section thicknesses

Solid vault

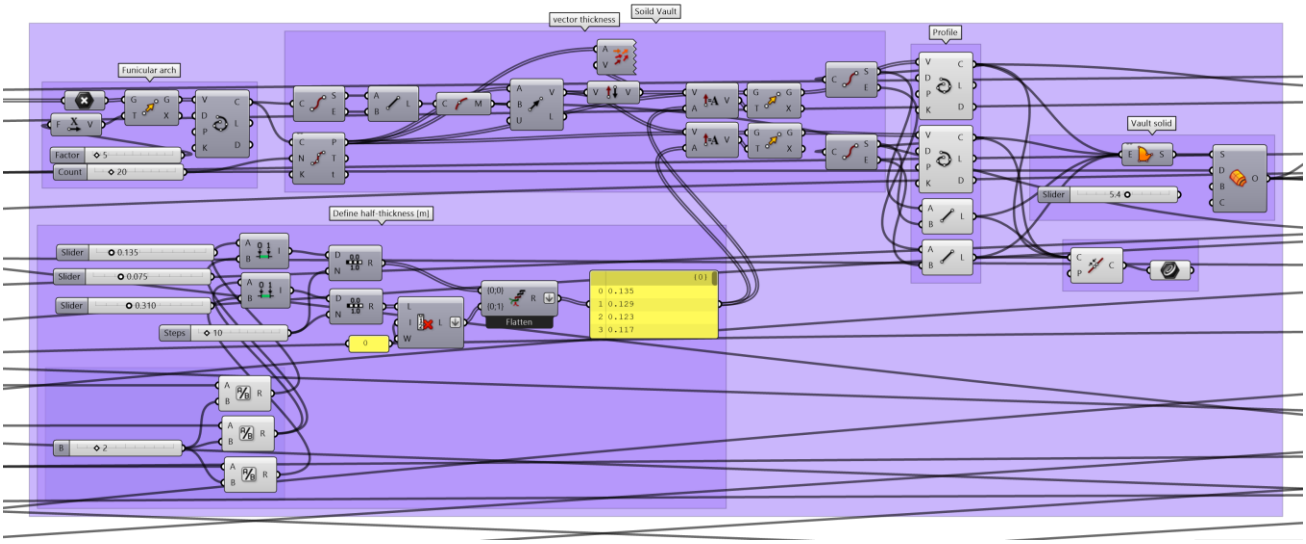

Fig. 9.10 Solid vault definition

Infill

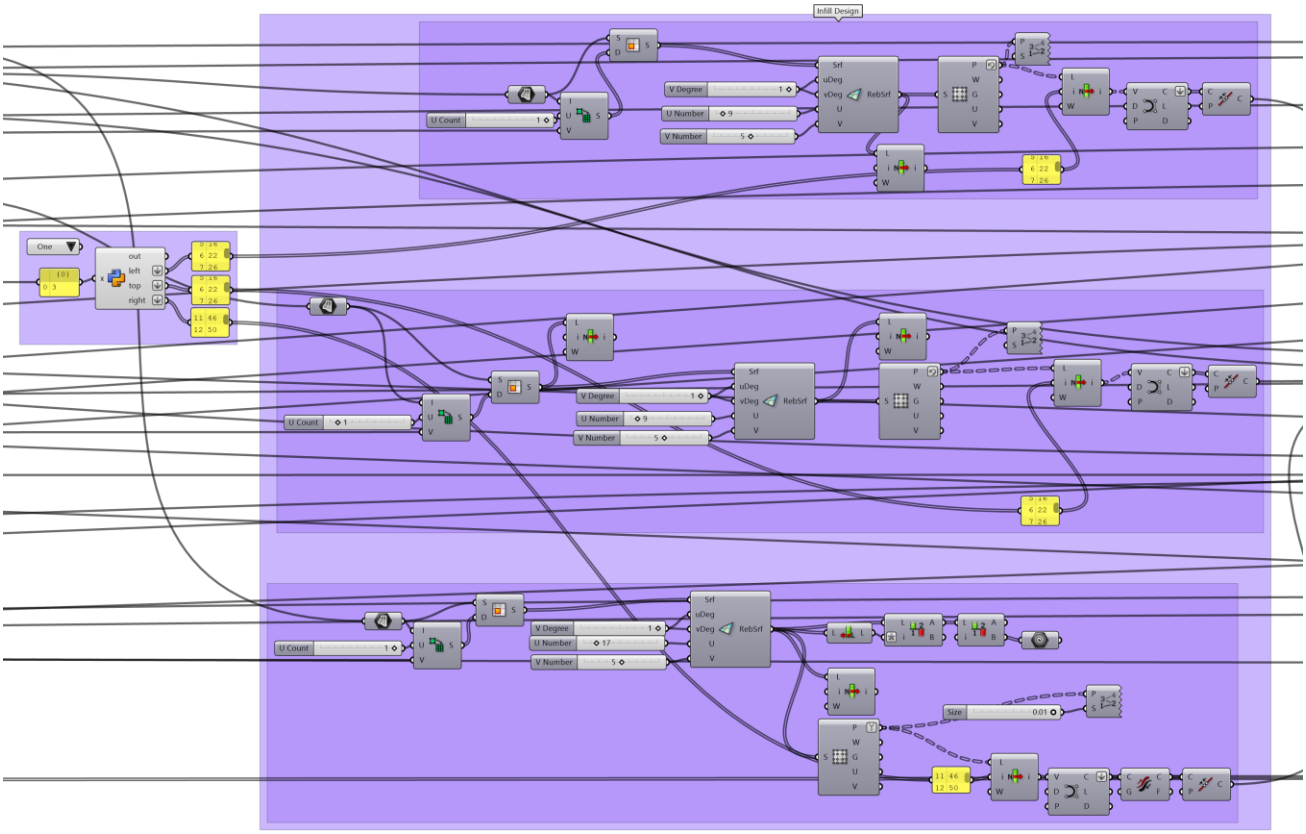

Fig. 9.11 Infill definition

Infill list

```
__author__ = "rodif"
__version__ = "2020.10.22"

import rhinoscriptsyntax as rs
left = 1
top = 1
right = 1
if x == "1":
    left = 0,1,2,5,10,35,40,41,42,43,44,39,14,9,2,3,4
    top = 0,1,2,5,10,35,40,41,42,43,44,39,14,9,2,3,4
    right = 0,1,2,5,10,70,75,80,81,82,83,84,79,74,14,9,2,3,4
elif x == "2":
    left = 0,1,2,15,20,25,36,42,38,29,24,19,2,3,4
    top = 0,1,2,15,20,25,36,42,38,29,24,19,2,3,4
    right = 0,1,2,15,20,25,42,55,60,65,76,82,78,69,64,59,42,29,24,19,2,3,4
elif x == "3":
    left = 0,1,2,6,10,16,22,26,30,36,42,38,34,28,22,18,14,8,2,3,4
    top = 0,1,2,6,10,16,22,26,30,36,42,38,34,28,22,18,14,8,2,3,4
    right =
0,1,2,6,10,16,22,26,30,36,42,46,50,56,62,66,70,76,82,78,74,68,62,58,54,48,42,38,34,28,22,18,14
,8,2,3,4
elif x == "4":
    left =
0,1,2,7,6,5,10,11,12,17,16,15,20,21,22,27,26,25,30,31,32,37,36,35,40,41,42,43,44,39,38,37,32,3
3,34,29,28,27,22,23,24,19,18,17,12,13,14,9,8,7,2,3,4
    top =
0,1,2,7,6,5,10,11,12,17,16,15,20,21,22,27,26,25,30,31,32,37,36,35,40,41,42,43,44,39,38,37,32,3
3,34,29,28,27,22,23,24,19,18,17,12,13,14,9,8,7,2,3,4
    right =
0,1,2,7,6,5,10,11,12,17,16,15,20,21,22,27,26,25,30,31,32,37,36,35,40,41,42,47,46,45,50,51,52,5
7,56,55,60,61,62,67,66,65,70,71,72,77,76,75,80,81,82,83,84,79,78,77,72,73,74,69,68,67,62,63,64
,59,58,57,52,53,54,49,48,47,42,43,44,39,38,37,32,33,34,29,28,27,22,23,24,19,18,17,12,13,14,9,8
,7,2,3,4
elif x == "5":
    left =
0,1,2,7,6,5,10,11,12,17,22,21,20,25,30,35,40,41,42,43,44,39,34,29,24,23,22,17,12,13,14,9,8,7,2
,3,4
    top =
0,1,2,7,6,5,10,11,12,17,22,21,20,25,30,35,40,41,42,43,44,39,34,29,24,23,22,17,12,13,14,9,8,7,2
,3,4
    right =
0,1,2,7,6,5,10,11,12,17,22,21,20,25,30,35,36,37,42,47,52,57,56,55,60,65,70,75,80,81,82,83,84,7
9,74,69,64,59,58,57,52,47,42,37,38,39,34,29,24,23,22,17,12,13,14,9,8,7,2,3,4
elif x == "6":
    left =
0,1,2,1,5,11,12,17,16,20,26,27,32,31,35,41,42,43,39,33,32,27,28,24,18,17,12,13,9,3,2,3,4
    top = 0,1,2,1,5,11,12,17,16,20,26,27,3
2,31,35,41,42,43,39,33,32,27,28,24,18,17,12,13,9,3,2,3,4
    right =
0,1,2,1,5,11,12,17,22,27,32,37,36,40,46,47,52,57,62,67,72,71,75,81,82,83,79,73,72,67,62,57,52,
47,48,44,38,37,32,27,22,17,12,13,9,3,2,3,4
```

Fig. 9.12 Infill list GhPython script

Slicing

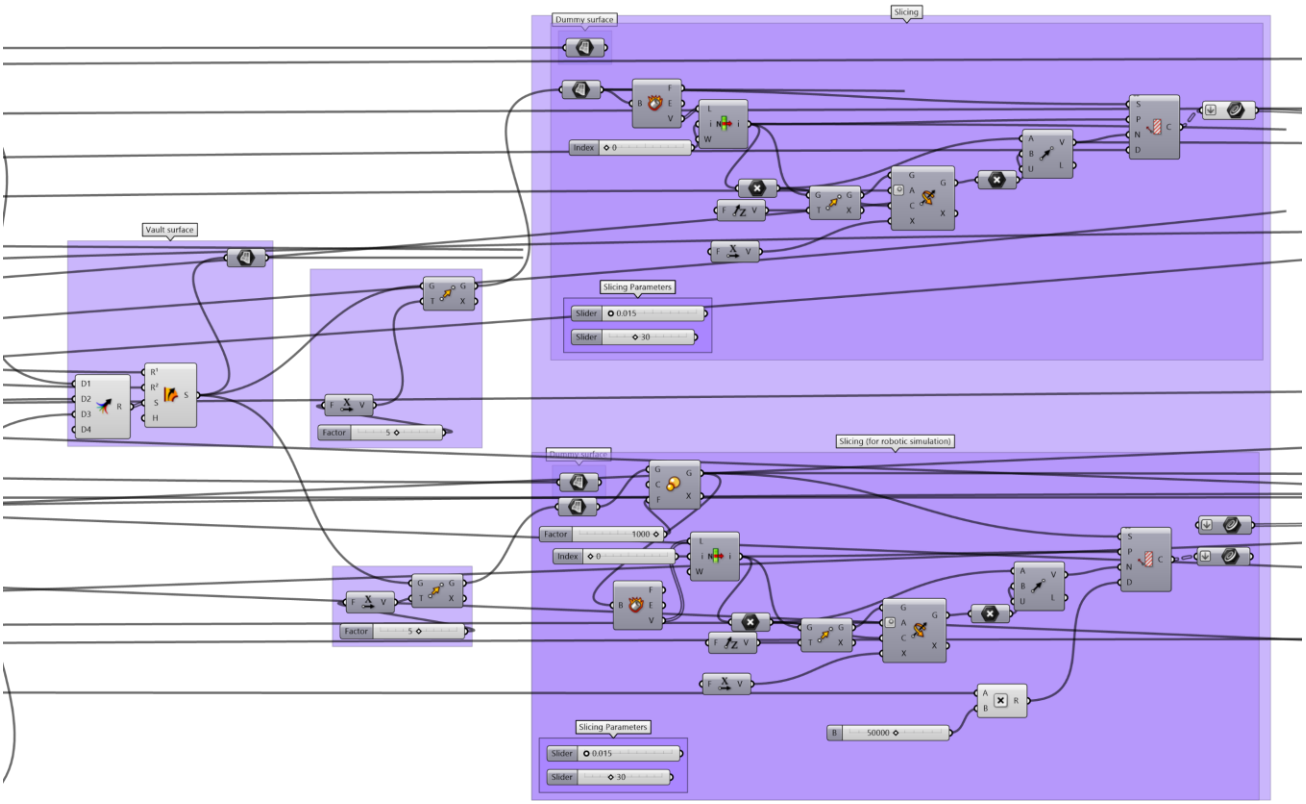

Fig. 9.13 Slicing definition

Robotic simulation

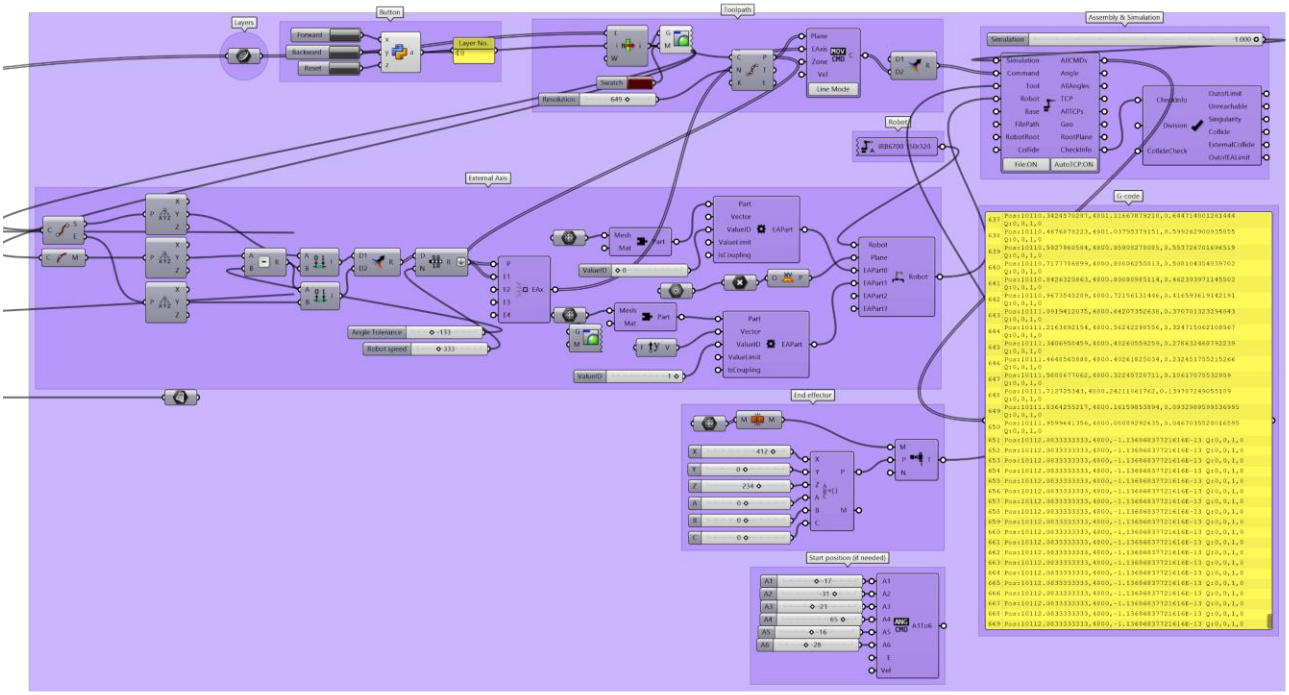

Fig. 9.14 Robotic simulation definition

Layer selection

```
1. import rhinoscriptsyntax as rs
2. import scriptcontext as sc
3. if x:
4.     sc.sticky["step"] = sc.sticky["step"] +1
5. if y:
6.     sc.sticky["step"] = sc.sticky["step"] -1
7. if z:
8.     sc.sticky["step"] = 0
9.
10.  a = sc.sticky["step"]
```

Fig. 9.15 Layer selection button GhPython script

Impact analysis

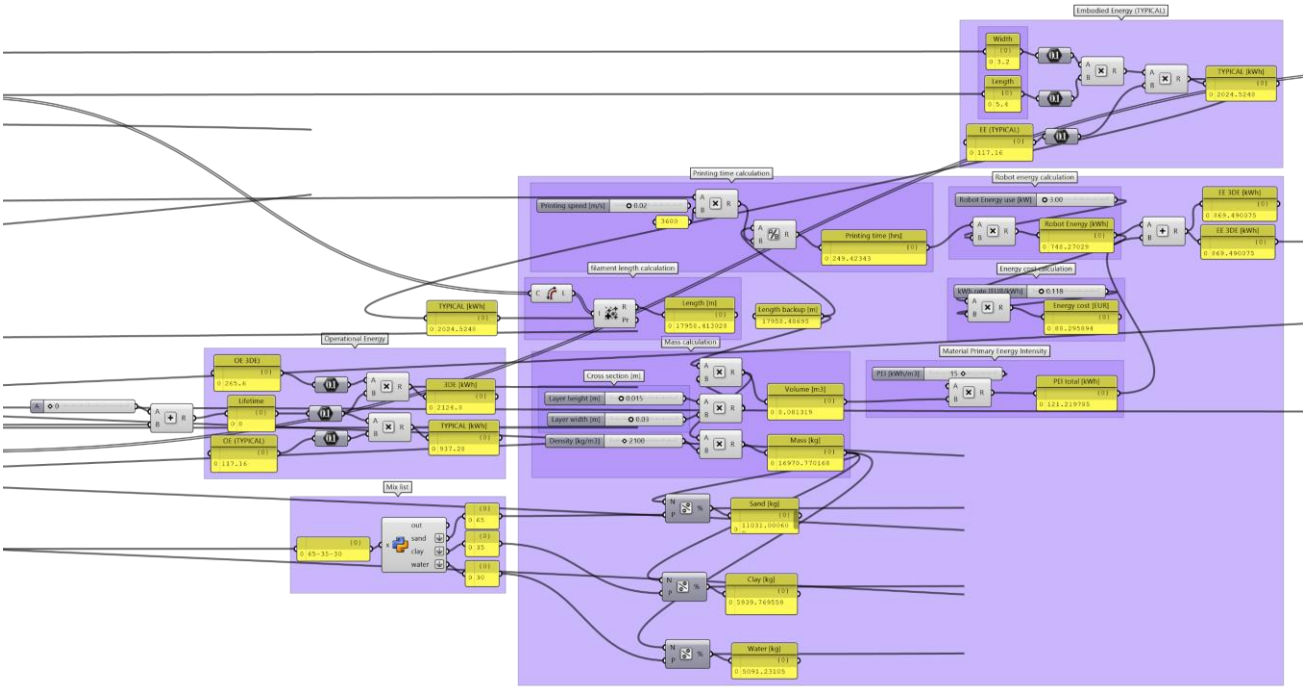

Fig. 9.16 Impact analysis definition

Arduino Sketch

```
#include <Stepper.h>

const int stepsPerRevolution = 19800;  // change this to fit the number of steps per
revolution
// for your motor


// initialize the stepper library on pins 6 through 7:
Stepper myStepper(stepsPerRevolution, 6, 7);
int driverDIR = 6;  //DIR- pin

int reverseSwitch = 2;  //limit switch as toggle
boolean setdir = LOW;  //toggle start/stop

int stepCount = 0;  // number of steps the motor has taken

//Interrupt Handler

void revmotor (){
  setdir = !setdir;
}

void setup() {
   attachInterrupt(digitalPinToInterrupt(reverseSwitch), revmotor, FALLING);
   Serial.begin(9600);
   delay(25);  //millisecond delay between pulses
}

void loop() {
  // read the sensor value:
  int sensorReading = analogRead(A0);

  Serial.println(sensorReading);
  digitalWrite(driverDIR,setdir);
  // map it to a range from 0 to 100:
  int motorSpeed = map(sensorReading, 0, 1023, 0, 100);
  // set the motor speed:
  if (motorSpeed > 0) {
    myStepper.setSpeed(motorSpeed);
    // step 1/100 of a revolution:
    if (setdir==LOW){
    myStepper.step(stepsPerRevolution / 100);}
    else
    {myStepper.step(stepsPerRevolution / 100000);}
  }
}
```

Fig. 9.17 Arduino sketch

ANSYS Workbench analyses

Property	Value	Unit
Density	1900	kg/m3
Orthotropic Elasticity		
Young's Modulus X direction	400	MPa
Young's Modulus Y direction	550	MPa
Young's Modulus Z direction	400	MPa
Poisson's Ratio XY	0.3	MPa
Poisson's Ratio YZ	0.3	MPa
Poisson's Ratio XZ	0.16	MPa
Shear Modulus XY	180	MPa
Shear Modulus YZ	200	MPa
Shear Modulus XZ	180	MPa
Tensile Yield Strength	0.12	MPa
Compressive Yield Strength	4	MPa
Tensile Ultimate Strength	0.37	MPa
Compressive Ultimate Strength	5	MPa

Fig. 9.18 3D printed earth material properties

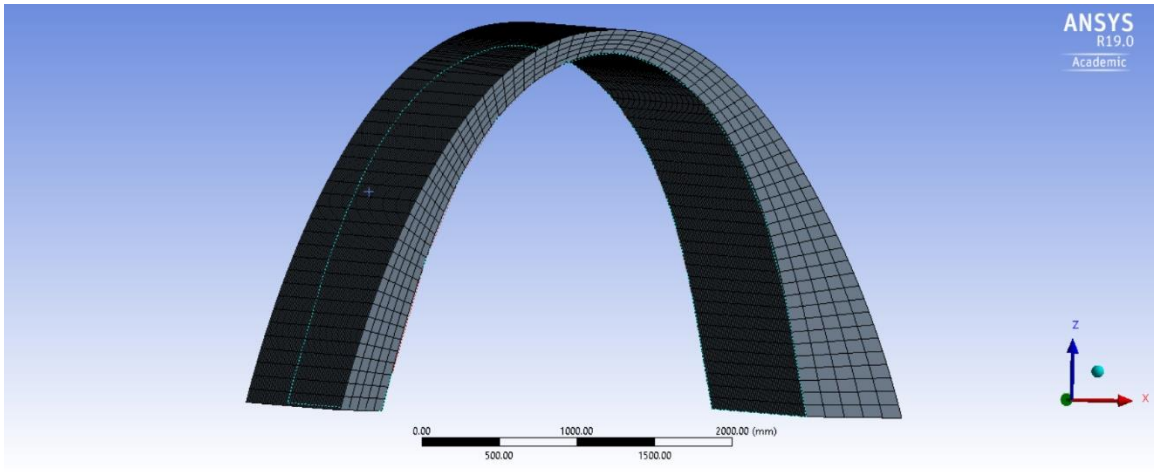

Fig. 9.19 ANSYS Workbench mesh resolution

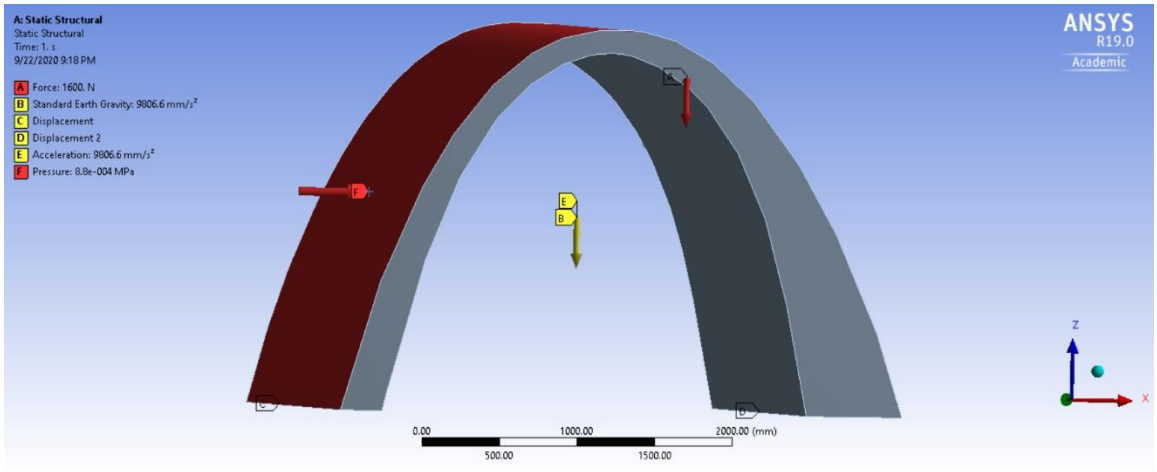

Fig. 9.20 ANSYS Workbench load case & boundary conditions

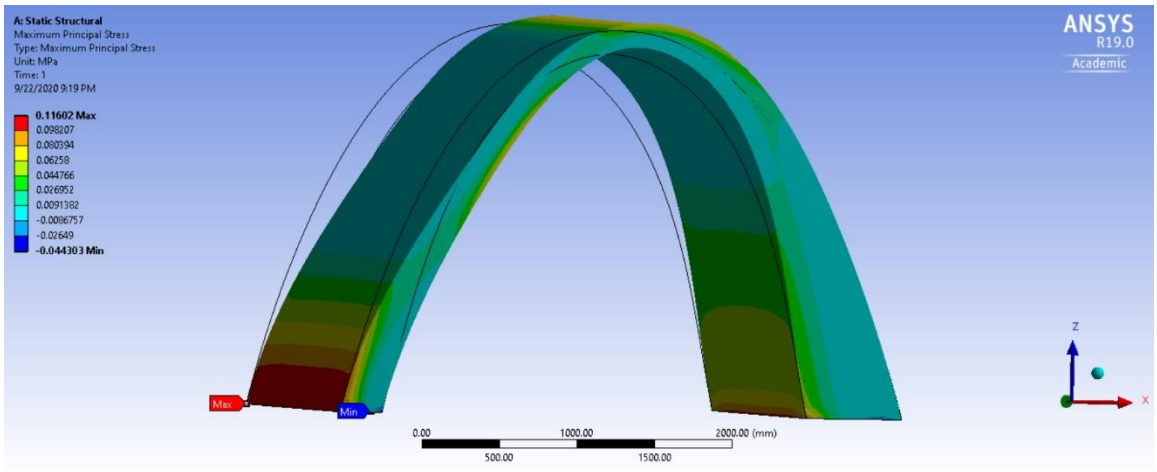

Figure 9.21 Maximum principal stresses

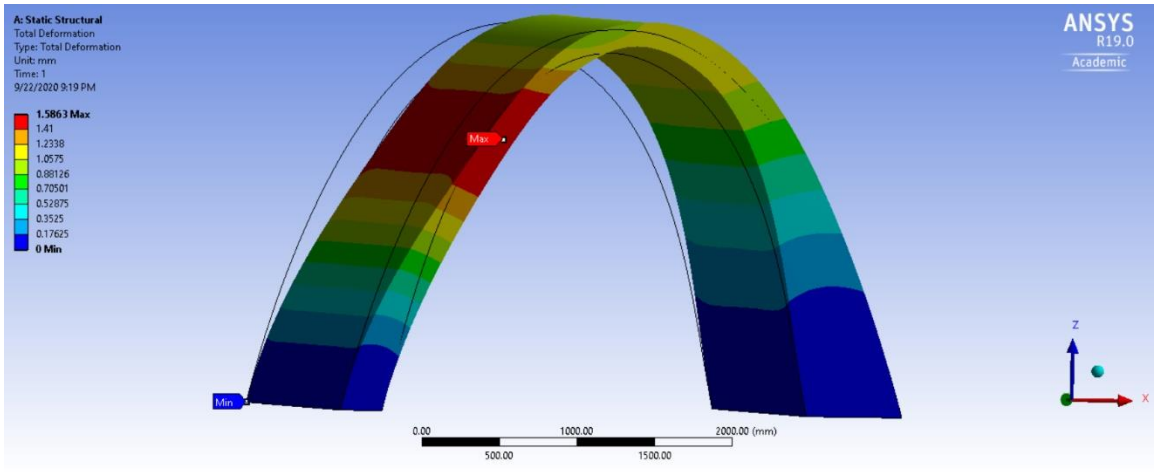

Figure 9.22 Total deformation [cm]

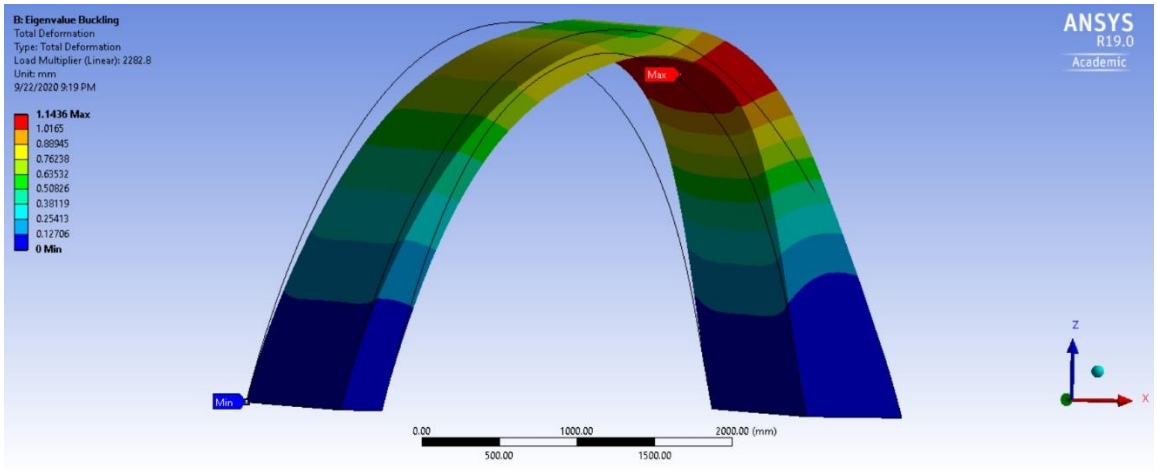

Figure 9.23 Buckling deformation (Linear)

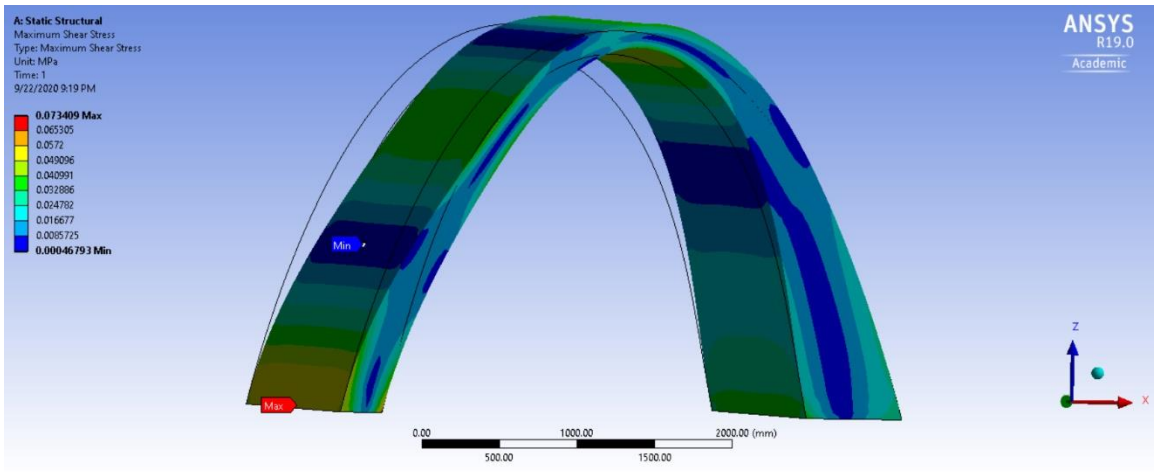

Figure 9.24 Maximum shear stress

Prototype printing settings

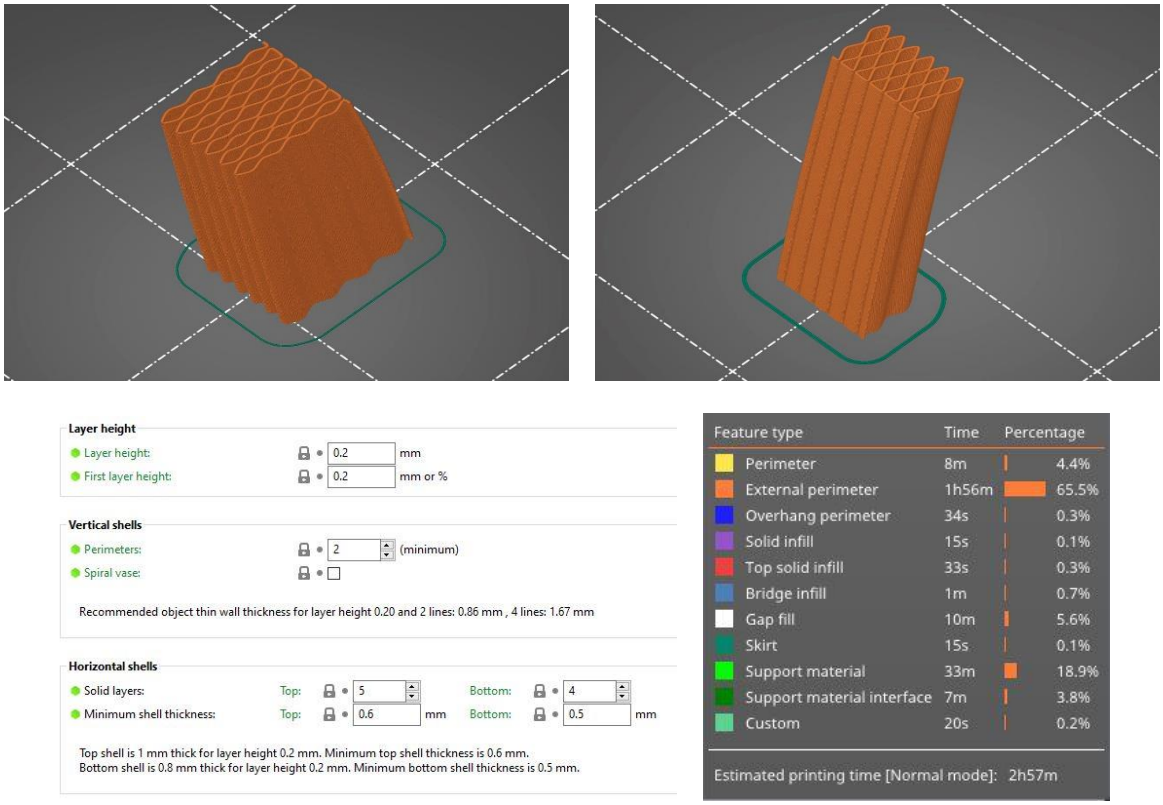

Fig. 9.25 Prototype printing settings

Planning

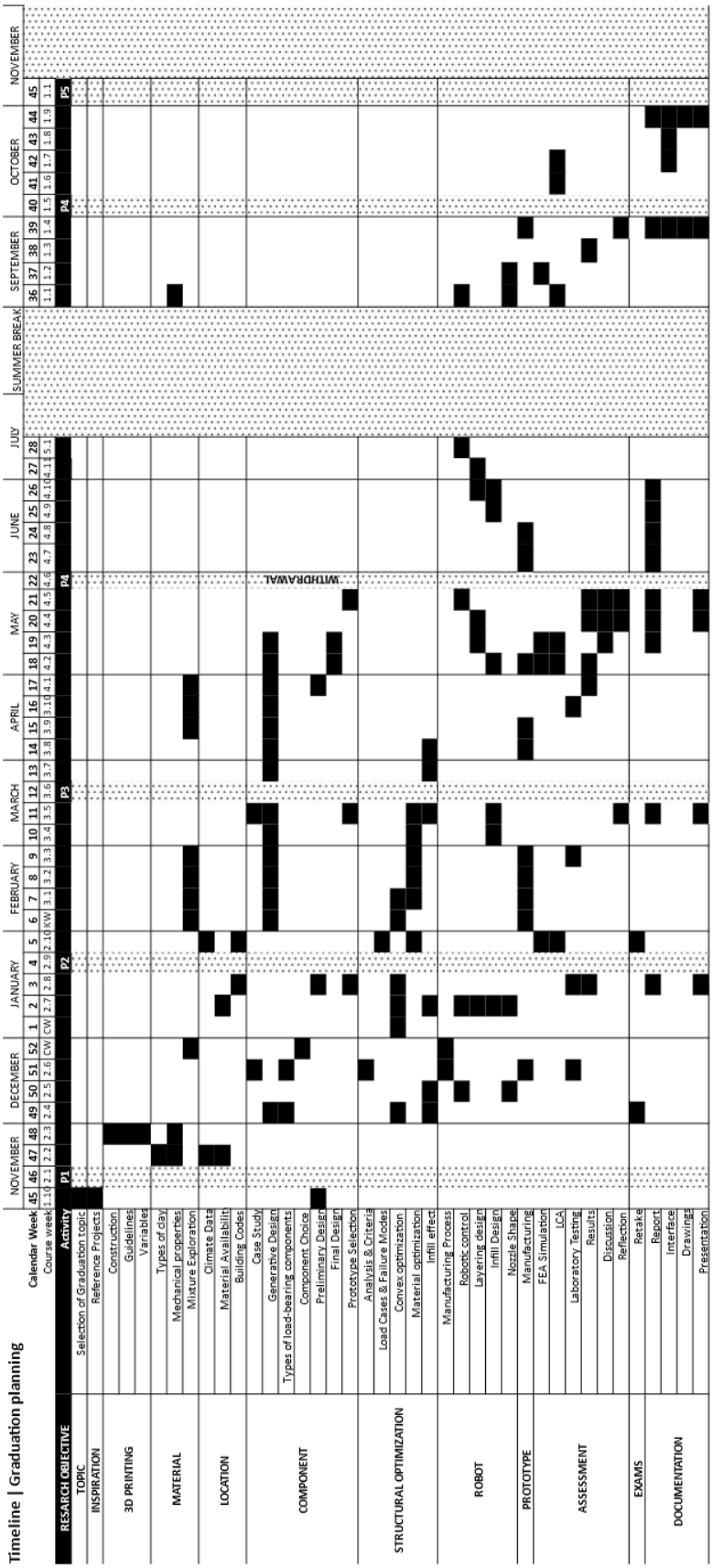

Fig. 9.26 Timeline